MOLECULAR GENETICS OF DEAFNESS:

THE ROLES OF MYO15 AND THYROID HORMONE

by

Qing Fang

A dissertation submitted in partial fulfillment
of the requirements for the degree of
Doctor of Philosophy
(Human Genetics)
in The University of Michigan
2010

Doctoral Committee:

Professor Sally A. Camper, Chair
Professor Miriam H. Meisler
Associate Professor Thomas M. Glaser
Associate Professor David C. Kohrman
Professor Karen H. Friderici, Michigan State University

Acknowledgments

First and foremost I would like to thank my parents, without whom I would not be the person that I am today. Their huge support gave me the biggest encouragement during the past several years.

I would like to thank my husband Wei, whose love and understanding create a peaceful family for me to get enjoyment and relaxation.

A special acknowledgment will be given to my mentor Dr. Sally Camper. It is hard to express in words how my life was changed by knowing Sally and being her student. She is warm, understanding and inspiring. She is the best mentor I have ever met.

Also I would like to thank my committee for all their support throughout these years. They are true scientists, and helped me in my development as a scientist.

Finally, special thanks to all the past and present members of the Camper lab, who have made my time full of fun and good memories.

Table of Contents

List of Figures

List of Tables

ABSTRACT

MOLECULAR GENETICS OF DEAFNESS:

THE ROLES OF MYO15 AND THYROID HORMONE

by

Qing Fang

Chair: Sally A. Camper

Deafness affects about 250 million people, and genetics contributes to approximately half of the cases. Environmental influences include exposure to noise, ototoxic drugs, physical trauma, and systemic diseases, such as hypothyroidism. This thesis presents functional analysis of a Mendelian cause of human deafness, mutations in the unconventional myosin MYO15, and a genetically complex disorder, susceptibility to hearing impairment due to hypothyroidism.

Mutations in the motor or tail domain of MYO15 cause congenital deafness and vestibular dysfunction. These domains are required for stereocilia elongation and WHIRLIN transport. Some isoforms of MYO15 contain a proline-rich region of unknown function. We generated a mouse model of a human mutation that eliminates these isoforms. These mutants have profound deafness but lack severe vestibular abnormalities, and have unique cochlear stereocilia pathology. Initial elongation occurs but is not maintained, implicating the proline-

rich region in hair bundle preservation. There is no evidence of allelic complementation for hearing or hair bundle maintenance in compound heterozygotes with different combinations of mutant alleles, proving functional importance of the full length MYO15 isoform.

Thyroid hormone (TH) has pleiotropic effects on cochlear development, and genomic variation influences the severity of the hearing problem. *Prop1*^{df} and *Pou1f1*^{dw} mutant mice lack pituitary thyrotropin, which causes severe TH deficiency and variable hearing impairments. DW-*Pou1f1*^{dw} mutants have multiple cochlear abnormalities and are profoundly deaf. In contrast, DF-*Prop1*^{df} mutants have mild hearing impairment and few permanent abnormalities. Transfer of these embryos to surrogates demonstrated that their susceptibility to hearing impairment is intrinsic to the fetus. A genome scan conducted on hearing progeny of an F1 intercross between DW-*Pou1f1*^{dw} carriers and *Mus castaneus* identified a single locus on chromosome 2, modifier of dw hearing, *Mdwh*, that rescues hearing despite persistent hypothyroidism. A known modifier in this region is neither necessary nor sufficient to rescue DW hearing, suggesting that *Mdwh* is a novel protective locus. Microarray analysis identified cochlear gene expression changes caused by hypothyroidism in *Pou1f1*^{dw} mice that are positional candidates for the modifier gene. Identification of the protective modifier will enhance our understanding of the mechanisms of hypothyroidism-induced hearing impairment and may lead to rational therapeutics.

CHAPTER 1

Introduction

Deafness is a common human health problem with about 250 million people affected worldwide. Approximately half of the deaf cases have a genetic basis. Hereditary deafness can be categorized by their genetic inheritance pattern (dominant, recessive, sex chromosome-linked, mitochondria-related), by their accompanying symptoms (syndromic, non-syndromic), and by age of onset (pre-lingual, post-lingual). More than 150 loci that cause genetic deafness have been mapped, although the genes underlying many of these loci have not been identified yet (Van Camp and Smith, Hereditary Hearing Loss Homepage: http://hereditaryhearingloss.org). Other causes of deafness include exposure to noise, ototoxic chemicals or medications, physical trauma, and systemic diseases.

The sensory cells critical for hearing are the hair cells. The number of hair cells is limited; for example, there are only about 3,000 hair cells in one mouse cochlea (Chen and Corey, 2002). Hair cells do not regenerate in humans and other mammals, which makes combating deafness a challenging task in the clinic.

There are several important advantages of the mouse that make it an ideal model system for the study of functional genomics of human deafness: the striking similarities in auditory structure and physiology between mice and humans, the relatively close evolutionary relationship of the two mammalian genomes, the ability to genetically manipulate mouse genome with desired genetic variation, and the convenient accessibility of mouse tissues for pathological analyses.

In this dissertation, I present my research in two areas: 1) a mouse model I developed of a human Mendelian, autosomal recessive deafness disorder *DFNB3* and 2) the variable effects of congenital hypothyroidism on hearing acuity using existing spontaneous, autosomal recessive mouse models of secondary hypothyroidism.

The model I generated of *DFNB3* precisely mimics a human mutation in the N-terminal proline-rich domain of the *MYO15* gene that causes congenital deafness. I show that this domain is essential for hearing and maintenance of cochlear stereocilia, but not required for gross vestibular function or the development of cochlear stereocilia. These discoveries lead to the hypothesis that the proline-rich domain is involved in transportation of novel cargo proteins that maintain the stereocilia.

The spontaneous mutants *Prop1*^{df} and *Pou1f1*^{dw} lack thyroid hormone because of pituitary dysfunction, and the degree of hearing deficit in both mutants is strongly influenced by genetic background. I present studies on the mechanism of thyroid hormone action in the cochlea and genetic studies that

address the influence of genetic background on the phenotype. I found that the predominant action of the genetic background is intrinsic to the fetus and not a maternal effect. I also present evidence that the modifier of hypothyroidism-induced deafness is a novel locus on Chr 2 that could be identified by conventional approaches.

Overall these studies lead us to a better understanding of the developmental and physiological mechanisms underlying the auditory processes in a Mendelian nonsyndromic deafness disorder, *DFNB3*, and a complex syndromic hearing impairment that can be caused by genetics and enviroment: thyroid hormone regulation of hearing acuity.

Inner ear structure

The mammalian ear consists of the outer, the middle and the inner ear (Fig. 1-1). The major role of the outer and the middle ear is to collect the sound and conduct it to the inner ear by vibration of the eardrum and movement of the ossicular chain within the middle-ear cavity. The inner ear is composed of vestibular and cochlear compartments, where the mechanical sound waves are converted into neural impulses and transmitted through the post-cochlear auditory pathway to the brain. The vestibular compartments contain the otolithic organs (saccule and utricle) and the semi-circular canals, which detect linear and rotational acceleration, respectively. The cochlea, a snail-shaped structure, contains the organ of Corti and is responsible for hearing. The organ of Corti is the sensory epithelium running along the inside of the cochlea from the base to

the apex. Two types of highly specialized sensory cells, inner hair cells (IHCs) and outer hair cells (OHCs), exist in the organ of Corti and are critical for mechano-electro-transduction (MET). On the apical surface of each hair cell, actin-rich cellular projections, called stereocilia, are arranged in a staircase pattern and bundled by lateral links and tip links connecting the adjacent rows. MET channels are located on the cell membranes of the shorter stereocilia and are thought to be close to and associated to the tip-link attachment sites (Beurg et al., 2009). When the sound waves cause the deflection of stereocilia bundles towards the longest rows, the tension of the tip links generates the mechanical force that opens the ion channels. Cations, mostly potassium, enter through the channels and depolarize the hair cells, which results in neurotransmitter release and excitation of the auditory nerves connected to the base of the hair cells.

Unconventional myosins in the inner ear

The myosin protein superfamily is large. The human genome contains ~40 myosin genes that can be divided into ~12 classes based on analysis of their head and tail domain structures (Berg et al., 2001). Class II myosins, also called conventional myosins, are primarily expressed in skeletal muscles. All of the other myosins expressed in non-muscle cells are known as unconventional myosins.

Myosins are actin-based motors with a conserved catalytic domain (motor domain), which hydrolyzes ATP and produces energy to create force and mechanical movement along actin filaments. The C-terminal tails found in most

myosins are quite diverse and are involved in binding different proteins. An N-terminal extension beyond the motor domain is present in some myosins and thought to endow class-specific properties.

Unconventional myosins participate in many cellular processes such as cell movement and signal transduction (Mermall et al., 1998). Recent research shows unconventional myosins also play the fundamental roles in establishing cell polarity (Yin et al., 2000) and the polymerization of actin (Evangelista et al., 2000; Lechler et al., 2000; Lee et al., 2000). Stereocilia of hair cells in the inner ear are actin-based structures. Five unconventional myosins are expressed in cochlear hair cells: MYO1, MYO3A, MYO6, MYO7A and MYO15A. Defects in these myosins are responsible for deafness in both humans and mice (Table 1-1). I discuss each of these myosins in the next section.

MYO1

Class I myosins include eight isozymes, that exhibit different expression levels in auditory and vestibular epithelia (Dumont et al., 2002). MYO1A is mutated in human hereditary deafness *DFNA48* (Donaudy et al., 2003). MYO1C is located near both ends of the tip links (Garcia et al., 1998), which is consistent with the identification of MYO1C as the adaptation motor of MET in the inner ear (Gillespie, 2004). Adaptation serves to reset the open probability of transduction channels near the rest value after stereocilia bundle deflection. No mutations in *MYO1C* have been reported in humans to date. A mouse missense mutation in *Myo1c* gene causes altered adaptation, but knocking out *Myo1c* gave

inconclusive results (Gillespie, 2004; Stauffer et al., 2005). It is possible that more than one MYO1 isozyme contributes to the adaptation motor.

MYO3A

Mutations in a human class III myosin cause progressive, nonsyndromic hearing loss *DFNB30* (Walsh et al., 2002). MYO3A is localized at the tips of stereocilia, and is thought to be important for the elongation of stereocilia (Schneider et al., 2006). Mechanistically, MYO3A is thought to be required for transporting espin 1 to the plus ends of actin filaments (Salles et al., 2009). Espin is an actin-bundling protein that acts as a scaffold to determine the placement, dimensions, flexibility and signaling of stereocilia (Sekerkova et al., 2006).

Both MYO3A and its ortholog NINAC in *Drosophila* contain domains N-terminal to the motor that display serine and threonine kinase activity (Ng et al., 1996). The protein kinase domain is required for normal visual processing in *Drosophila* (Li et al., 1998). Site-specific mutations in the protein kinase domain and the myosin domain, however, lead to different phenotypes: mutation of the kinase domain results in a defective electroretinography (ERG) phenotype but no retinal degeneration, while mutation in the myosin domain causes both an abnormal ERG phenotype and retinal degeneration (Porter and Montell, 1993). In mouse cochlea, the absence of the MYO3A kinase domain causes a stereocilia phenotype that is distinct from mutants lacking of the tail domain (Schneider et al., 2006). Thus, the MYO3A/NINAC example provides precedent for independent functions of the protein domains N-terminal to the myosin motor.

MYO6

MYO6 is mutated in humans with dominant deafness *DFNA22*, recessive deafness *DFNB37* and *Snell's Waltzer* mice, which have recessive deafness and vestibular dysfunction (Avraham et al., 1995; Melchionda et al., 2001; Ahmed et al., 2003). MYO6 is unique among motor myosins because it moves towards the negative end of the actin filaments, i.e. from the tips of the stereocilia to the cuticular plate at the apical surface of the hair cells. In the inner ear, the expression of MYO6 is concentrated at the cuticular plate at the base of the stereocilia (Hasson et al., 1997). The stereocilia of *Snell's Waltzer* mutants start to develop normally, then fuse together to form giant stereocilia (Self et al., 1999), suggesting that the role of MYO6 is to anchor the membrane at the base of the stereocilia on the apical hair cell surface. In addition, MYO6 and otoferlin interact to recycle synaptic vesicles at the IHC ribbon synapse at the base of the hair cells (Roux et al., 2009). Otoferlin is the major calcium sensor and essential for the exocytosis at the ribbon synapses in IHCs with innervation of afferant nerves (Roux et al., 2006).

MYO7A

Myo7a is the unconventional myosin gene affected in *shaker 1* mice and a large allelic series of mouse mutants, and in humans, mutations in *MYO7A* cause two forms of non-syndromic deafness *DFNA11* and *DFNB2* and one syndromic deafness Usher syndrome type 1B (*USH1B*) (Guilford et al., 1994; Gibson et al.,

1995; Weil et al., 1995; Tamagawa et al., 1996; Liu et al., 1997b; Liu et al., 1997a; Weil et al., 1997). Within the inner ear, MYO7A is expressed in the stereocilia, cuticular plate and the cytoplasm of both IHCs and OHCs (Hasson et al., 1995).

In stereocilia, MYO7A interacts with Harmonin, Sans and Protocadherin 15 (PCDH15) (Boeda et al., 2002; Adato et al., 2005; Senften et al., 2006), which are also Usher syndrome type 1 proteins that form the network to control the cohesion of the growing hair bundle during inner ear development. MYO7A is also involved in regulating the length of stereocilia by interacting with Twinfilin-2 (Peng et al., 2009; Rzadzinska et al., 2009). Twinfillin-2 is a capping protein for the barbed ends of actin filaments, that is localized at the tips of the shorter rows of stereocilia. During stereocilia development, Twinfilin-2 restricts excessive elongation of the shorter row of stereocilia, thereby maintaining the mature staircase architecture of cochlear hair bundles (Peng et al., 2009).

MYO15

MYO15 is important for elongation of the vestibular and cochlear stereocilia. *Myo15* is identified as the gene mutated in human deafness, *DFNB3*, and mouse deafness mutants *shaker 2* (*sh2*) and *shaker 2J (sh2J)* (Liang et al., 1998; Probst et al., 1998; Anderson et al., 2000). The molecular motor of MYO15 is inactivated in *sh2* mice by an amino acid substitution in the highly conserved putative actin-binding domain. The lesion in *sh2J* mice deletes the FERM and PDZ ligand domains in the mysoin tail. Both *sh2* and *sh2J* mutants

exhibit short cochlear and vestibular stereocilia, profound deafness, and balance dysfunction that results in circling behavior and head bobbing. The PDZ binding domain, which is located at the carboxy terminus of MYO15, and the motor domain are necessary for binding WHIRLIN and transporting it to the stereocilia tips. These conclusions are based on the fact that *shaker 2* and *shaker 2J* mutants are unable to transport WHIRLIN properly (Anderson et al., 2000; Belyantseva et al., 2003). MYO15 protein contains an N-terminal proline-rich domain, in which two mutations were found to cause deafness in humans (Nal et al., 2007). The function of this proline-rich domain of MYO15A is unknown and is the focus of my research presented in Chapter 2.

Overall, given that the normal function of inner ear hair cells relies on filamentous actin structures, it is not surprising that multiple unconventional myosins play important roles in the development and physiology of hair cells. Each of these myosins has an independent, unique function, as mutations specific to each myosin gene cause distinguishable hair cell phenotypes. A full understanding of the function of each myosin gene and protein will improve our knowledge of the normal auditory system. We anticipate that advancing the basic understanding will ultimately improve the patient care and rehabilitation of hearing loss in clinical settings .

Thyroid Hormone and Hearing

Hearing is one of the most sensitive functions controlled by thyroid hormone (TH). Deafness arises if there is insufficient TH available during sensitive periods in the fetal and early neonatal period in both humans and rodents (Trotter, 1960; Deol, 1973; Uziel, 1986). TH is required for the timely coordination of a complex set of differentiation events in the maturing cochlea. The mechanisms that prompt the progression of these developmental events are poorly understood.

Physiology of the hypothalamic-pituitary-thyroid axis

The brain produces thyrotropin-releasing hormone (TRH), which stimulates the thyrotrope cells of the anterior pituitary gland to secrete thyroid-stimulating hormone (TSH) (Fig. 1-2). TSH stimulates the thyroid gland to produce and secrete TH into the blood stream where it is carried to target organs all over the body. The thyroid gland releases two major forms of TH, T4 and T3. T3 is the main active form of hormone, although T4 is more abundant than T3 in the serum. TH is transported through the cell membrane by specific TH transporters. At the target tissue, T3 is generated from T4 by type 2 deiodinase (encoded by the *Dio2* gene) and is inactivated by type 3 deiodinase (encoded by the *Dio3* gene). Thyroid hormone receptors (THR) in the pituitary and hypothalamus sense the levels of thyroid hormone and regulate TRH and TSH production in order to maintain homeostasis. THR in the target organs are ligand-modulated transcription factors that affect expression of many genes.

Animal models for study on hypothyroidism-induced hearing loss

The etiology of hypothyroidism can be classified into two major types according to where the abnormality resides. Primary hypothyroidism is caused by defective thyroid glands, and secondary hypothyroidism is caused by a lack of thyroid gland stimulation because of hypothalamus or pituitary gland dysfunction. Thyroid hormone resistance (RTH), caused by defects in THRs or reduced intracellular availability of activated TH in peripheral tissues, can produce phenotypes similar to those caused by TH deficiencies.

A models have been used to study the pathophysiological mechanism of hypothyroidism-induced hearing loss. Most of these animals exhibit primary hypothyroidism caused by loss of response to pituitary stimulation. *Tshr*$^{hyt/hyt}$ mice have poorly functioning TSH receptors, which influence thyroid gland function (O'Malley et al., 1995; Li et al., 1999). *Pax8*$^{-/-}$ mice have defective development of both the thyroid gland and the otocyst, consistent with the normal expression of this transcription factor in both structures during embryogenesis (Christ et al., 2004). Another approach is to induce hypothyroidism by administering thyrotoxic agents, such as propothiouracil (PTU) or methimidiazole (MMI), that destroy thyroid gland function directly in rats or mice (Uziel et al., 1983; Uziel et al., 1985b; Uziel et al., 1985a; Knipper et al., 2000). Animal models that carry mutations in THRs (*Thrb*$^{-/-}$ mice) exhibit severe hearing impairment, providing a model for human endocrine disorder of RTH (Forrest et al., 1996). Mice lacking

Dio2 enzyme activity (*Dio2*$^{-/-}$ mice) are unable to produce bioactive TH (Ng et al., 2004).

Thesis Review

In my dissertation, I chose to study two secondary hypothyroidism mouse models: *Pou1f1*^{dw} and *Prop1*^{df}. These two strains carry mutations in the pituitary transcription factors *Pou1f1* and *Prop1*, respectively, which cause thyrotropin (TSH) deficiency and secondarily, the absence of TH. Compared to other mouse models of hypothyroidism, *Pou1f1*^{dw} and *Prop1*^{df} mutants have several advantages. 1) The mutant mice are viable and live ~ 40% longer than their normal littermates, while *Pax8*$^{-/-}$ mice die at young age (P21). This makes it impossible to determine whether processes are temporarily affected because developmental delay or permanently disrupted. 2) There is no need for drug treatment to create the TH deficiency, which avoids the potential side effects of thyrotoxic agents. 3) The simple, autosomal recessive inheritance of hypothyroidism simplifies breeding and compared to THR double mutants. 4) The ability to correct the defects by TH replacement makes these mouse models superior to other genetic models.

It is very interesting that despite the same extent of hypothyroidism, *Pou1f1*^{dw} and *Prop1*^{df} mutants exhibit very different degrees of hearing impairment. *Pou1f1*^{dw} mutants are profoundly deaf while *Prop1*^{df} mutants only have a mild hearing loss (Karolyi et al., 2007). Genetic background accounts for the differential hearing losses between these two mouse strains. Thus, *Pou1f1*^{dw}

and *Prop1*^{df} mutants provide invaluable tools to identify the genes and pathways that are the most sensitive to TH regulation in inner ear development.

Chapters 3 to 5 in this dissertation describe my research projects on hypothyroidism-induced deafness. Chapter 3 focuses on the detailed morphological, physiological, and gene expression analyses of *Pou1f1*^{dw} mutants during the course of cochlear development. The processes affected in *Pou1f1*^{dw} mutants, shown in Chapter 3, were examined in *Prop1*^{df} mutants in Chapter 4. Moreover, in Chapter 4, we designed embryo transfer experiments to prove that the fetal genetic backgrounds, but not maternal effects, are the major factors underlying differential hearing impairment in *Pou1f1*^{dw} and *Prop1*^{df} mutants. Further work on identifying a genetic modifier of hypothyroidism-induced deafness was carried out and the progress towards indentifying this modifier is presented in Chapter 5.

Control of TH action by hormone availability in the cochlea

TH activity can be controlled at several steps preceding its regulation on a target gene through binding to THR. Cellular uptake of TH is mediated by various types of transporters including L type amino acid, organic anion and monocarboxylate families (Abe et al., 2002; Friesema et al., 2005; Taylor and Ritchie, 2007). *MCT1* and *MCT2* monocarboxylate transporters were found to be expressed in the inner ear (Okamura et al., 2001). Mutations in *MCT8* are associated with syndromes that include hearing impairment, for example, human X-linked neurological syndrome and Allen-Herndon-Dudley syndrome, with which patients have symptoms as global developmental delay, central hypotonia,

spastic quadriplegia, dystonic movements, rotary nystagmus, and impaired gaze and hearing (Dumitrescu et al., 2004; Verma, 2008). This underscores the importance of TH transport for inner ear function.

Both *Dio2* and *Dio3* are expressed in the cochlea (Campos-Barros et al., 2000; Ng et al., 2009). *Dio2*, is induced in the cochlea before auditory function begins (Campos-Barros et al., 2000). The most pronounced neurological phenotype in *Dio2*$^{-/-}$ mice is deafness, suggesting that this enzyme amplifies local T3 levels to stimulate the onset of hearing (Ng et al., 2004). *Dio3*$^{-/-}$ mice display deafness with premature cochlear differentiation, indicating a protective role for type 3 deiodinase in auditory development (Ng et al., 2009).

The *CRYM* gene encodes mu-crystallin, which is an intracellular, cytosolic T3 binding protein (Suzuki et al., 2007). Human *CRYM* mutations cause nonsyndromic deafness (Abe et al., 2003). One mutation in the *CRYM* gene causes deafness by impairing the ability of the protein to bind T3 (Oshima et al., 2006). Auditory function is normal in *Crym*$^{-/-}$ mice (Suzuki et al., 2007), however, which may reflect the difference in the chain of events that lead to cellular response to TH between humans and mammals.

Deafness genes could be affected by hypothyroidism

The regulation of gene expression by TH is mediated by THR. There are multiple thyroid hormone receptor genes and isoforms. The majority of the isoforms have domains that confer transcriptional activation, DNA binding, ligand binding, and protein dimerization. Thyroid hormone response elements (TRE)

are the DNA fragments that bind THRs directly. Depending on the TRE sequence in any given regulatory element, TH can induce transcriptional activation or repression. The mechanism is that the binding of TH to THR induces a conformational change that converts THR from a transcriptional repressor to an activator or vice versa, dictated by the sequence of the TRE. TH and the TRE regulate the recruitment of co-repressors or co-activators to THRs. Thus, a normal level of TH is necessary to have the proper balance of gene repression and activation.

In order to understand the mechanism whereby TH affects the structural development and physiological function of the inner ear, the genes that are activated and repressed by TH in the cochlea need to be identified. There are already several examples of the genes that are affected by hypothyroidism and are proven to be relevant to genetic forms of deafness (Table 1-2). Here, we give a brief review of these hypothyroidism-related deafness genes.

Tecta **and** ***Tectb*** genes encode α- and β-tectorin, respectively. Both proteins are important components of the tectorial membrane (TM) in the organ of Corti in the cochlea. The TM, a collagen-rich extracellular matrix, makes contact with the tips of the stereocilia of cochlear hair cells. The sound transduced into the inner ear will vibrate the basilar membrane that contains the sensory epithelium against the TM. These vibrations activate mechanoelectrical transduction of the hair cells. Both *Tecta* and *Tectb* mutant mice exhibit moderate-to-severe hearing impairment while the hearing loss in *Tectb*$^{-/-}$ mice is

only evident at low frequencies (< 20 kHz), and *TECTA* mutations are also linked with deafness in humans (Richardson et al., 2008). THRβ mutant mice, *Thrb*$^{-/-}$, have significantly elevated expression levels of α- and β-tectorin and obvious thickening and enlargement of TM (Winter et al., 2009). These results indicate that transcription of *Tecta* and *Tectb* genes may be repressed by TH/THR pathway, and that alterations in *Tecta* and *Tectb* gene expression can influence the composition and morphology of the TM. It is important to note, however, that the functional significance of thyroid hormone dependent alterations in *Tecta* and *Tectb* expression are not clear given the highly pleiotropic effects of thyroid hormone.

Prestin (Slc26A5) is the motor protein of cochlear OHCs and responsible for OHC electromotility and cochlear amplification (Zheng et al., 2000; Liberman et al., 2002). TH appears to regulate the expression and localization of prestin by binding THRβ (Weber et al., 2002; Winter et al., 2006). I show, however, that *Pou1f1*^{dw} mutants, which have a permanent TH deficiency, eventually develop normal prestin expression and subcellular localization despite the persistent absence of TH (Chapter 3). In humans, mutations in prestin are associated with profound deafness (Liu et al., 2003).

Kcnq4 encodes a voltage-dependent potassium channel that is localized to the basolateral membrane of hair cells (Beisel et al., 2000; Rocha-Sanchez et al., 2007). In humans, *KCNQ4* mutations cause non-syndromic, autosomal

dominant deafness, *DFNA2* (Kubisch et al., 1999). A mouse model of *Kcnq4* loss of function has progressive hearing loss and evolving degeneration of OHCs (Kharkovets et al., 2006). *THR*α mutant mice, *Thra*$^{-/-}$, have normal expression of KCNQ4 in the OHC even under conditions of induced hypothyroidism (Winter et al., 2006), which suggests that *Kcnq4* gene expression is regulated by THRα that may repress the transcription.

Kcnma1 encodes the α-subunit of the large Ca^{2+}-activated potassium channels, named BK or maxi-K channels. BK channels are localized at the apical aspect of IHCs, just below the cuticular plate, while BK is concentrated in the basal portion of the OHCs (Hafidi et al., 2005). Hypothyroid animal models have a significant reduction in BK expression in IHCs and OHCs (Brandt et al., 2007; Sendin et al., 2007; Winter et al., 2007). BK expression in the OHCs developed normally even under hypothyroidism induced by MMI treatment in *Thra*$^{-/-}$ mice, which indicates that THRα exerts a repressive action on the expression of BK in OHCs (Winter et al., 2007). *BK*α mutant mice, *BK*$\alpha^{-/-}$, exhibit progressive hearing loss (Ruttiger et al., 2004).

SK2 is calcium-activated, small conductance potassium channel, encoded by the *Kcnn2* gene. SK2 channels are required both for expression of functional acetyl choline receptors (AChRs), and for establishing and/or maintaining efferent terminals in the cochlea (Kong et al., 2008). In *SK2*$^{-/-}$ mice, there is no significant threshold shift on Auditary Brainstem Response (ABR) test, but the

efferent-evoked suppression of Distortion Product of Otoacoustic Emissions (DPOAEs) is absent (Murthy et al., 2009). SK2 expression is reduced in hypothyroid rats but preserved in *Thra*$^{-/-}$ mice (Winter et al., 2007).

Otoferlin (Otof) is thought to be the major calcium sensor and essential for exocytosis at the ribbon synapses at the bases of cochlear hair cell (Roux et al., 2006). Mutations in the human *OTOF* gene cause nonsyndromic, autosomal recessive deafness, *DFNB9* (Mirghomizadeh et al., 2002; Varga et al., 2003). Athyroid *Pax8*$^{-/-}$ mice and methimazole (MMI)-treated hypothyroid rats have significantly reduced or completely absent expression of OTOF (Brandt et al., 2007), which implies that TH regulates OTOF expression, either directly or indirectly.

In conclusion, TH has pleiotropic effects on the development and maintenance of auditory function. TH deficiency causes abnormalities in multiple processes within the inner ear that can contribute to hearing impairment. Uncovering the deafness genes regulated by TH could help us have a better understanding of the development and physiology of normal hearing.

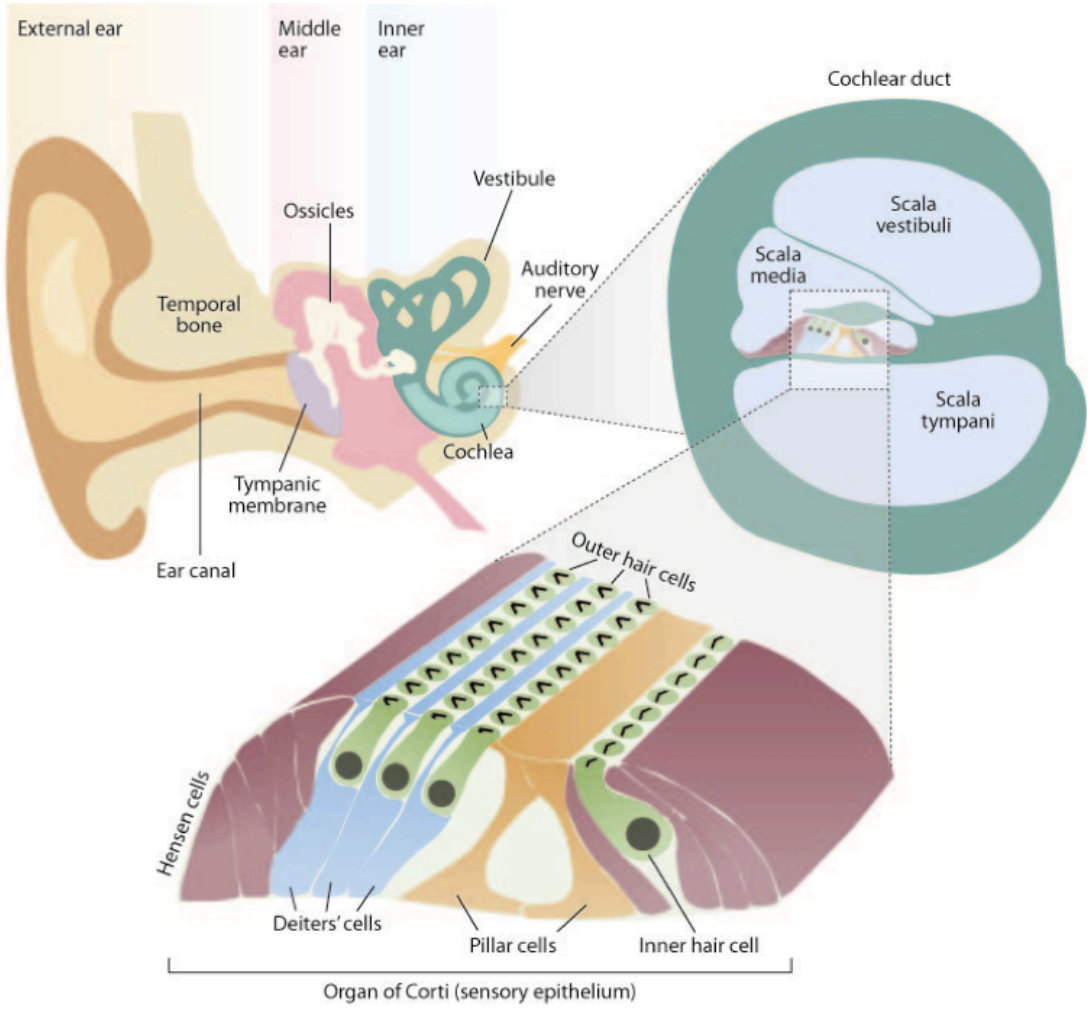

Figure 1-1. Structure of the inner ear. Schematic drawing from Dror AA and Avraham KB, Hearing loss: mechanisms revealed by genetics and cell biology, Annu. Rev. Genet. 43:411-437, 2009.

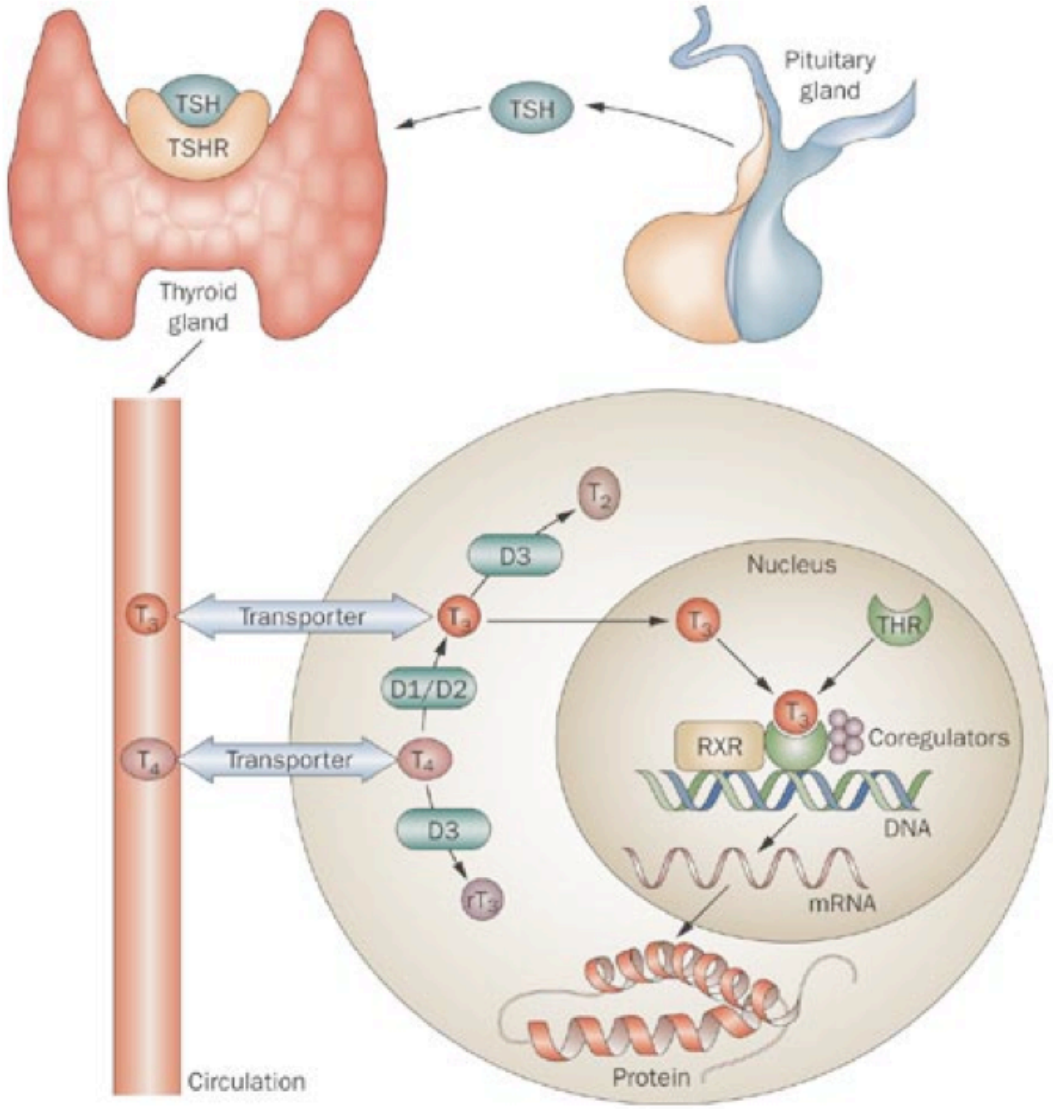

Figure 1-2. Hypothalamic-Pituitary-Thyroid Axis. Picture from Dayan CM and Panicker V, Novel insights into thyroid hormones from the study of common genetic variation, Nature Reviews Endocrinology, 5: 211-218, 2009. D1=deiodinase 1, D2=deiodinase 2, D3=deiodinase 3, rT3=reverse T3, RXR= retinoid X receptor, T2=di-iodothyronine, THR=thyroid hormone receptor, TSHR=TSH receptor.

Table 1-1. Unconventional myosins and deafness in mouse and human				
	Mouse		Human	
Gene	**mutants**	**features**	**types**	**features**
MYO1	*Myo1c*^{Y61G}	Inhibited fast and slow adaptation	*DFNA48* (MYO1A)	Post-lingual, progressive, moderate-to-severe
MYO3A	N.A.	N.A.	*DFNB30*	Post-lingual, progressive
MYO6	*Snell's Waltzer*	Deafness Vestibular dysfunction Fused stereocilia; abnormal retinal electrophysiology	*DFNA22*	Post-lingual, progressive
			DFNB37	Congenital deafness, other features vary
MYO7A	*shaker 1* (There is a series of *Myo7a* alleles with different stereocilia phenotypes.)	Deafness Vestibular dysfunction Disorganized stereocilia	*DFNA11*	Progressive deafness
			DFNB2	Congenital deafness
			USHER 1B	Deafness and progressive blindness
MYO15	*shaker 2, shaker 2J*	Deafness Vestibular dysfunction Short stereocilia	*DFNB3*	Congenital deafness, vestibular dysfunction

Table 1-2. Deafness genes potentially regulated by TH		
Gene	**Mutant hearing loss**	**Function in the inner ear**
Tecta, Tectb	Moderate to severe	Composition of tectorial membrane
Prestin (*Slc26a5*)	Congenital, profound	OHC molecular motor
KCNQ4	Post-lingual, progressive	Maintain the resting potential of OHCs
BK channel (*Kcnma1, Slo1*)	Progressive	Fast after-hyperpolarization (AHP) following action potentials of OHCs
SK2	No elevation of ABR thresholds, but absent efferent-evoked suppression of DPOAEs	Generating a hyperpolarizing response to efferent stimulation
Otoferlin	Severe to profound	Ca^{2+} sensor, exocytosis

REFERENCES

Abe S, Katagiri T, Saito-Hisaminato A, Usami S, Inoue Y, Tsunoda T, Nakamura Y (2003) Identification of CRYM as a candidate responsible for nonsyndromic deafness, through cDNA microarray analysis of human cochlear and vestibular tissues. Am J Hum Genet 72:73-82.

Abe T, Suzuki T, Unno M, Tokui T, Ito S (2002) Thyroid hormone transporters: recent advances. Trends Endocrinol Metab 13:215-220.

Adato A, Michel V, Kikkawa Y, Reiners J, Alagramam KN, Weil D, Yonekawa H, Wolfrum U, El-Amraoui A, Petit C (2005) Interactions in the network of Usher syndrome type 1 proteins. Hum Mol Genet 14:347-356.

Ahmed ZM, Morell RJ, Riazuddin S, Gropman A, Shaukat S, Ahmad MM, Mohiddin SA, Fananapazir L, Caruso RC, Husnain T, Khan SN, Griffith AJ, Friedman TB, Wilcox ER (2003) Mutations of MYO6 are associated with recessive deafness, DFNB37. Am J Hum Genet 72:1315-1322.

Anderson DW, Probst FJ, Belyantseva IA, Fridell RA, Beyer L, Martin DM, Wu D, Kachar B, Friedman TB, Raphael Y, Camper SA (2000) The motor and tail regions of myosin XV are critical for normal structure and function of auditory and vestibular hair cells. Hum Mol Genet 9:1729-1738.

Avraham KB, Hasson T, Steel KP, Kingsley DM, Russell LB, Mooseker MS, Copeland NG, Jenkins NA (1995) The mouse Snell's waltzer deafness gene encodes an unconventional myosin required for structural integrity of inner ear hair cells. Nat Genet 11:369-375.

Beisel KW, Nelson NC, Delimont DC, Fritzsch B (2000) Longitudinal gradients of KCNQ4 expression in spiral ganglion and cochlear hair cells correlate with progressive hearing loss in DFNA2. Brain Res Mol Brain Res 82:137-149.

Belyantseva IA, Boger ET, Friedman TB (2003) Myosin XVa localizes to the tips of inner ear sensory cell stereocilia and is essential for staircase formation of the hair bundle. Proc Natl Acad Sci U S A 100:13958-13963.

Berg JS, Powell BC, Cheney RE (2001) A millennial myosin census. Mol Biol Cell 12:780-794.

Beurg M, Fettiplace R, Nam JH, Ricci AJ (2009) Localization of inner hair cell mechanotransducer channels using high-speed calcium imaging. Nat Neurosci 12:553-558.

Boeda B, El-Amraoui A, Bahloul A, Goodyear R, Daviet L, Blanchard S, Perfettini I, Fath KR, Shorte S, Reiners J, Houdusse A, Legrain P, Wolfrum U, Richardson G, Petit C (2002) Myosin VIIa, harmonin and cadherin 23, three Usher I gene products that cooperate to shape the sensory hair cell bundle. EMBO J 21:6689-6699.

Brandt N, Kuhn S, Munkner S, Braig C, Winter H, Blin N, Vonthein R, Knipper M, Engel J (2007) Thyroid hormone deficiency affects postnatal spiking activity and expression of Ca2+ and K+ channels in rodent inner hair cells. J Neurosci 27:3174-3186.

Campos-Barros A, Amma LL, Faris JS, Shailam R, Kelley MW, Forrest D (2000) Type 2 iodothyronine deiodinase expression in the cochlea before the onset of hearing. Proc Natl Acad Sci U S A 97:1287-1292.

Chen ZY, Corey DP (2002) Understanding inner ear development with gene expression profiling. J Neurobiol 53:276-285.

Christ S, Biebel UW, Hoidis S, Friedrichsen S, Bauer K, Smolders JW (2004) Hearing loss in athyroid pax8 knockout mice and effects of thyroxine substitution. Audiol Neurootol 9:88-106.

Deol MS (1973) An experimental approach to the understanding and treatment of hereditary syndromes with congenital deafness and hypothyroidism. J Med Genet 10:235-242.

Donaudy F, Ferrara A, Esposito L, Hertzano R, Ben-David O, Bell RE, Melchionda S, Zelante L, Avraham KB, Gasparini P (2003) Multiple mutations of MYO1A, a cochlear-expressed gene, in sensorineural hearing loss. Am J Hum Genet 72:1571-1577.

Dumitrescu AM, Liao XH, Best TB, Brockmann K, Refetoff S (2004) A novel syndrome combining thyroid and neurological abnormalities is associated with mutations in a monocarboxylate transporter gene. Am J Hum Genet 74:168-175.

Dumont RA, Zhao YD, Holt JR, Bahler M, Gillespie PG (2002) Myosin-I isozymes in neonatal rodent auditory and vestibular epithelia. J Assoc Res Otolaryngol 3:375-389.

Evangelista M, Klebl BM, Tong AH, Webb BA, Leeuw T, Leberer E, Whiteway M, Thomas DY, Boone C (2000) A role for myosin-I in actin assembly through interactions with Vrp1p, Bee1p, and the Arp2/3 complex. J Cell Biol 148:353-362.

Forrest D, Erway LC, Ng L, Altschuler R, Curran T (1996) Thyroid hormone receptor beta is essential for development of auditory function. Nat Genet 13:354-357.

Friesema EC, Jansen J, Milici C, Visser TJ (2005) Thyroid hormone transporters. Vitam Horm 70:137-167.

Garcia JA, Yee AG, Gillespie PG, Corey DP (1998) Localization of myosin-Ibeta near both ends of tip links in frog saccular hair cells. J Neurosci 18:8637-8647.

Gibson F, Walsh J, Mburu P, Varela A, Brown KA, Antonio M, Beisel KW, Steel KP, Brown SD (1995) A type VII myosin encoded by the mouse deafness gene shaker-1. Nature 374:62-64.

Gillespie PG (2004) Myosin I and adaptation of mechanical transduction by the inner ear. Philos Trans R Soc Lond B Biol Sci 359:1945-1951.

Guilford P, Ayadi H, Blanchard S, Chaib H, Le Paslier D, Weissenbach J, Drira M, Petit C (1994) A human gene responsible for neurosensory, non-syndromic recessive deafness is a candidate homologue of the mouse sh-1 gene. Hum Mol Genet 3:989-993.

Hafidi A, Beurg M, Dulon D (2005) Localization and developmental expression of BK channels in mammalian cochlear hair cells. Neuroscience 130:475-484.

Hasson T, Heintzelman MB, Santos-Sacchi J, Corey DP, Mooseker MS (1995) Expression in cochlea and retina of myosin VIIa, the gene product

defective in Usher syndrome type 1B. Proc Natl Acad Sci U S A 92:9815-9819.
Hasson T, Gillespie PG, Garcia JA, MacDonald RB, Zhao Y, Yee AG, Mooseker MS, Corey DP (1997) Unconventional myosins in inner-ear sensory epithelia. J Cell Biol 137:1287-1307.
Karolyi IJ, Dootz GA, Halsey K, Beyer L, Probst FJ, Johnson KR, Parlow AF, Raphael Y, Dolan DF, Camper SA (2007) Dietary thyroid hormone replacement ameliorates hearing deficits in hypothyroid mice. Mamm Genome 18:596-608.
Kharkovets T, Dedek K, Maier H, Schweizer M, Khimich D, Nouvian R, Vardanyan V, Leuwer R, Moser T, Jentsch TJ (2006) Mice with altered KCNQ4 K+ channels implicate sensory outer hair cells in human progressive deafness. EMBO J 25:642-652.
Knipper M, Zinn C, Maier H, Praetorius M, Rohbock K, Kopschall I, Zimmermann U (2000) Thyroid hormone deficiency before the onset of hearing causes irreversible damage to peripheral and central auditory systems. J Neurophysiol 83:3101-3112.
Kong JH, Adelman JP, Fuchs PA (2008) Expression of the SK2 calcium-activated potassium channel is required for cholinergic function in mouse cochlear hair cells. J Physiol 586:5471-5485.
Kubisch C, Schroeder BC, Friedrich T, Lutjohann B, El-Amraoui A, Marlin S, Petit C, Jentsch TJ (1999) KCNQ4, a novel potassium channel expressed in sensory outer hair cells, is mutated in dominant deafness. Cell 96:437-446.
Lechler T, Shevchenko A, Li R (2000) Direct involvement of yeast type I myosins in Cdc42-dependent actin polymerization. J Cell Biol 148:363-373.
Lee WL, Bezanilla M, Pollard TD (2000) Fission yeast myosin-I, Myo1p, stimulates actin assembly by Arp2/3 complex and shares functions with WASp. J Cell Biol 151:789-800.
Li D, Henley CM, O'Malley BW, Jr. (1999) Distortion product otoacoustic emissions and outer hair cell defects in the hyt/hyt mutant mouse. Hear Res 138:65-72.
Li HS, Porter JA, Montell C (1998) Requirement for the NINAC kinase/myosin for stable termination of the visual cascade. J Neurosci 18:9601-9606.
Liang Y et al. (1998) Genetic mapping refines DFNB3 to 17p11.2, suggests multiple alleles of DFNB3, and supports homology to the mouse model shaker-2. Am J Hum Genet 62:904-915.
Liberman MC, Gao J, He DZ, Wu X, Jia S, Zuo J (2002) Prestin is required for electromotility of the outer hair cell and for the cochlear amplifier. Nature 419:300-304.
Liu XZ, Walsh J, Tamagawa Y, Kitamura K, Nishizawa M, Steel KP, Brown SD (1997a) Autosomal dominant non-syndromic deafness caused by a mutation in the myosin VIIA gene. Nat Genet 17:268-269.
Liu XZ, Walsh J, Mburu P, Kendrick-Jones J, Cope MJ, Steel KP, Brown SD (1997b) Mutations in the myosin VIIA gene cause non-syndromic recessive deafness. Nat Genet 16:188-190.

Liu XZ, Ouyang XM, Xia XJ, Zheng J, Pandya A, Li F, Du LL, Welch KO, Petit C, Smith RJ, Webb BT, Yan D, Arnos KS, Corey D, Dallos P, Nance WE, Chen ZY (2003) Prestin, a cochlear motor protein, is defective in non-syndromic hearing loss. Hum Mol Genet 12:1155-1162.

Melchionda S, Ahituv N, Bisceglia L, Sobe T, Glaser F, Rabionet R, Arbones ML, Notarangelo A, Di Iorio E, Carella M, Zelante L, Estivill X, Avraham KB, Gasparini P (2001) MYO6, the human homologue of the gene responsible for deafness in Snell's waltzer mice, is mutated in autosomal dominant nonsyndromic hearing loss. Am J Hum Genet 69:635-640.

Mermall V, Post PL, Mooseker MS (1998) Unconventional myosins in cell movement, membrane traffic, and signal transduction. Science 279:527-533.

Mirghomizadeh F, Pfister M, Apaydin F, Petit C, Kupka S, Pusch CM, Zenner HP, Blin N (2002) Substitutions in the conserved C2C domain of otoferlin cause DFNB9, a form of nonsyndromic autosomal recessive deafness. Neurobiol Dis 10:157-164.

Murthy V, Maison SF, Taranda J, Haque N, Bond CT, Elgoyhen AB, Adelman JP, Liberman MC, Vetter DE (2009) SK2 channels are required for function and long-term survival of efferent synapses on mammalian outer hair cells. Mol Cell Neurosci 40:39-49.

Nal N, Ahmed ZM, Erkal E, Alper OM, Luleci G, Dinc O, Waryah AM, Ain Q, Tasneem S, Husnain T, Chattaraj P, Riazuddin S, Boger E, Ghosh M, Kabra M, Morell RJ, Friedman TB (2007) Mutational spectrum of MYO15A: the large N-terminal extension of myosin XVA is required for hearing. Hum Mutat 28:1014-1019.

Ng KP, Kambara T, Matsuura M, Burke M, Ikebe M (1996) Identification of myosin III as a protein kinase. Biochemistry 35:9392-9399.

Ng L, Hernandez A, He W, Ren T, Srinivas M, Ma M, Galton VA, St Germain DL, Forrest D (2009) A protective role for type 3 deiodinase, a thyroid hormone-inactivating enzyme, in cochlear development and auditory function. Endocrinology 150:1952-1960.

Ng L, Goodyear RJ, Woods CA, Schneider MJ, Diamond E, Richardson GP, Kelley MW, Germain DL, Galton VA, Forrest D (2004) Hearing loss and retarded cochlear development in mice lacking type 2 iodothyronine deiodinase. Proc Natl Acad Sci U S A 101:3474-3479.

O'Malley BW, Jr., Li D, Turner DS (1995) Hearing loss and cochlear abnormalities in the congenital hypothyroid (hyt/hyt) mouse. Hear Res 88:181-189.

Okamura H, Spicer SS, Schulte BA (2001) Developmental expression of monocarboxylate transporter in the gerbil inner ear. Neuroscience 107:499-505.

Oshima A, Suzuki S, Takumi Y, Hashizume K, Abe S, Usami S (2006) CRYM mutations cause deafness through thyroid hormone binding properties in the fibrocytes of the cochlea. J Med Genet 43:e25.

Peng AW, Belyantseva IA, Hsu PD, Friedman TB, Heller S (2009) Twinfilin 2 regulates actin filament lengths in cochlear stereocilia. J Neurosci 29:15083-15088.

Porter JA, Montell C (1993) Distinct roles of the Drosophila ninaC kinase and myosin domains revealed by systematic mutagenesis. J Cell Biol 122:601-612.

Probst FJ, Fridell RA, Raphael Y, Saunders TL, Wang A, Liang Y, Morell RJ, Touchman JW, Lyons RH, Noben-Trauth K, Friedman TB, Camper SA (1998) Correction of deafness in shaker-2 mice by an unconventional myosin in a BAC transgene. Science 280:1444-1447.

Richardson GP, Lukashkin AN, Russell IJ (2008) The tectorial membrane: one slice of a complex cochlear sandwich. Curr Opin Otolaryngol Head Neck Surg 16:458-464.

Rocha-Sanchez SM, Morris KA, Kachar B, Nichols D, Fritzsch B, Beisel KW (2007) Developmental expression of Kcnq4 in vestibular neurons and neurosensory epithelia. Brain Res 1139:117-125.

Roux I, Hosie S, Johnson SL, Bahloul A, Cayet N, Nouaille S, Kros CJ, Petit C, Safieddine S (2009) Myosin VI is required for the proper maturation and function of inner hair cell ribbon synapses. Hum Mol Genet 18:4615-4628.

Roux I, Safieddine S, Nouvian R, Grati M, Simmler MC, Bahloul A, Perfettini I, Le Gall M, Rostaing P, Hamard G, Triller A, Avan P, Moser T, Petit C (2006) Otoferlin, defective in a human deafness form, is essential for exocytosis at the auditory ribbon synapse. Cell 127:277-289.

Ruttiger L, Sausbier M, Zimmermann U, Winter H, Braig C, Engel J, Knirsch M, Arntz C, Langer P, Hirt B, Muller M, Kopschall I, Pfister M, Munkner S, Rohbock K, Pfaff I, Rusch A, Ruth P, Knipper M (2004) Deletion of the Ca2+-activated potassium (BK) alpha-subunit but not the BKbeta1-subunit leads to progressive hearing loss. Proc Natl Acad Sci U S A 101:12922-12927.

Rzadzinska AK, Nevalainen EM, Prosser HM, Lappalainen P, Steel KP (2009) MyosinVIIa interacts with Twinfilin-2 at the tips of mechanosensory stereocilia in the inner ear. PLoS One 4:e7097.

Salles FT, Merritt RC, Jr., Manor U, Dougherty GW, Sousa AD, Moore JE, Yengo CM, Dose AC, Kachar B (2009) Myosin IIIa boosts elongation of stereocilia by transporting espin 1 to the plus ends of actin filaments. Nat Cell Biol 11:443-450.

Schneider ME, Dose AC, Salles FT, Chang W, Erickson FL, Burnside B, Kachar B (2006) A new compartment at stereocilia tips defined by spatial and temporal patterns of myosin IIIa expression. J Neurosci 26:10243-10252.

Sekerkova G, Zheng L, Mugnaini E, Bartles JR (2006) Differential expression of espin isoforms during epithelial morphogenesis, stereociliogenesis and postnatal maturation in the developing inner ear. Dev Biol 291:83-95.

Self T, Sobe T, Copeland NG, Jenkins NA, Avraham KB, Steel KP (1999) Role of myosin VI in the differentiation of cochlear hair cells. Dev Biol 214:331-341.

Sendin G, Bulankina AV, Riedel D, Moser T (2007) Maturation of ribbon synapses in hair cells is driven by thyroid hormone. J Neurosci 27:3163-3173.

Senften M, Schwander M, Kazmierczak P, Lillo C, Shin JB, Hasson T, Geleoc GS, Gillespie PG, Williams D, Holt JR, Muller U (2006) Physical and functional interaction between protocadherin 15 and myosin VIIa in mechanosensory hair cells. J Neurosci 26:2060-2071.

Stauffer EA, Scarborough JD, Hirono M, Miller ED, Shah K, Mercer JA, Holt JR, Gillespie PG (2005) Fast adaptation in vestibular hair cells requires myosin-1c activity. Neuron 47:541-553.

Suzuki S, Suzuki N, Mori J, Oshima A, Usami S, Hashizume K (2007) micro-Crystallin as an intracellular 3,5,3'-triiodothyronine holder in vivo. Mol Endocrinol 21:885-894.

Tamagawa Y, Kitamura K, Ishida T, Ishikawa K, Tanaka H, Tsuji S, Nishizawa M (1996) A gene for a dominant form of non-syndromic sensorineural deafness (DFNA11) maps within the region containing the DFNB2 recessive deafness gene. Hum Mol Genet 5:849-852.

Taylor PM, Ritchie JW (2007) Tissue uptake of thyroid hormone by amino acid transporters. Best Pract Res Clin Endocrinol Metab 21:237-251.

Trotter WR (1960) The association of deafness with thyroid dysfunction. Br Med Bull 16:92-98.

Uziel A (1986) Periods of sensitivity to thyroid hormone during the development of the organ of Corti. Acta Otolaryngol Suppl 429:23-27.

Uziel A, Marot M, Rabie A (1985a) Corrective effects of thyroxine on cochlear abnormalities induced by congenital hypothyroidism in the rat. II. Electrophysiological study. Brain Res 351:123-127.

Uziel A, Legrand C, Rabie A (1985b) Corrective effects of thyroxine on cochlear abnormalities induced by congenital hypothyroidism in the rat. I. Morphological study. Brain Res 351:111-122.

Uziel A, Pujol R, Legrand C, Legrand J (1983) Cochlear synaptogenesis in the hypothyroid rat. Brain Res 283:295-301.

Varga R, Kelley PM, Keats BJ, Starr A, Leal SM, Cohn E, Kimberling WJ (2003) Non-syndromic recessive auditory neuropathy is the result of mutations in the otoferlin (OTOF) gene. J Med Genet 40:45-50.

Verma S (2008) Allan-Herndon-Dudley syndrome. Indian J Pediatr 75:402-404.

Walsh T, Walsh V, Vreugde S, Hertzano R, Shahin H, Haika S, Lee MK, Kanaan M, King MC, Avraham KB (2002) From flies' eyes to our ears: mutations in a human class III myosin cause progressive nonsyndromic hearing loss DFNB30. Proc Natl Acad Sci U S A 99:7518-7523.

Weber T, Zimmermann U, Winter H, Mack A, Kopschall I, Rohbock K, Zenner HP, Knipper M (2002) Thyroid hormone is a critical determinant for the regulation of the cochlear motor protein prestin. Proc Natl Acad Sci U S A 99:2901-2906.

Weil D, Kussel P, Blanchard S, Levy G, Levi-Acobas F, Drira M, Ayadi H, Petit C (1997) The autosomal recessive isolated deafness, DFNB2, and the

Usher 1B syndrome are allelic defects of the myosin-VIIA gene. Nat Genet 16:191-193.
Weil D, Blanchard S, Kaplan J, Guilford P, Gibson F, Walsh J, Mburu P, Varela A, Levilliers J, Weston MD, et al. (1995) Defective myosin VIIA gene responsible for Usher syndrome type 1B. Nature 374:60-61.
Winter H, Braig C, Zimmermann U, Engel J, Rohbock K, Knipper M (2007) Thyroid hormone receptor alpha1 is a critical regulator for the expression of ion channels during final differentiation of outer hair cells. Histochem Cell Biol 128:65-75.
Winter H, Braig C, Zimmermann U, Geisler HS, Franzer JT, Weber T, Ley M, Engel J, Knirsch M, Bauer K, Christ S, Walsh EJ, McGee J, Kopschall I, Rohbock K, Knipper M (2006) Thyroid hormone receptors TRalpha1 and TRbeta differentially regulate gene expression of Kcnq4 and prestin during final differentiation of outer hair cells. J Cell Sci 119:2975-2984.
Winter H, Ruttiger L, Muller M, Kuhn S, Brandt N, Zimmermann U, Hirt B, Bress A, Sausbier M, Conscience A, Flamant F, Tian Y, Zuo J, Pfister M, Ruth P, Lowenheim H, Samarut J, Engel J, Knipper M (2009) Deafness in TRbeta mutants is caused by malformation of the tectorial membrane. J Neurosci 29:2581-2587.
Yin H, Pruyne D, Huffaker TC, Bretscher A (2000) Myosin V orientates the mitotic spindle in yeast. Nature 406:1013-1015.
Zheng J, Shen W, He DZ, Long KB, Madison LD, Dallos P (2000) Prestin is the motor protein of cochlear outer hair cells. Nature 405:149-155.

CHAPTER 2

Proline-rich domain of MYO15 is necessary for hearing and stereocilia maintenance

ABSTRACT

Mutations in the unconventional myosin *Myo15* are responsible for profound congenital deafness and vestibular dysfunction in *shaker 2* (*sh2*) and *shaker 2J* (*sh2J*) mice (Probst et al., 1998; Anderson et al., 2000). The *sh2* mutation is thought to inactivate the motor, while the *sh2J* deletion is expected to produce a protein lacking the C-terminal PDZ ligand domain that is important for binding WHIRLIN (WHRN) and transporting it to the tips of the stereocilia, which is required for normal elongation of the stereocilia. Stereocilia are abnormally short in *sh2*, *sh2J* and *Whrn* mutants, and WHRN transport is defective in both the *sh2* and *sh2J* mutants. Mutations in the human ortholog, *MYO15*, cause deafness, *DFNB3* (Wang et al., 1998). Alternatively spliced *MYO15* transcripts predict multiple isoforms of MYO15 (Liang et al., 1999). The presence or absence of a large evolutionarily conserved proline-rich region N-terminal to the motor domain of MYO15 is dictated by inclusion or exclusion of exon 2, and lesions in exon 2

* I was the lead person for all aspects of this project, from experimental design to analysis, and writing the chapter.

cause deafness in humans (Nal et al., 2007). Elegant studies in cochlear explants demonstrated that isoforms lacking the proline rich domain are sufficient to rescue stereocilia elongation and WHRN transport (Belyantseva et al., 2005). To test whether the proline-rich region has a distinct function, we generated a mouse model that recapitulates a human nonsense mutation in the proline-rich domain using knock-in technology. These knock-in mutants have profound deafness, but they differ from *sh2* and *sh2J* mice in hair bundle morphology and the absence of circling behavior. Vestibular evoked response tests are consistent with subtle vestibular abnormalities. Cochlear stereocilia initially appear normally elongated with WHRN localized at the tips, but the stereocilia are not maintained, implicating the proline-rich region in preserving the hair bundle. Classic genetic analysis of compound heterozygous mice containing different combinations of *Myo15* mutant alleles revealed no evidence of allelic complementation for hearing or hair bundle maintenance, consistent with the functional importance of full length MYO15 isoforms containing the proline-rich domain for normal mammalian hearing. This new, isoform-specific *Myo15* mutant mouse demonstrates a unique function for the proline-rich domain that is more critical for auditory function than for vestibular function.

INTRODUCTION

Myosin XV (MYO15) is an unconventional myosin protein specifically expressed in the inner ear, pituitary gland, and selected cell types in other endocrine organs (Liang et al., 1999; Lloyd et al., 2001). Mutations in *Myo15* are

responsible for profound congenital deafness and vestibular dysfunction in two spontaneous mouse mutants: *shaker 2* (*sh2*) and *shaker 2J* (*sh2J*), and in humans with *DFNB3* (Liang et al., 1999). There is no evidence to date for endocrine organ dysfunctions associated with MYO15 mutations. MYO15 localizes at the tips of stereocilia in both auditory and vestibular sensory cells (Belyantseva et al., 2003), and MYO15 is required for the elongation of stereocilia of both cell types during inner ear development (Belyantseva et al., 2005). Both *sh2* and *sh2J* mice have very short stereocilia (Anderson et al., 2000). The *sh2* mutation is thought to inactivate the motor, while the *sh2J* deletion is expected to produce a protein lacking the C-terminal PDZ ligand domain that is important for binding WHIRLIN (WHRN) and transporting it to the tips of the stereocilia (Belyantseva et al., 2005). *Whirlin* mutants have short stereocilia similar to those in *sh2* and *sh2J* mutants (Anderson et al., 2000; Mustapha et al., 2007).

Multiple isoforms of MYO15 are predicted by alternatively spliced transcripts (Liang et al., 1999). Inclusion of exon 26 in the *Myo15* transcript predicts truncation of the protein following the IQ motifs (the regulatory domain of the myosin that binds to myosin light chains), which would eliminate over 1400 amino acids of the tail, including domains of myosin tail homology, FERM, PDZ, and SH3 (Liang et al., 1999). The presence or absence of a large proline-rich region N-terminal to the motor domain of MYO15 is dictated by inclusion or exclusion of exon 2 (Fig. 2-1). For simplicity, we use P to represent the proline-rich domain, M for the motor domain and T for the tail domains of MYO15. Thus, MYO15

isoforms PMT, PM and MT refer to the full-length isoform with all domains, short isoform with only proline-rich domain plus motor domain and short isoforms with only motor plus tail domains, respectively (Fig. 2-1).

The 1223 amino acid N-terminal proline-rich domain is about one third of the full length MYO15 and mostly encoded by the unusually large exon 2 of *Myo15* gene (Liang et al., 1999). The proline-rich domain is evolutionarily conserved, and the function is unknown, although proline-rich motifs are often involved in binding proteins with SH3 domains (Holt and Koffer, 2001). The mutations, *E1105X* and *G1112fsX1124*, are located in exon 2 and cause deafness in two human families (Nal et al., 2007). The degree of hearing loss among the affected family members ranged from severe to profound. Both mutations predict the loss of full-length MYO15 proteins, while maintaining isoforms produced from transcripts without exon 2. This suggests that isoforms of MYO15 containing the proline-rich domain (PMT and/or PM) are critical for normal hearing.

The MYO15 isoform MT, which lacks the N-terminal proline-rich domain, is sufficient to rescue the short stereocilia defect in *sh2* mutant cochlea explants (Belyantseva et al., 2005). Hair cells transfected by the gene gun exhibited stereocilia elongation and transportation of WHRN to the tips. This suggests that the proline-rich domain of MYO15 may not be necessary for grossly normal stereocilia morphology or WHRN transportation. Yet the proline-rich domain may be required for other more specific aspects of stereocilia morphology or hearing function based on the fact that mutations within exon 2 are associated with hearing impairment in human patients.

We hypothesize that the N-terminal proline-rich region of MYO15 has a distinct function different from that of the motor and tail domains of MYO15 protein for hearing. To test this hypothesis, we generated isoform-specific antibodies for MYO15 and a mouse model that recapitulates a human nonsense mutation in the proline-rich domain using knock-in technology. In normal mice, MYO15 isoforms bearing the proline rich region are enriched in the short stereocilia rows, while isoforms bearing only the motor and tail regions are predominate in the longest stereocilia rows. The *Myo15* knock-in mutants exhibit profound deafness, but differ from *sh2* and *sh2J* mice in the absence of circling behavior and the characters of hair bundle pathology. Cochlear stereocilia in *Myo15* knock-in mutants appear to be normally elongated initially, but the sereocilia are not maintained, implicating the proline-rich region in structural preservation. Classic genetic analysis of compound heterozygous mice containing different combinations of *Myo15* mutant alleles revealed no allelic complementation, consistent with the functional importance of a full length MYO15 isoform containing the proline-rich domain for normal mammalian hearing.

MATERIALS & METHODS

Generation of *Myo15*$^{E1086X/E1086X}$ Mice

The position equivalent to human *E1105X* in the mouse is *E1086X.* Fig. 2-2A shows the scheme of the gene-targeting strategy to generate a mouse model of the human *E1105X* mutation *Myo15* gene. Briefly, two homologous

combination arms containing the genomic sequences of exon 2 (5' arm) and exon 3 to exon 7 (3' arm) of *Myo15* were amplified by PCR using 129X1/SvJ genomic DNAs as the template. The GAG to TAA mutation of amino acid 1086, which creates a new cutting site of restrictive enzyme MseI, was introduced into 5' arm by using QuickChange II XL Site-Directed Mutagenesis Kit from Stratagene. The two arms were inserted into the plasmid vector pflox (Chui et al., 1997), which was previously modified by removing the HSVtk cassette. All constructs were sequenced. We screened 480 R1 ES cells resistant to neomycin for homologous recombination and monoinsertion events by Southern blot analysis (Fig. 2-2 B)(Nagy et al., 1993). Two clones were injected into C57BL/6J blastocysts to create chimeric animals. Male chimeras were mated with C57BL/6 females. Germline transmission of the mutant *Myo15* allele was detected from two independent ES clones by PCR amplification of a fragment in the NEO cassette in agouti pups. Positive F1 progeny were crossed with EIIA–Cre mice (Lakso et al., 1996). F2 animals carrying an allele in which the neomycin-resistant selection cassette was deleted were detected by PCR (primers 5'-CCACAGTCTGAGGACCGAGT-3' and 5' GGTCTTGGTCTGGATGCTCT-3') and MseI digestion. The wild type allele generates 445 bp and 30 bp products and $Myo15^{E1086X}$ allele generates 324 bp, 121 bp and 30 bp products (Fig. 2-2 C). The heterozygous animals were intercrossed to generate $Myo15^{E1086X/E1086X}$, $Myo15^{+/E1086X}$ and $Myo15^{+/+}$ mice. For simplicity, *ΔP* is used to refer to *E1086X* mutation in this article.

Mice

Shaker 2, *shaker 2J*, and C57BL/6J mice were obtained from the Jackson Laboratory (Bar Harbor, ME, USA). All procedures were approved by the University of Michigan Committee on Use and Care of Animals. The *Myo15*$^{\Delta P/\Delta P}$ mice were bred to *Myo15*$^{+/sh2J}$ mice to generate *Myo15*$^{\Delta P/sh2J}$ F1 progeny mice. At least three animals of each genotype were analyzed at each age. P0 is designated as the day of birth.

Assessment of Hearing

Auditory brainstem responses (ABRs) and Distortion Product Otoacoustic Emissions (DPOAEs) were recorded and analyzed as described (Karolyi IJ et al., 2007). Five to six animals of each genotype were tested at 4, 20, and 48 kHZ for ABRs and 12, 24, and 48 kHz for DPOAEs.

Scanning Electron Microscopy

Animals were euthanized and temporal bones were removed and fixed with 2.5% glutaraldehyde in 0.1M of sodium cacodylate buffer pH 7.4 with 2mM $CaCl_2$ (Electron Microscopy Sciences, Cat # 15960). Cochleae were processed using the OTOTO method, which involves immersing the tissues alternately in thiocarbohydrazide and osmium tetroxide (Osborne and Comis, 1991). Cochleae were critical point dried and mounted on stubs using colloidal silver paste. Samples were examined with an Amray 1000B SEM or a field-emission SEM (S-4800, Hitachi).

Antibodies

PB888 antisera is a gift from Dr. Thomas Friedman at the NIDCD. It was produced against an epitope in the mouse *Myo15* gene just 5' to the *E1086X* mutation. PB48 antibody was generated in rabbits against an epitope in the tail region of MYO15 (Lloyd et al., 2001). Generation of the WHRN antibody (HL5137) was previously described (Belyantseva et al., 2005).

Immunofluorescence Study

The cochleae were dissected and fixed with 4% paraformaldehyde in PBS for 2 h. The organ of Corti (OC) sensory epithelia were permeabilized in 0.5% Triton X-100 in PBS for 30 min followed by three time 10-min washes in PBS. Nonspecific binding sites were blocked by 5% goat serum and 2% BSA in PBS for 1 h at room temperature. Samples were incubated with primary antibodies (1:200 dilution for PB48, PB888 and HL5137 antibodies) at 4^{o}C for overnight. The next day, samples were rinsed in PBS for several times and incubated with the anti-rabbit TRITC-conjugated secondary antibody (Amersham Pharmacia Biosciences) for 40 min. F-actin was visualized by Alexa 488–phalloidin staining (Invitrogen). Tissues were photographed and analyzed by confocal microscopy with a Zeiss laser scanning microscope LSM-510.

RESULTS

Hearing function is impaired in *Myo15*$^{\Delta P/\Delta P}$ mice

The ABR test was used to measure the hearing levels of *Myo15*$^{\Delta P/\Delta P}$ mice at 2,4, and 6-weeks of age. A representative ABR threshold graph at 20kHz is shown in Fig. 2-3 A. *Myo15*$^{\Delta P/\Delta P}$ mice exhibit 70~80 dB SPL thresholds at 2-weeks old, which represent a severe degree of hearing loss. At 4-weeks old, the ABR thresholds of *Myo15*$^{\Delta P/\Delta P}$ mice are elevated to ~100 dB SPL, and this profound hearing loss level is also detected at 6-weeks of age. Our ABR results of *Myo15*$^{\Delta P/\Delta P}$ mice show that within the first couple weeks after the onset of hearing at 2-weeks old in normal mice, the auditory function of *Myo15*$^{\Delta P/\Delta P}$ mice undergoes progressive degeneration.

To further characterize the hearing impairment in the *Myo15*$^{\Delta P/\Delta P}$ mice, we assessed the outer hair cell (OHC) function by tests of DPOAE. The *Myo15*$^{\Delta P/\Delta P}$ mice demonstrated no DPOAE beyond that of postmortem animals since 2-weeks old. Fig. 2-3 B is the representative DPOAE graphs from 2-weeks and 6-weeks old wild type littermates and mutant animals at a stimulation frequency of 12 kHz. This data indicates that the OHCs in the *Myo15*$^{\Delta P/\Delta P}$ mice are dysfunctional from an early development stage.

MYO15 protein isoforms exhibit differential localization in hair cell stereocilia

The *E1086X* mutation is predicted to produce normal and truncated MYO15 protein isoforms. MYO15 isoforms containing the proline-rich domain (isoforms PMT and PM) will be truncated, but isoforms containing only motor and tail domains (isoform MT) will be retained as intact, normal isoforms. In order to

examine the expression and localization of different MYO15 isoforms in the *Myo15*$^{\Delta P/\Delta P}$ mice, we did immunostaining on a whole-mount preparation of auditory sensory epithelia using antibodies that specifically recognize the proline-rich domain (PB888) or the tail domain (PB48) of MYO15, respectively. The positions of epitopes recognized by these two antibodies are shown in Fig. 2-4 A. PB888 staining of P17 mice reveales MYO15 isoforms containing the proline-rich domain (PMT and PM) localize at the tips of shorter rows of stereocilia in both IHCs and OHCs (Fig. 2-4 B and C, arrow). *Myo15*$^{\Delta P/\Delta P}$ mice have little or no staining with PB888 (Fig. 2-4 D and E). The same staining results were seen in P32 mice (data not shown). This suggests that truncated MYO15 protein isoforms are unstable and/or are diffusely distributed because there is no localization in the stereocilia. In contrast, staining results with the MYO15 tail-specific antibody, PB48, show tail containing isoforms of MYO15 (PMT and MT) in the tips of long and short stereocilia of wild type mice. Only the isoform MT is left in the longest stereocilia of *Myo15*$^{\Delta P/\Delta P}$ mice (Fig. 2-4 F-I, arrowhead). This suggests that the proline-rich domain, encoded by exon 2, is necessary for localization of MYO15 to the shorter stereocilia.

Stereocilia in the cochlear hair cells form normally but degenerate later in *Myo15*$^{\Delta P/\Delta P}$ mice

In *Myo15*$^{sh2/sh2}$ and *Myo15*$^{sh2J/sh2J}$ mice, both IHCs and OHCs exhibit very short lengths of stereocilia (Anderson et al., 2000), which suggests that MYO15 is important for elongation of hair bundles during development. We examined

the stereocilia morphology of *Myo15*$^{\Delta P/\Delta P}$ mice by SEM. Interestingly, we found that the lengths and stair-case pattern of stereocilia are pretty well preserved in both IHCs and OHCs of *Myo15*$^{\Delta P/\Delta P}$ mice at early development ages (Fig. 2-5 B). By P50, however, the shorter rows of stereocilia have degenerated and disappeared, while the longest rows of stereocilia are still normally maintained (Fig. 2-5 E). The degeneration of shorter rows in mutant mice is first observed at about 4 weeks of age, which is also the age that mutant mice exhibited no ABR response to sound (Fig. 2-3 A). Since the MYO15 isoforms PMT and PM are specifically localized at the tips of shorter rows of stereocilia (Fig. 2-4), loss of these isoforms in *Myo15*$^{\Delta P/\Delta P}$ mice may account for the degeneration of stereocilia where they are located.

Normal transportation of WHRN in *Myo15*$^{\Delta P/\Delta P}$ mice

In *Myo15*$^{sh2/sh2}$ and *Myo15*$^{sh2J/sh2J}$ mice, WHRN cannot be transported to the tips of stereocilia because the motor domain and PDZ binding domain at the C-terminus of MYO15 are required (Belyantseva et al., 2005). However, in *Myo15*$^{\Delta P/\Delta P}$ mice, the transportation of WHRN is not affected by the loss of Myo15 isoforms PMT and PM (Fig. 2-6). Because WHRN was not detected at the tips of stereocilia in *sh2* or *sh2J* mice, we conclude that the transportation of WHRN in the stereocilia does not require MYO15 N-terminal proline-rich domain.

***Myo15 E1086X* and *sh2J* alleles cannot complement each other**

Myo15$^{+/\Delta P}$ mice were bred with *Myo15*$^{+/sh2J}$ mice to obtain *Myo15*$^{\Delta P/sh2J}$

offspring, in which only MYO15 isoform MT and isoform PM exist in the hair cells. The ABR test results showed that *Myo15*$^{\Delta P/sh2J}$ mice exhibit ~100 dB SPL threshold at all frequencies tested (Fig. 2-7 A), which means *Myo15 E1086X* and *sh2J* alleles cannot complement on hearing function. The stereocilia morphology of *Myo15*$^{\Delta P/sh2J}$ mice was examined by SEM. We found that the *Myo15*$^{\Delta P/sh2J}$ mice have the similar phenotype of stereocilia as *Myo15*$^{\Delta P/\Delta P}$ mice: hair cell stereocilia form normally but short rows degenerate at late development stage (Fig. 2-7 C, arrows). Our data shows that *Myo15 E1086X* and *sh2J* alleles cannot complement on both hearing function and stereocilia morphology. Therefore, it is necessary for the proline-rich domain of MYO15 protein to be assembled with motor and tail domains together for normal hearing.

DISCUSSION

MYO15 isoforms have different subcellular localizations

It is not unusual for genes expressed in auditory hair cells to produce multiple protein isoforms with different spatial and temporal expression patterns. Examples of such proteins include ion channels (e.g. KCNQ4), scaffold proteins (e.g. Harmonin), and tip link proteins (e.g. Protocadherin15) (Reiners et al., 2005; Ahmed et al., 2006; Xu et al., 2007). Here, we show that MYO15 protein isoforms also have different localizations: isoforms containing the proline-rich domain are mostly at the tips of the short rows of stereocilia, while isoforms with only the motor and tail domains are enriched at the tips of the longest stereocilia. Previous studies with a MYO15 antibody that recognizes the tail domain revealed

that immunoreactivity is scaled to the lengths of stereocilia, with the most robust staining in the longest rows of stereocilia (Rzadzinska et al., 2004). Here, using antibodies that differentially recognize the proline-rich domain and the tail domain of MYO15, we showed in this study that different MYO15 isoforms localize in different stereocilia rows. These observations imply that the distinct subcellular localization of different MYO15 isoforms contributes to the apparent gradient of overall MYO15 protein concentration in the stereocilia. Thus, the phenotypes of the *Myo15*$^{\Delta P/\Delta P}$ mice are unlikely to be caused by reduced dosage of the whole MYO15 protein pool within the cells. Instead, MYO15 isoforms containing the proline-rich domain have specific roles in the maintenance and function of the shorter stereocilia.

The *E1086X* mutation introduces a stop codon into exon 2 of the *Myo15* gene. Quantitative PCR analyses demonstrate that transcripts spliced from exon 2 to exon 3 are present in the similar quantities in normal and mutant mice (data not shown). This reveals that the *Myo15* transcripts containing the mutation do not undergo nonsense-mediated decay. We found no evidence for MYO15 isoforms PMT and PM in the shorter rows of stereocilia in the *Myo15*$^{\Delta P/\Delta P}$ mice, however. Thus, the truncated isoforms PMT and PM are not stable and degraded quickly. Based on immunostaining results, an appropriate amount of isoform MT is still preserved at the tips of longest row of stereocilia. This suggests that the transcription, splicing and translation processes involved in producing this isoform are not affected by the *E1086X* mutation. This provides additional evidence that the phenotypes of *Myo15*$^{\Delta P/\Delta P}$ mice are not likely to be

due to the disruption of the whole MYO15 protein pool, and it also supports the hypothesis that the N-terminal proline-rich domain of MYO15 has distinct function(s) in the cochlear hair cells.

MYO15 isoforms with proline-rich domain are important for maintenance of shorter stereocilia

MYO15 is important for stereocilia elongation and transporting WHRN to the tips of stereocilia (Belyantseva et al., 2005). The *sh2* and *sh2J* mice are unable to localize WHRN at the stereocilia tips and accordingly all rows of stereocilia are very short in these *Myo15* mutants and in *whirler* mutants (Belyantseva et al., 2005; Delprat et al., 2005). Compared to *sh2* and *sh2J* mice, the phenotype of $Myo15^{\Delta P/\Delta P}$ mice is striking; the transportation of WHRN and elongation of stereocilia appears normal initially, but stereocilia degenerate later. This proves that the N-terminal proline-rich domain of Myo15 is not required for transportation of WHRN or stereocilia elongation. This is also consistent with the results of previous experiments that demonstrated correction of stereocilia lengths in *sh2* mutant cochlear explants by introduction of a MYO15 expression construct bearing only motor and tail domains (Belyantseva et al., 2005). The *ex-vivo* nature of the explant experiment, however, made it impossible to test the physiological function of the transfected hair cells. Here, the $Myo15^{\Delta P/\Delta P}$ mouse model proves that without the proline-rich domain of MYO15, normal hearing is not acquired even though the stereocilia reach normal lengths.

We detected the degeneration of shorter rows of stereocilia in young

Myo15$^{\Delta P/\Delta P}$ mice, revealing a functional role for the N-terminal proline-rich domain in maintaining the integrity of hair bundles. This function may be accomplished by interaction between the proline-rich domain of MYO15 and its binding proteins involved in regulation of actin polymerization at the tips of stereocilia. Many proline-rich proteins participate in delivering actin monomers to specific cellular locations where actin-rich membrane protrusions, such as ruffles, filopodia and microspikes, are formed (Holt and Koffer, 2001). A potential interacting protein with proline-rich motifs that regulates actin polymerization is Profilin. There are no reports of mutations in the *profilin* gene causing deafness in both mammals and humans. A couple of examples, however, illustrate the connection of unconventional myosin with actin regulating protein in hair cells. Twinfilin 2 plays a role in the regulation of stereocilia elongation by restricting excessive elongation of the shorter row stereocilia (Peng et al., 2009). This function of Twinfilin 2 is fulfilled by interacting with MYO7A (Rzadzinska et al., 2009). MYO3A and espin, an actin bundling protein, interact directly to boost the elongation of stereocilia (Salles et al., 2009). It is noteworthy that the tips of the shorter stereocilia are the site of mechanoelectrical transduction (MET). It is possible that the turnover and dynamic localization of the actin regulating protein/myosin complex are influenced by interactions between MYO15 and components of the MET machinery, and *vice-versa*.

MYO15 N-terminal proline-rich domain and mechanoelectrotransduction

Mechanically sensitive transducer channels are present only at the bottom of the tip links, not in the tallest row stereocilia, as demonstrated by measuring calcium entry during hair bundle stimulation (Beurg et al., 2009). The co-localization of MET channels and MYO15 proline-rich domain containing isoforms leads us to hypothesize that these MYO15 isoforms are involved in the regulation of MET at the tips of the short rows of stereocilia. The interaction between the proline-rich domain of MYO15 and components of the transduction channel may not be direct, however, and may differ between IHCs and OHCs. In support of this idea, IHCs of *Myo15*$^{sh2/sh2}$ mice have defects in the fast adaptation and calcium sensitivity aspects of MET, though the MET response has a normal amplitude and speed of activation (Stepanyan and Frolenkov, 2009). The OHCs of *Myo15*$^{sh2/sh2}$ mice, however, have normal MET and maintain a very slight staircase structure. Stepanyan and Frolenkov hypothesize that the abnormalities in *Myo15*$^{sh2/sh2}$ IHC function are attributable to the absence of the staircase pattern. Our preliminary data suggests that IHCs of young (P3-P9) *Myo15*$^{\Delta P/\Delta P}$ mice exhibit MET currents in the normal range and fast adaptation (Frolenkov and Indzhykulian, unpublished data). If confirmed, this is consistent with the idea that MET requires the staircase architecture of the hair bundle.

The integrated long isoform of MYO15 is required for normal hearing

Compound heterozygous mice, *Myo15*$^{\Delta P/sh2J}$, have profound hearing impairment and pathology of stereocilia maintenance similar to *Myo15*$^{\Delta P/\Delta P}$ mice. The *Myo15*$^{\Delta P/sh2J}$ mice are expected to have half doses of isoforms PM and MT

in the hair cells. Even though the proline-rich domain and tail domain exist individually coupled to the motor domain within the cells, these proteins cannot execute all the functions necessary for hearing. Thus, normal hearing requires the integrated isoform PMT of MYO15, a single molecule containing all three domains. This indicates the possibility of intramolecular interaction between MYO15 proline-rich domain and tail domain to regulate protein activity.

MYO7A and Diaphanous 1 are examples of hair cell proteins with intermolecular regulation. The tail of *Drosophila* Myo7a can bind to its head-neck domain and inhibits the ATPase activity of the protein (Yang et al., 2009). *Diaphanous 1*, which is mutated in humans with *DFNA1*, is activated by binding of its GBD domain to GTP-Rho, disrupting the intramolecular association between the GBD domain and the tail (Watanabe et al., 1999). Although the importance of these intramolecular interactions for hearing function remains unclear, it is likely that this mechanism is involved in the highly dynamic regulation of hair cell stereocilia. To examine whether there is an autoregulation between the proline-rich domain and other domains within MYO15 protein, biochemical and biophysical assays need to be developed in the future.

In conclusion, we created a novel mouse model, *Myo15*$^{\Delta P/\Delta P}$, that eliminates isoforms with the proline-rich domain of MYO15 protein while preserving other MYO15 isoforms. *Myo15*$^{\Delta P/\Delta P}$ mice are differentiated from *sh2* or *sh2J* mice in vestibular function, hair bundle pathology, and transport of WHRN protein, which indicates that the proline-rich domain of MYO15 plays a

distinct role in the development and maintenance of auditory sensory cells. *Myo15*$^{\Delta P/\Delta P}$ mice will be an invaluable tool for us to understand the function of unconventional myosins in normal hearing.

ACKNOWLEDGEMENTS

I would like to thank Dr. Jonathan Bird and Dr. Thomas B. Friedman at NIDCD for providing the antibodies, Dr. Gregory I. Frolenkov at University of Kentucky for the high resolution SEM examination on hair cell stereocilia, Dr. David F. Dolan at Kresge Hearing Research Institue of the University of Michigan for ABR and DPOAE measurements, and the University of Michigan Transgenic Animal Model Core for ES cell electroporation and blastcysts microinjection steps in generation of the gene-targeted mice.

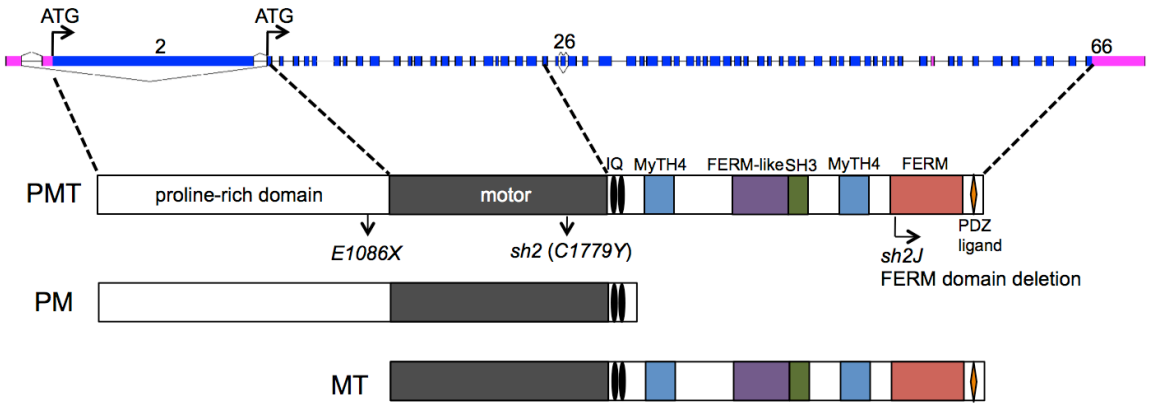

Figure 2-1. *Myo15* gene structure and protein isoforms.
The *Myo15* gene has 66 exons. Exon 2 encodes the proline-rich domain of MYO15. Two translation start sites are located in exon 2 and exon 3, respectively. Alternative splicing of exon 2 results in the inclusion or exclusion of the proline-rich domain in MYO15. Alternative splicing involving exon 26 would produce a protein that is truncated shortly after the IQ motifs. Arrows indicate two spontaneous mouse mutations, *sh2* and *sh2J*, and the induced mutation, *E1086X*, that is discussed in the thesis. Selected MYO15 isoforms are designated as PMT, PM and MT (P=proline-rich domain, M= motor domain, T= tail domain).

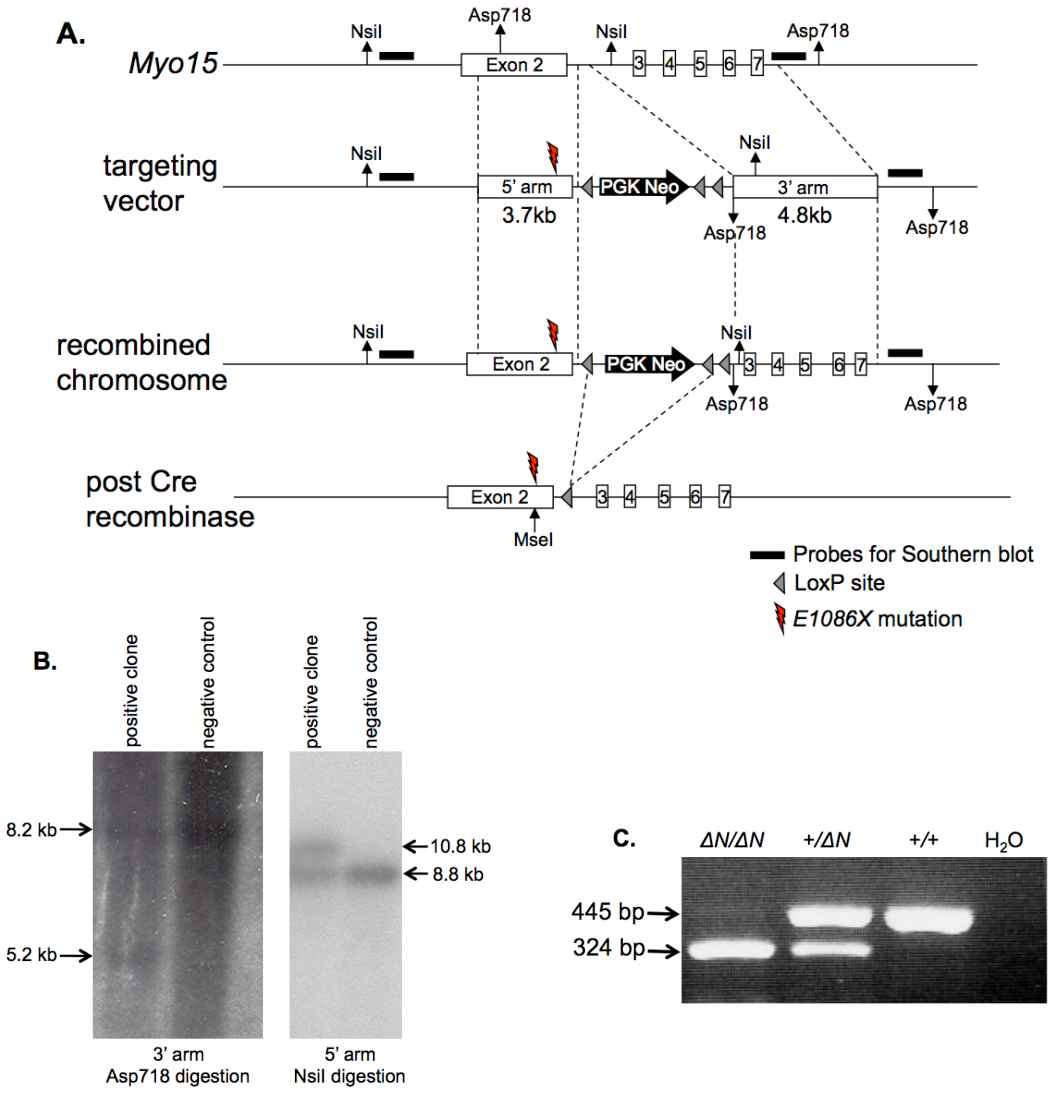

Figure 2-2. Targeted mutation in exon 2 of the *Myo15* gene.
A*,** Maps of *Myo15* wild-type allele, the targeting construct and the resulting mutant alleles, which contain the *E1086X* mutation in exon 2 of *Myo15* gene. The *E1086X* mutation creates a new MseI cutting site. White boxes represent exons, arrowheads indicate loxP sites. The neomycin cassette was secondary removed using Cre recombinase, generating the $Myo15^{E1086X}$ ($Myo15^{\Delta P}$) allele. The two probes used to validate homologous recombination in ES cells by Southern blot analysis are indicated. ***B, Southern blot analysis of Asp718 and NsiI-digested genomic DNA derived from neomycin-resistant ES cell clones as well as negative controls. ***C,*** PCR analysis of wild-type (+/+), heterozygous (*+/ΔP*), and homozygous mutant (*ΔP/ΔP*) mice.

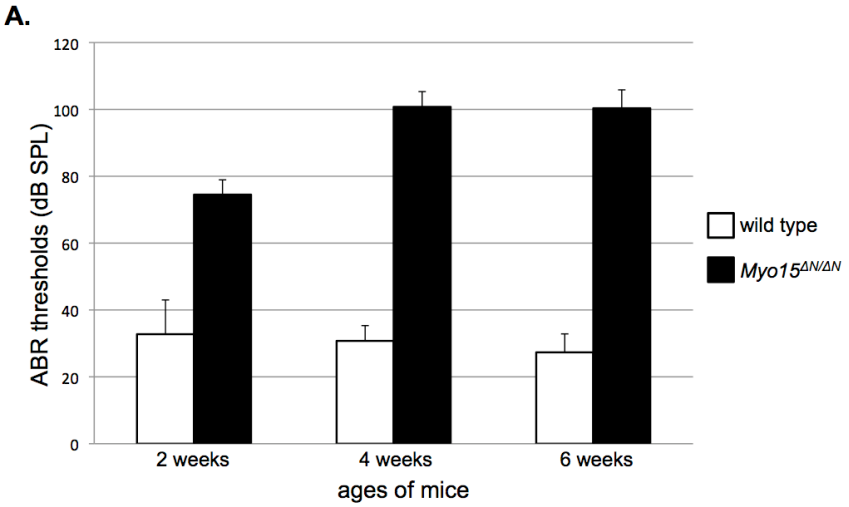
A.
ABR thresholds (dB SPL)
120
100
80
60
40
20
0
2 weeks
4 weeks
6 weeks
ages of mice
wild type
Myo15ΔN/ΔN

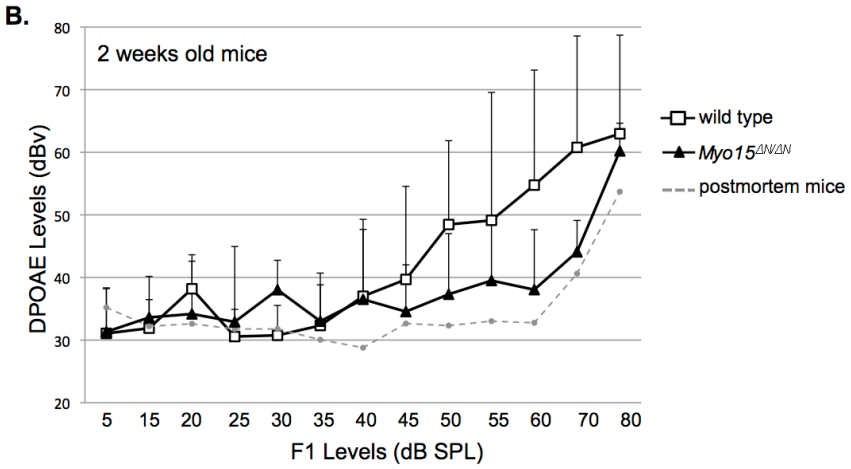
B.
2 weeks old mice
DPOAE Levels (dBv)
80
70
60
50
40
30
20
5 15 20 25 30 35 40 45 50 55 60 70 80
F1 Levels (dB SPL)
wild type
Myo15ΔN/ΔN
postmortem mice

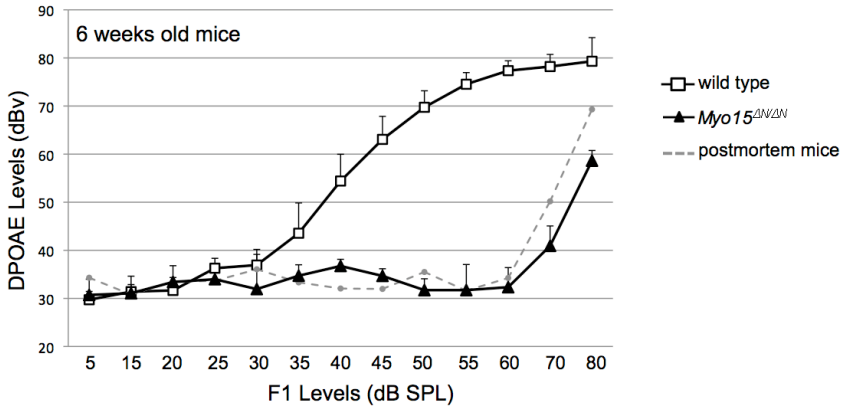
6 weeks old mice
DPOAE Levels (dBv)
90
80
70
60
50
40
30
20
5 15 20 25 30 35 40 45 50 55 60 70 80
F1 Levels (dB SPL)
wild type
Myo15ΔN/ΔN
postmortem mice

Figure 2-3. Assessment of hearing impairment in *Myo15*$^{\Delta P/\Delta P}$ mice.
A, Representative ABR thresholds at 20 kHz for wild type (white columns) and *Myo15*$^{\Delta P/\Delta P}$ (black columns) mice at ages of 2, 4 and 6 weeks old. ***B,*** Representative DPOAE measurements at 12 kHz for living wild-type and *Myo15*$^{\Delta P/\Delta P}$ mice at ages of 2 and 6 weeks old (white squares and black triangles, respectively). The noise floor is shown as DPOAEs of postmortem wild type mice (grey dashed line with dots).

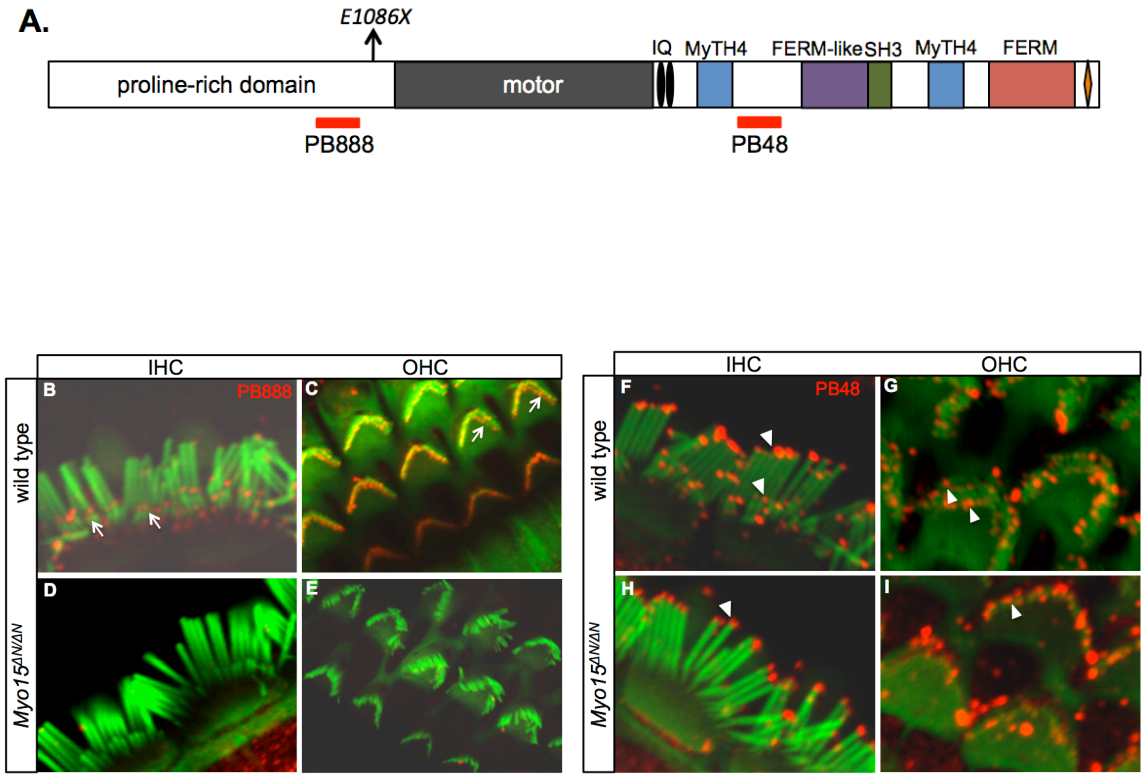

Figure 2-4. Localization of different MYO15 isoforms in the stereocilia of wild type and *Myo15*$^{\Delta P/\Delta P}$ mice.

A, Schematic representation of full-length MYO15 protein and its domains. Horizontal red rectangles indicate the location of the amino-acid residues of the antigens that were used to immunize rabbits. ***(B-E),*** Immunostaining by PB888 antibody on whole mount preparation of sensory epithelia from wild type and *Myo15*$^{\Delta P/\Delta P}$ mice. Arrows indicate the localization of MYO15 isoforms containing the proline rich domain, which is recognized by the PB888 antibody, in the short rows of stereocilia in IHCs and OHCs of wild type mice. ***(F-I),*** Immunostaining with the PB48 antibody on whole mount preparations of sensory epithelia from wild type and *Myo15*$^{\Delta P/\Delta P}$ mice. PB48 recognizes all the MYO15 isoforms carrying the tail domain, which localize in all rows of stereocilia in wild types, but are absent from the short rows in *Myo15*$^{\Delta P/\Delta P}$ mice (indicated by the arrowheads).

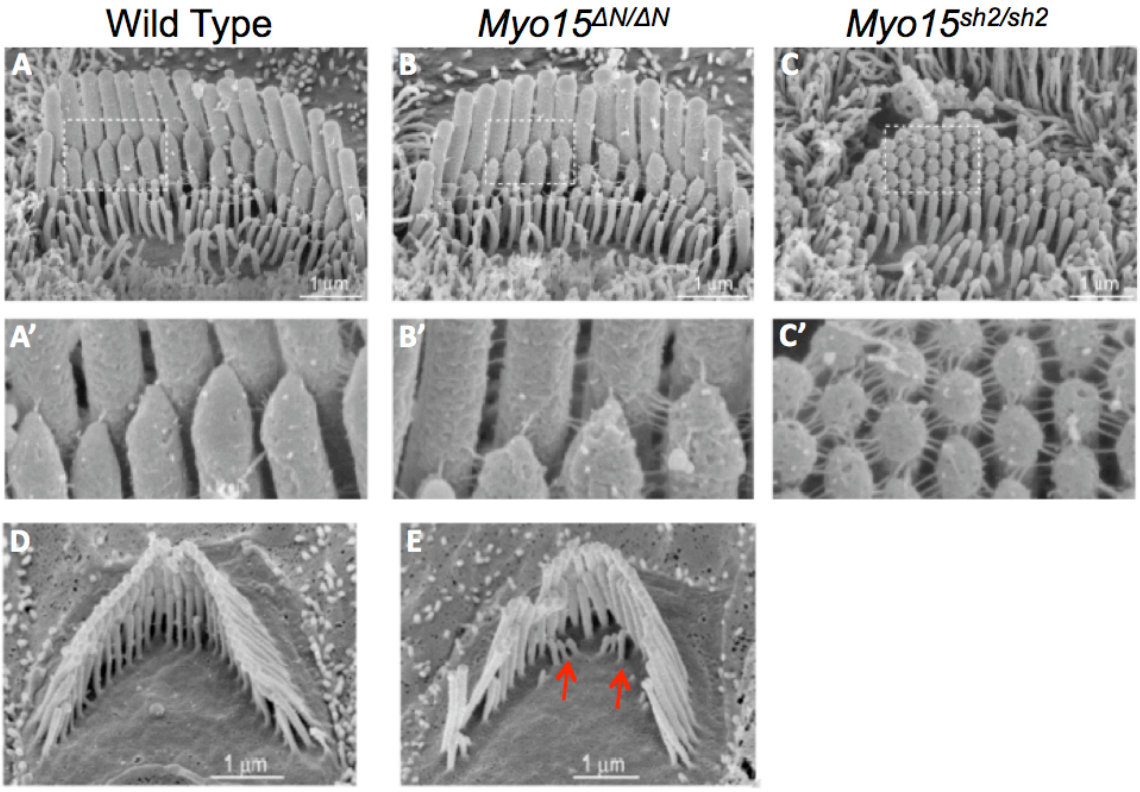

Figure 2-5. Stereocilia morphology of *Myo15*$^{\Delta P/\Delta P}$ mice.
(A-C), SEM images of OHCs stereocilia in wild type (**A**), *Myo15*$^{\Delta P/\Delta P}$ **(B)** and *Myo15*$^{sh2/sh2}$ (**C**) mice at P6~P8 days old. All samples are from approximately the same mid-cochlear location. ***(A'-C'),*** Higher magnification images of the areas in the dashed line rectangles in (**A-C**). ***(D, E),*** SEM images of OHCs stereocilia in wild type (**D**) and *Myo15*$^{\Delta P/\Delta P}$ **(E)** mice at P50 days old. Red arrows indicate a few remaining stereocilia undergoing degeneration in the short rows. Most of the stereocilia in the shortest row have been lost completely at this time.

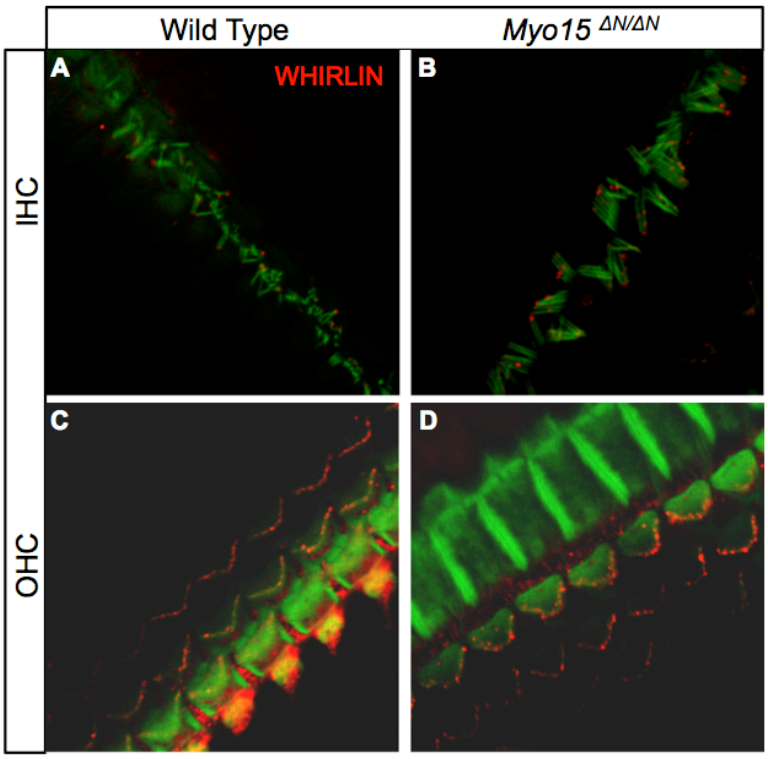

Figure 2-6. Transportation of WHIRLIN appears normal in *Myo15*$^{\Delta P/\Delta P}$ mice. An anti-WHIRLIN antibody was used to immunostain whole mount preparations of cochlear sensory epithelia of wild type **(A, C)** and *Myo15*$^{\Delta P/\Delta P}$ **(B, D)** mice (red) and phallodin staining (green) reveals actin rich structures.

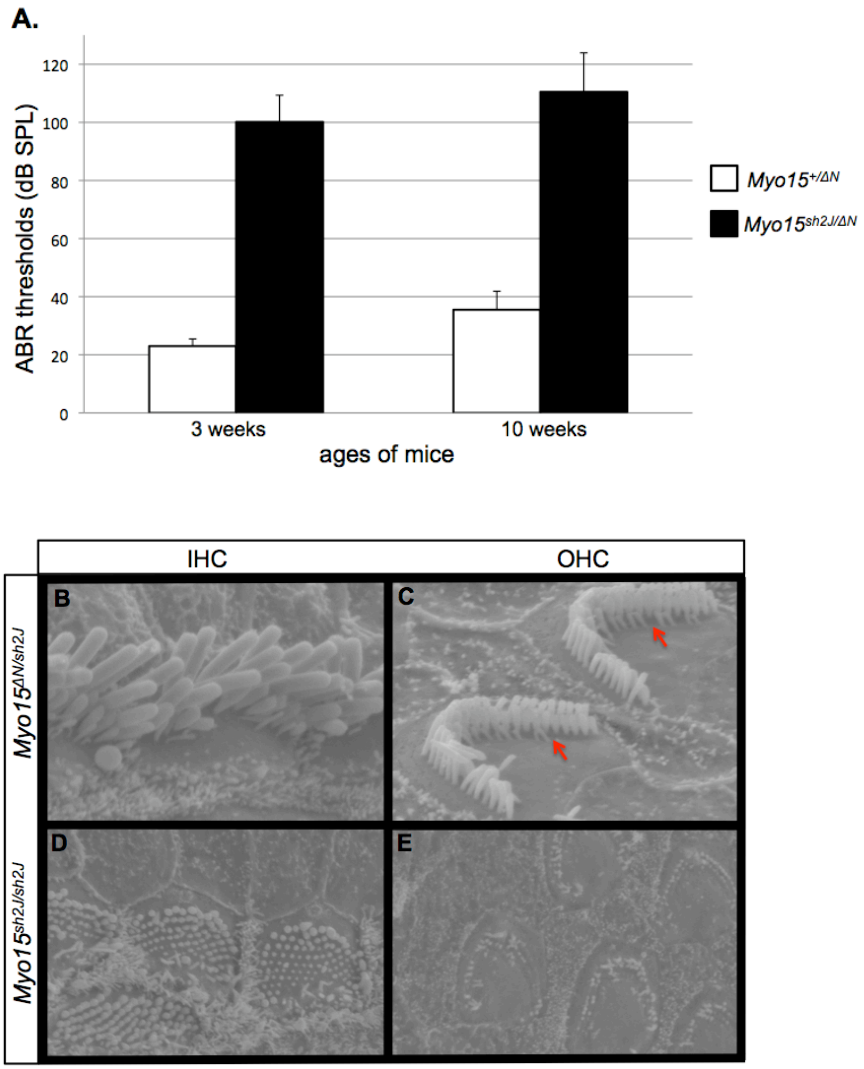

Figure 2-7. *E1086X* and *sh2J* alleles of *Myo15* do not complement each other in hearing function or stereocilia morphology.
A, ABR thresholds of *Myo15*$^{+/\Delta P}$ *and Myo15*$^{sh2J/+\Delta P}$ mice at 20 kHZ. ***(B-E),*** SEM images of stereocilia from IHCs and OHCs of *Myo15*$^{sh2J/+\Delta P}$ (**B,C**) and *Myo15*$^{sh2J/sh2J}$ (**D,E**) mice. Red arrows indicate the degenerating stereocilia in the short row of *Myo15*$^{sh2J/+\Delta P}$ OHCs.

REFERENCES

Ahmed ZM, Goodyear R, Riazuddin S, Lagziel A, Legan PK, Behra M, Burgess SM, Lilley KS, Wilcox ER, Griffith AJ, Frolenkov GI, Belyantseva IA, Richardson GP, Friedman TB (2006) The tip-link antigen, a protein associated with the transduction complex of sensory hair cells, is protocadherin-15. J Neurosci 26:7022-7034.

Anderson DW, Probst FJ, Belyantseva IA, Fridell RA, Beyer L, Martin DM, Wu D, Kachar B, Friedman TB, Raphael Y, Camper SA (2000) The motor and tail regions of myosin XV are critical for normal structure and function of auditory and vestibular hair cells. Hum Mol Genet 9:1729-1738.

Belyantseva IA, Boger ET, Friedman TB (2003) Myosin XVa localizes to the tips of inner ear sensory cell stereocilia and is essential for staircase formation of the hair bundle. Proc Natl Acad Sci U S A 100:13958-13963.

Belyantseva IA, Boger ET, Naz S, Frolenkov GI, Sellers JR, Ahmed ZM, Griffith AJ, Friedman TB (2005) Myosin-XVa is required for tip localization of whirlin and differential elongation of hair-cell stereocilia. Nat Cell Biol 7:148-156.

Beurg M, Fettiplace R, Nam JH, Ricci AJ (2009) Localization of inner hair cell mechanotransducer channels using high-speed calcium imaging. Nat Neurosci 12:553-558.

Chui D, Oh-Eda M, Liao YF, Panneerselvam K, Lal A, Marek KW, Freeze HH, Moremen KW, Fukuda MN, Marth JD (1997) Alpha-mannosidase-II deficiency results in dyserythropoiesis and unveils an alternate pathway in oligosaccharide biosynthesis. Cell 90:157-167.

Delprat B, Michel V, Goodyear R, Yamasaki Y, Michalski N, El-Amraoui A, Perfettini I, Legrain P, Richardson G, Hardelin JP, Petit C (2005) Myosin XVa and whirlin, two deafness gene products required for hair bundle growth, are located at the stereocilia tips and interact directly. Hum Mol Genet 14:401-410.

Holt MR, Koffer A (2001) Cell motility: proline-rich proteins promote protrusions. Trends Cell Biol 11:38-46.

Lakso M, Pichel JG, Gorman JR, Sauer B, Okamoto Y, Lee E, Alt FW, Westphal H (1996) Efficient in vivo manipulation of mouse genomic sequences at the zygote stage. Proc Natl Acad Sci U S A 93:5860-5865.

Liang Y, Wang A, Belyantseva IA, Anderson DW, Probst FJ, Barber TD, Miller W, Touchman JW, Jin L, Sullivan SL, Sellers JR, Camper SA, Lloyd RV, Kachar B, Friedman TB, Fridell RA (1999) Characterization of the human and mouse unconventional myosin XV genes responsible for hereditary deafness DFNB3 and shaker 2. Genomics 61:243-258.

Lloyd RV, Vidal S, Jin L, Zhang S, Kovacs K, Horvath E, Scheithauer BW, Boger ET, Fridell RA, Friedman TB (2001) Myosin XVA expression in the pituitary and in other neuroendocrine tissues and tumors. Am J Pathol 159:1375-1382.

Mustapha M, Beyer LA, Izumikawa M, Swiderski DL, Dolan DF, Raphael Y, Camper SA (2007) Whirler mutant hair cells have less severe pathology than shaker 2 or double mutants. J Assoc Res Otolaryngol 8:329-337.
Nagy A, Rossant J, Nagy R, Abramow-Newerly W, Roder JC (1993) Derivation of completely cell culture-derived mice from early-passage embryonic stem cells. Proc Natl Acad Sci U S A 90:8424-8428.
Nal N, Ahmed ZM, Erkal E, Alper OM, Luleci G, Dinc O, Waryah AM, Ain Q, Tasneem S, Husnain T, Chattaraj P, Riazuddin S, Boger E, Ghosh M, Kabra M, Morell RJ, Friedman TB (2007) Mutational spectrum of MYO15A: the large N-terminal extension of myosin XVA is required for hearing. Hum Mutat 28:1014-1019.
Peng AW, Belyantseva IA, Hsu PD, Friedman TB, Heller S (2009) Twinfilin 2 regulates actin filament lengths in cochlear stereocilia. J Neurosci 29:15083-15088.
Probst FJ, Fridell RA, Raphael Y, Saunders TL, Wang A, Liang Y, Morell RJ, Touchman JW, Lyons RH, Noben-Trauth K, Friedman TB, Camper SA (1998) Correction of deafness in shaker-2 mice by an unconventional myosin in a BAC transgene. Science 280:1444-1447.
Reiners J, van Wijk E, Marker T, Zimmermann U, Jurgens K, te Brinke H, Overlack N, Roepman R, Knipper M, Kremer H, Wolfrum U (2005) Scaffold protein harmonin (USH1C) provides molecular links between Usher syndrome type 1 and type 2. Hum Mol Genet 14:3933-3943.
Rzadzinska AK, Schneider ME, Davies C, Riordan GP, Kachar B (2004) An actin molecular treadmill and myosins maintain stereocilia functional architecture and self-renewal. J Cell Biol 164:887-897.
Rzadzinska AK, Nevalainen EM, Prosser HM, Lappalainen P, Steel KP (2009) MyosinVIIa interacts with Twinfilin-2 at the tips of mechanosensory stereocilia in the inner ear. PLoS One 4:e7097.
Salles FT, Merritt RC, Jr., Manor U, Dougherty GW, Sousa AD, Moore JE, Yengo CM, Dose AC, Kachar B (2009) Myosin IIIa boosts elongation of stereocilia by transporting espin 1 to the plus ends of actin filaments. Nat Cell Biol 11:443-450.
Stepanyan R, Frolenkov GI (2009) Fast adaptation and Ca2+ sensitivity of the mechanotransducer require myosin-XVa in inner but not outer cochlear hair cells. J Neurosci 29:4023-4034.
Wang A, Liang Y, Fridell RA, Probst FJ, Wilcox ER, Touchman JW, Morton CC, Morell RJ, Noben-Trauth K, Camper SA, Friedman TB (1998) Association of unconventional myosin MYO15 mutations with human nonsyndromic deafness DFNB3. Science 280:1447-1451.
Watanabe N, Kato T, Fujita A, Ishizaki T, Narumiya S (1999) Cooperation between mDia1 and ROCK in Rho-induced actin reorganization. Nat Cell Biol 1:136-143.
Xu T, Nie L, Zhang Y, Mo J, Feng W, Wei D, Petrov E, Calisto LE, Kachar B, Beisel KW, Vazquez AE, Yamoah EN (2007) Roles of alternative splicing in the functional properties of inner ear-specific KCNQ4 channels. J Biol Chem 282:23899-23909.

Yang Y, Baboolal TG, Siththanandan V, Chen M, Walker ML, Knight PJ, Peckham M, Sellers JR (2009) A FERM domain autoregulates Drosophila myosin 7a activity. Proc Natl Acad Sci U S A 106:4189-4194.

APPENDIX

Disruption of the proline rich domain of MYO15 results in subtle vestibular dysfunction but no circling behavior or hyperactivity disorder

INTRODUCTION

The inner ear contains the developmentally related cochlea and peripheral vestibular labyrinth. Given the similar physiology between these two organs, hearing loss and vestibular dysfunction may be expected to occur simultaneously in some individuals segregating mutations in inner ear genes. Many mouse mutants with hearing deficits also exhibit head tossing and circling behavior that is thought to be associated with vestibular dysfunction. The close association with deafness and circling behavior, however, may represent an ascertainment bias because the hyperactivity disorder is obvious and easy to detect in spontaneous mutants or in mutagenesis screens. Recent mutagenesis projects have incorporated hearing testing as a routine screen (Hardisty-Hughes et al., 2010) and identified many deafness mutants without vestibular defects (Schwander et al., 2007). The *Otoferlin* (*Otof*) mutant mouse is such an example. Otoferlin protein is highly expressed in both cochlear and vestibular hair cells of mouse inner ears (Roux et al., 2006), yet mice carrying mutations in *Otof* gene, either the genetically engineered *Otof*-deficient mice (Roux et al., 2006) or mice with ENU-induced mutations (Longo-Guess et al., 2007; Schwander et al., 2007), are deaf but have apparently normal vestibular function.

Different alleles of a gene that cause inner ear defects may or may not include an obvious vestibular abnormality. For example, *waltzer* mutants have a null allele of *Cdh23* that causes a circiling and head tossing phenotype, while an ENU-induced missense mutation in *Cdh23* does not arouse this behavior in *salsa* mice (Wilson et al., 2001; Schwander et al., 2009). The discrepancy between auditory and vestibular phenotypes could arise from differences in timing of developments, proteins or protein isoform expression, interacting proteins, and/or functional requirements between cochlea and vestibular organs.

Myo15 is expressed in both cochlear and vestibular hair cells and is crucial in regulating the elongation of stereocilia of both sensory cell types during inner ear development (Belyantseva et al., 2003). In addition to profound, congenital deafness, all previously described alleles of *Myo15* exhibit head tossing and circling behavior, which indicate vestibular dysfunction (Probst et al., 1998). This includes *sh2*, *sh2J*, *sh2-2J*, and *sh2-3J* mutant mice (Mouse Genome Informatics (MGI) website, http://www.informatics.jax.org/). The vestibular hair cells in *sh2* and *sh2J* mutants have extremely short stereocilia and lack whirlin staining at the tips (Belyantseva et al., 2005), which presumably leads to lack of vestibular function.

Here, we report that a unique, highly conserved, proline-rich domain of MYO15 protein may have different roles in auditory and vestibular systems. The stereocilia of cochlear and vestibular hair cells of $Myo15^{\Delta N/\Delta N}$ mice differ from previously reported alleles in that they seem normal initially, and although the mutant mice are deaf, they do not show any obvious head tossing or circling

behavior. We have begun to investigate the vestibular function in *Myo15*$^{\Delta N/\Delta N}$ mice and find evidence of subtle deviations in electrophysiology from normal mice. Here we report progress to date on this analysis.

RESULTS

We compared the behavior of *Myo15*$^{\Delta N/\Delta N}$ and *Myo15*$^{sh2/sh2}$ mutants in their cages. *Myo15*$^{sh2/sh2}$ mutants spontaneously circle and toss their heads. They occasionally stop circling, but if handled or suspended by the tail, they begin to circle when released in the cage. In contrast, wild type mice were not observed to circle, even after handling. The *Myo15*$^{\Delta N/\Delta N}$ mutants were indistinguishable from wild type, and they showed no obvious signs of excessive movement or hyperactivity of any kind.

To obtain a more quantitative behavioral assessment, the *Myo15*$^{\Delta N/\Delta N}$ mice were analyzed at 6 weeks and 3 months of age by the Center for Integrative Genomics at University of Michigan. SHIRPA (**S**mithKline Beecham Pharmaceuticals; **H**arwell, MRC Mouse Genome Centre and Mammalian Genetics Unit; **I**mperial College School of Medicine at St Mary's; **R**oyal London Hospital, St Bartholomew's and the Royal London School of Medicine; **P**henotype **A**ssessment) protocol was used for the assessment (Rogers et al., 1997). As the primary screen in the protocol, each mouse begins by being observed undisturbed in a viewing jar. Then the mouse is transferred to the arena for testing of transfer arousal and observation of normal behavior. A sequence of manipulations follows with tail suspension and use of the grid across

the width of the arena. Finally, the animal is restrained in a supine position to record autonomic behaviors prior to measurement of the righting reflex. There were no significant differences between *Myo15*$^{\Delta N/\Delta N}$ mice and controls for all the behavioral tests in the primary screen.

A more challenging test is part of the secondary screen in the SHIRPA protocol. An accelerating rota-rod is used to quantify the balance and coordination abilities of the mice. The time that a mouse can remain on a rotating drum was recorded, and there was no significant difference between *Myo15*$^{\Delta N/\Delta N}$ and control mice, although substantial variations were seen among the mice in the same genotype group (Fig. 2-8 A). In contrast, the *Myo15*$^{sh2/sh2}$ mutants are not even able to attempt the rota-rod task. Thus, *Myo15*$^{\Delta N/\Delta N}$ mice do not show obvious balance or hyperactivity disorder on the basis of these behavioral assessments.

To more directly test for vestibular function at the electrophysiological level, we measured vestibular evoked potentials (VsEPs) on *Myo15*$^{\Delta N/\Delta N}$ mice. VsEPs are elicited by stimuli that activate vestibular sensors and vestibular neurons and recorded via electrodes placed on the surface of the scalp (Jones et al., 2005). Compared to wild type controls, *Myo15*$^{\Delta N/\Delta N}$ mice have significantly elevated VsEP thresholds at 8 weeks of age (Fig. 2-8 B, *Myo15*$^{\Delta N/\Delta N}$: -1.5 +/- 2.5 dB, controls: -11.1 +/- 2.5 dB). The P1-N1 peaks on VsEPs measurement are generated by the peripheral vestibular nerve innervating the utricle and saccule. The latency of P1-N1 peaks provides a measure of the timing of neural transmission and conduction through the vestibular neural pathways, and the

amplitude of the peaks reflects the size and general synchrony of the population of neurons responding to the stimulus. It shows that the *Myo15*$^{\Delta N/\Delta N}$ mice have significantly prolonged P1-N1 latencies (Fig. 2-8 C) and significantly reduced P1-N1 amplitudes (Fig. 2-8 C). These results are consistent with loss of end organ sensitivity and slowed sensory transduction/neural activation in the *Myo15*$^{\Delta N/\Delta N}$ vestibular system.

The stereocilia morphology of vestibular hair cells was examined by phalloidin staining and scanning electronic microscopy (SEM). Unlike *sh2* and *sh2J* mutants, the lengths of vestibular stereocilia in *Myo15*$^{\Delta N/\Delta N}$ mice are similar to wild type controls at P50 (Fig. 2-9), which indicates that the elongation and maintenance of vestibular stereocilia does not require the proline-rich domain of MYO15 protein.

DISCUSSION

We discovered that *Myo15*$^{\Delta N/\Delta N}$ mice differ from all previous mutant alleles of *Myo15* by having normal activity. No overt evidence of hyperactivity, head tossing or circling were observed, and quantitative tests confirmed normal locomotor activity, coordination and balance. We cannot rule out differences in behavior with more challenging tasks such as swimming test or vestibular colic reflex (See Future Directions).

Despite the normal activity and coordination of *Myo15*$^{\Delta N/\Delta N}$ mice, we detected electrophysiological abnormalities. There are other examples of mice whose behavior was judged as normal, but VsEPs were severely diminished

(Jones et al., 2005). It is not surprising, therefore, that *Myo15*$^{\Delta N/\Delta N}$ mice exhibit normal behavior with reduced vestibular sensory input on VsEPs measurements. The reason probably comes from the remarkable plasticity and compensation abilities in the vestibulomotor systems.

The phenotypes of the *shaker 2* and *shaker 2J* mutants revealed that *Myo15* is required for elongation of cochlear and vestibular stereocilia. The *Myo15*$^{\Delta N/\Delta N}$ mice demonstrated that the proline-rich domain is not necessary for elongation, but it is required for maintenance of cochlear stereocilia. The cochlear stereocilia of *Myo15*$^{\Delta N/\Delta N}$ mice initially elongate and form the staircase pattern normally, but the stereocilia deteriorate prior to adulthood (see Chapter 2). While we did not observe any obvious degeneration of vestibular stereocilia, preliminary studies suggest that the proline-rich isoform is expressed in only a small subset of vestibular hair cells, and this area could have been missed (Bird, unpublished). Further analyses that define the spatial and temporal expression of different Myo15 isoforms in the vestibular system more precisely will be informative for future studies that investigate whether vestibular stereocilia of *Myo15*$^{\Delta N/\Delta N}$ mice undergo degeneration during maturation or aging (See Future Directions).

In conclusion, this novel *Myo15*$^{\Delta N/\Delta N}$ mouse model has severe auditory deficits but mild electrophysiological, vestibular dysfunction and no obvious balance or behavioral disorder. Therefore, *Myo15*$^{\Delta N/\Delta N}$ mice are an unique tool to elucidate the distinct functions of the Myo15 proline-rich domain in the development and/or function of auditory and vestibular systems.

ACKNOWLEDGEMENTS

I would like to thank Janet Hoff for conducting the behavior tests, Dr. Sherri Jones at Eastern Carolina University for VsEPs measurements, and Dr. Gregory Frolenkov at University of Kentucky for examination of the vestibular morphology by high resolution SEM.

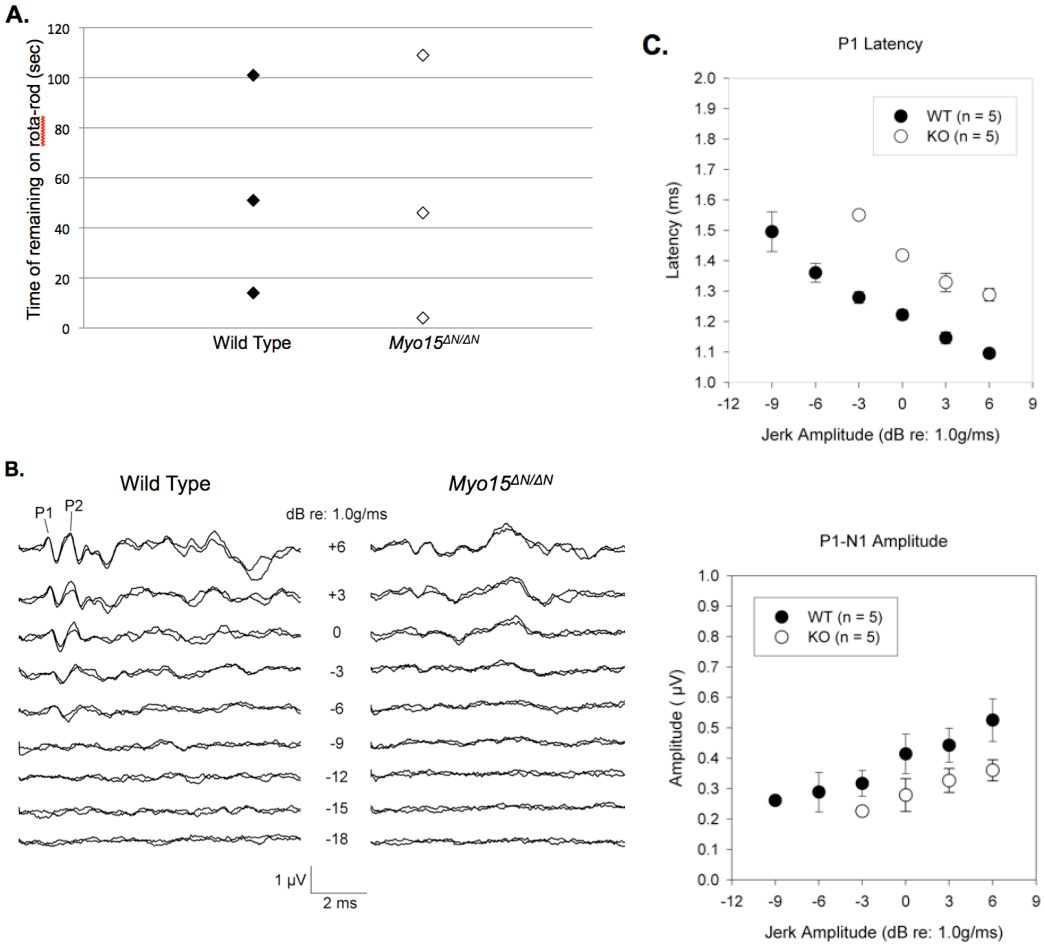

Figure 2-8. Assessment of vestibular function in *Myo15$^{\Delta N/\Delta N}$* mice.
A, The length of time that wild type and *Myo15$^{\Delta N/\Delta N}$* mice remain on the rota-rod in the behavior assay. ***B,*** Representative waveforms of VsEP measurements for wild type (left) and *Myo15$^{\Delta N/\Delta N}$* (right) mice. All responses shown here were recorded at +6 dB re: 1.0 g/ms. ***C,*** Latency of P1 waves and P1-N1 amplitudes for wild type (black circles) and *Myo15$^{\Delta N/\Delta N}$* (open circles) mice.

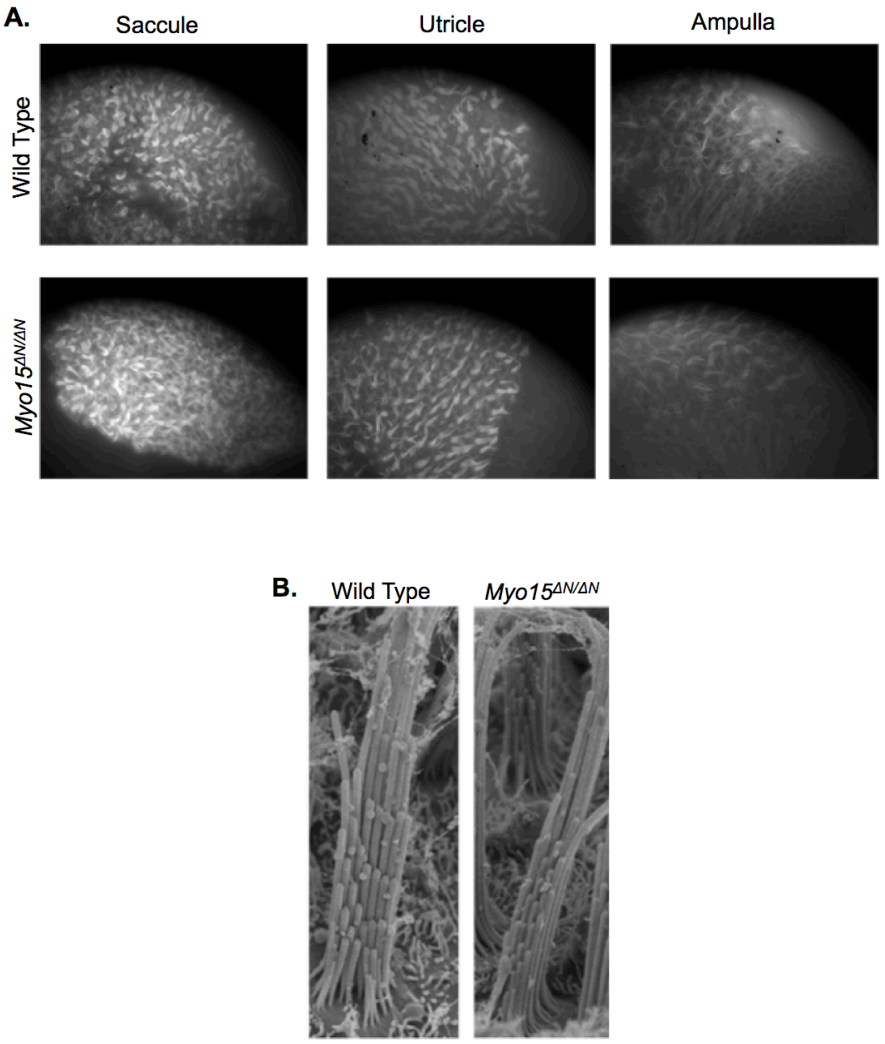

Figure 2-9. Stereocilia morphology of vestibular hair cells in *Myo15*$^{\Delta N/\Delta N}$ mice.
A, Images of phalloidin staining on stereocilia in the saccule, utricle and ampulla of wild type (upper row) and *Myo15*$^{\Delta N/\Delta N}$ (lower row) mice. ***B,*** SEM images of stereocilia in vestibular hair cells for wild type (left) and *Myo15*$^{\Delta N/\Delta N}$ (right) mice.

REFERENCES

Belyantseva IA, Boger ET, Friedman TB (2003) Myosin XVa localizes to the tips of inner ear sensory cell stereocilia and is essential for staircase formation of the hair bundle. Proc Natl Acad Sci U S A 100:13958-13963.

Belyantseva IA, Boger ET, Naz S, Frolenkov GI, Sellers JR, Ahmed ZM, Griffith AJ, Friedman TB (2005) Myosin-XVa is required for tip localization of whirlin and differential elongation of hair-cell stereocilia. Nat Cell Biol 7:148-156.

Hardisty-Hughes RE, Parker A, Brown SD (2010) A hearing and vestibular phenotyping pipeline to identify mouse mutants with hearing impairment. Nat Protoc 5:177-190.

Jones SM, Jones TA, Johnson KR, Yu H, Erway LC, Zheng QY (2006) A comparison of vestibular and auditory phenotypes in inbred mouse strains. Brain Res 1091:40-46.

Jones SM, Johnson KR, Yu H, Erway LC, Alagramam KN, Pollak N, Jones TA (2005) A quantitative survey of gravity receptor function in mutant mouse strains. J Assoc Res Otolaryngol 6:297-310.

Longo-Guess C, Gagnon LH, Bergstrom DE, Johnson KR (2007) A missense mutation in the conserved C2B domain of otoferlin causes deafness in a new mouse model of DFNB9. Hear Res 234:21-28.

Probst FJ, Fridell RA, Raphael Y, Saunders TL, Wang A, Liang Y, Morell RJ, Touchman JW, Lyons RH, Noben-Trauth K, Friedman TB, Camper SA (1998) Correction of deafness in shaker-2 mice by an unconventional myosin in a BAC transgene. Science 280:1444-1447.

Rogers DC, Fisher EM, Brown SD, Peters J, Hunter AJ, Martin JE (1997) Behavioral and functional analysis of mouse phenotype: SHIRPA, a proposed protocol for comprehensive phenotype assessment. Mamm Genome 8:711-713.

Roux I, Safieddine S, Nouvian R, Grati M, Simmler MC, Bahloul A, Perfettini I, Le Gall M, Rostaing P, Hamard G, Triller A, Avan P, Moser T, Petit C (2006) Otoferlin, defective in a human deafness form, is essential for exocytosis at the auditory ribbon synapse. Cell 127:277-289.

Schwander M, Xiong W, Tokita J, Lelli A, Elledge HM, Kazmierczak P, Sczaniecka A, Kolatkar A, Wiltshire T, Kuhn P, Holt JR, Kachar B, Tarantino L, Muller U (2009) A mouse model for nonsyndromic deafness (DFNB12) links hearing loss to defects in tip links of mechanosensory hair cells. Proc Natl Acad Sci U S A 106:5252-5257.

Schwander M, Sczaniecka A, Grillet N, Bailey JS, Avenarius M, Najmabadi H, Steffy BM, Federe GC, Lagler EA, Banan R, Hice R, Grabowski-Boase L, Keithley EM, Ryan AF, Housley GD, Wiltshire T, Smith RJ, Tarantino LM, Muller U (2007) A forward genetics screen in mice identifies recessive deafness traits and reveals that pejvakin is essential for outer hair cell function. J Neurosci 27:2163-2175.

Wilson SM, Householder DB, Coppola V, Tessarollo L, Fritzsch B, Lee EC, Goss D, Carlson GA, Copeland NG, Jenkins NA (2001) Mutations in Cdh23 cause nonsyndromic hearing loss in waltzer mice. Genomics 74:228-233.

CHAPTER 3

Hypothyroidism causes deafness and permanent defects in potassium channel gene expression and function in *Pit1*^{dw} mutants

ABSTRACT

The absence of thyroid hormone (TH) during late gestation and early infancy can cause irreparable deafness in both humans and rodents. A variety of rodent models have been utilized in an effort to identify the underlying molecular mechanism. Here, we characterize a mouse model of secondary hypothyroidism, **pi**tuitary **t**ranscription factor **1** (*Pit1*^{dw}), which has profound, congenital deafness and is responsive to oral TH replacement. These mutants have tectorial membrane abnormalities, including a prominent Hensen's stripe, elevated β-tectorin composition, and disrupted striated-sheet matrix. They lack distortion product otoacoustic emissions and cochlear microphonic responses, and exhibit reduced endocochlear potentials, suggesting defects in outer hair cell function and potassium recycling. Auditory system and hair cell physiology, histology and anatomy studies reveal novel defects of thyroid hormone deficiency related to deafness: (1) permanently impaired expression of KCNJ10 in the stria vascularis of *Pit1*^{dw} mice, which likely contributes to the reduced endocochlear

* This work was previously published as: Mustapha M, Fang Q, Gong TW, Dolan DF, Raphael Y, Camper SA, Duncan RK. *J Neurosci.* 2009 Jan 28; 29(4): 1212-23. I performed the immunohistochemical analyses by whole mount and sectioning and maintained animal colony.

potential, (2) significant outer hair cell loss in the mutants, which may result from cellular stress induced by the lower KCNQ4 expression and current levels in *Pit1*^{dw} mutant outer hair cells and (3) sensory and strial cell deterioration, which may have implications for thyroid hormone dysregulation in age related hearing impairment. In summary, we suggest that these defects in outer hair cell and strial cell function are important contributors to the hearing impairment in *Pit1*^{dw} mice.

INTRODUCTION

The organ of Corti is a neuroepithelium with sensory cells known as inner (IHC) and outer hair cells (OHC). Its maturation in the early postnatal period in mice and during the late prenatal period in humans is highly sensitive to thyroid hormone (TH), as TH deficiency during these periods can cause irreparable hearing deficits (Deol, 1973; Van't Hoff and Stuart, 1979; Uziel et al., 1983; Vanderschueren-Lodeweyckx et al., 1983; Uziel, 1986). TH activates and represses expression of many genes by interacting with TH receptors (THR). Some TH regulated genes encode functionally important proteins that are involved in structural development and/or physiological processes of the inner ear. Although several candidate genes have been proposed based on studies with rodent models of hypothyroidism, the molecular basis for the permanent nature of hypothyroidism-induced hearing loss is still unclear (Uziel, 1986; Knipper et al., 1998; Rusch et al., 1998; Knipper et al., 2000; Zheng et al., 2000;

Abe et al., 2003; Cantos et al., 2003; Rueda et al., 2003; Winter et al., 2006; Brandt et al., 2007; Sendin et al., 2007).

To explore the mechanism whereby TH affects the development and function of the inner ear, we characterized Snell dwarf (*Pit1*^{dw}, officially *Pou1f1*^{dw}), a mouse model of secondary hypothyroidism. These mice have an inactivating missense mutation in the *Pit1* gene, which encodes a POU-homeodomain transcription factor that is highly expressed in the pituitary gland (Camper et al., 1990; Li et al., 1990). The gene is necessary for development of the cells that produce growth hormone (GH), prolactin (PRL), and thyroid-stimulating hormone (TSH) (Gage et al., 1996). If untreated, homozygous mutants exhibit growth insufficiency, infertility, hypothyroidism, and deafness. Auditory brainstem response (ABR) testing revealed profound deafness in *Pit1*^{dw} mutants at both 3 weeks and 6 weeks of age, but continuous oral thyroid hormone supplementation initiated late in gestation was effective in preventing hearing deficits (Karolyi et al., 2007). These mutant mice are viable and healthy, living approximately 40% longer than their normal littermates (Brown-Borg et al., 1996). We selected these mutants for further characterization because of their viability, profound deafness, simple, autosomal recessive inheritance of hypothyroidism, and responsiveness to TH supplementation (Karolyi et al., 2007).

We report physiological, morphological, and gene expression analyses over the course of cochlear development in normal and *Pit1*^{dw} mutant mice. Tectorial membrane (TM) composition, morphology, and ultrastructure are

altered. OHC function is permanently compromised, as demonstrated by the absence of distortion product oto-acoustic emissions (DPOAE) and cochlear microphonics (CM). In addition to defects in OHC function, *Pit1*^{dw} mice have reduced endocochlear potential (EP). We examined expression of prestin and KCNQ4 in OHCs, as well as KCNQ1 and KCNJ10 in the stria vascularis, as candidates for underlying mechanisms. We identified some processes that are developmentally delayed but eventually mature in the absence of thyroid hormone and others that suffer lasting deficits, likely contributing to the permanent hearing problems caused by hypothyroidism. This study advances our understanding of the role of TH in development of normal hearing, including permanent effects on the tectorial membrane, expression of the potassium channel genes KCNQ4 and KCNJ10, the survival of OHC cells, and deterioration of the intermediate cells in the stria vascularis.

METHODS

Animal care and genotyping

All experiments were approved by the University Committee on the Use and Care of Animals and conducted in accord with the principles and procedures outlined in the NIH Guidelines for the Care and Use of Experimental Animals. Mice were obtained from the Jackson Laboratory (Bar Harbor, ME, USA) in 1990 and maintained at the University of Michigan. Previously described procedures for animal care and genotyping were used, including feeding mice a higher fat chow designed for breeding (PMI5020), delaying weaning of mutants until

approximately 35 days, and housing mutants with normal littermates to provide warmth (Karolyi et al., 2007). In all experiments, at least 3 animals of each genotype were analyzed for each age group studied unless stated otherwise. Postnatal day zero (P0) is designated as the day of birth.

Histology and gene expression analysis

Western blot analysis was performed with organ of Corti protein extracts collected from postnatal animals. Protein samples were homogenized in T-PER buffer (Pierce, Thermo Fisher Scientific, Rockford, IL), denatured in Laemmli sample buffer, and loaded onto SDS-polyacrylamids gels (12%). Gels were blotted onto nitrocellulose filters, and filters were probed with rabbit anti-beta tectorin antibody (gift from Dr. Richardson, University of Sussex, UK) at 1:1000 dilution. As a loading control, blots were subsequently probed with anti-glyceraldehyde-3-phosphate dehydrogenase (GAPDH) antibody (Santa Cruz Biotechnology sc-25778) at the dilution of 1:2000 and developed with an HRP-conjugated goat anti-rabbit (Pierce Biotechnology cat# 31462). Blots were developed with ECL substrate (Santa Cruz Biotechnology sc-2048).

Animals aged P8 and older were killed by CO_2 inhalation or decapitation. The temporal bones were avulsed and cochleae were quickly transferred into 4% paraformaldehyde in 0.1 M phosphate-buffered saline (PBS), pH 7.4. The footplate of the stapes was removed and each cochlea was perfused with the fixative introduced through the oval and round windows and extruded through a small opening made at the apex. The tissues were exposed to the fixative for 2

hours, followed by overnight incubation (with shaking) at 4 degrees in 8% EDTA for decalcification. No decalcification was applied to ears from animals younger than P10.

Fixed tissues were prepared for sectioning by embedding in paraffin or OCT. Soft bone specimens were dehydrated through a graded ethanol series and embedded in paraffin wax, sectioned at 6μm thickness, mounted, dried for 2 hours and stored at room temperature. Alternatively, soft bone specimens were incubated in 30% sucrose overnight at 4°C, embedded in OCT, cryosectioned at 6 μM thickness, mounted, dried for 15 minutes, and stored at -20°C.

Cochlear cryosections were blocked with 5% goat or donkey serum and 0.1% Triton X-100 in 0.1M PBS for 1 hour at room temperature, and incubated overnight at 4°C with a rabbit anti-serum against KCNJ10 (1:300, Alomone), or a rabbit polyclonal antibody against KCNQ4 (1:300) (Kharkovets et al., 2006), which was kindly provided by T. Jentsch (Hamburg University, Germany). Cochlear paraffin sections were dewaxed, rehydrated and boiled in 10 mM citric acid, pH 6, for 10 min to unmask epitopes followed by 1:1 H_2O_2:methanol (v/v) for 20 min to quench the endogenous peroxidase activity. The sections were incubated overnight at 4°C with a goat polyclonal antibody against prestin (N-20) (1:200, Santa Cruz) and mouse monoclonal antibody against synaptophysin (1:400, Sigma). Immunolabeling was visualized with TRITC-labeled secondary antibody (1:200, Jackson Immunoresearch) or Alexa Fluor 488 conjugated secondary antibodies (1:200, Invitrogen) and counter-stained with DAPI (Vector Laboratories). Sections from wild type and mutant animals were processed in

parallel for histology and immunostaining. Tissues were analyzed and photographed on a Leica DMRB epifluorescence microscope using identical light and exposures for mutant and wild type littermates.

For transmission electron microscopy analysis, animals were anesthetized and fixed by intracardiac perfusion with 2.5% glutaraldehyde in 0.15 M cacodylate buffer, pH 7.2, containing 1% tannic acid. The inner ear was removed and immersed into the same fixative for 2 h. The tissues were decalcified for 1 week in 3% EDTA with 0.25% glutaraldehyde at 4°C. The inner ears were post-fixed with 1% osmium tetroxide in phosphate buffer for 1 h. The specimens were dehydrated in increasing ethanol concentrations and embedded in Embed 812 epoxy resin. Sections were taken on a Leica Ultracut R using a diamond knife, stained with uranyl acetate and lead citrate, and examined on a Philips CM-100 TEM (Beyer et al., 2000) (Russell et al., 2007).

Scanning electron microscopy, whole mount and phalloidin epifluorescence analyses were carried out as previously described (Beyer et al., 2000; Mustapha et al., 2007).

Standard tests of auditory physiology

DPOAEs and EP were conducted as previously described (Karolyi et al., 2007).

CM measurements were carried out on mice that were anesthetized (ketamine 65 mg/kg, xylazine 3.5 mg/kg, and acepromazine 2 mg/kg) and given a dose of glycopyrrolate (0.2 mg/kg) to reduce secretions during surgery. Body

temperature was maintained through the use of water circulating heating pads and heat lamps. Additional anesthetic (ketamine and xylazine) was administered if needed to maintain anesthesia at a depth sufficient to insure immobilization and relaxation. Mice were placed into a head holder. The external pinna was removed and soft tissue dissected away from the bulla. The bulla wall was opened, and a single ball electrode, approximately 100 micrometer in diameter, was placed in the round window niche. The electrode was made from 2T 90% platinum/10% iridium wire and teflon coated, except for the ball. A teflon-coated silver return electrode was placed subcutaneously on the jawline. For CM recordings, the output frequency from the SRS 830 lock-in amplifier was stepped from 4 to 30 kHz, with a time constant of one second and a dwell time of 300 microseconds. The signal was passed through a programmable attenuator (TDT PA5) to produce a constant-amplitude signal. The signal from the round window electrode (Teflon-coated silver wire, with reference in the contralateral jawline) was sent though a Grass P15 amplifier (filter 0.1-50 kHz) to the input of the SRS830 lock-in amplifier. Signals were generated and data recorded with a MATLAB script written in-house.

Patch-clamp electrophysiology

Preparations of semi-intact mouse organ of Corti were obtained from mice 2 to 6 weeks old. Mice were anesthetized by intraperitoneal injection of ketamine (65 mg/kg) and xylazine (7 mg/kg) and killed by rapid decapitation. The bony labyrinth was extracted into cold perilymph-like saline (in mM, 142.0 NaCl, 5.8

KCl, 1.3 $CaCl_2$, 0.9 $MgCl_2$, 10 HEPES, 0.7 Na_2HPO_4, 2 Na-pyruvate, 5.8 glucose; pH 7.4; 305 mOsm), supplemented with amino acids and vitamins (1X MEM, Invitrogen). About three-quarters of the apical cochlear coil was separated from the modiolus and spiral ligament. All recordings were from OHC located approximately one-half turn from the cochlear apex. Viable hair cells were identified by their appearance, including features of bi-refringent membrane, columnar shape and absence of observable Brownian motion in cell organelles. Whole-cell voltage-clamp recordings were made with a MultiClamp 700B and Digidata 1440A data acquisition system using the pClamp 10.0 software suite (Molecular Devices). Data were sampled at 20 kHz and low-pass filtered at 4 kHz. For measurements of nonlinear capacitance, electronic compensation of membrane capacitance was necessarily omitted. Data were obtained from all three rows of OHC. Currents were recorded several minutes after break-in to the whole-cell configuration, in order to allow the cytoplasm and pipette solution to equilibrate. Electrodes were pulled from borosilicate glass capillaries (World Precision Instruments, Inc.) to a resistance of 3 - 6 MΩ. Drug perfusions, when necessary, were delivered locally through a multichannel micromanifold (ALA Scientific). All recordings were made at room temperature (21-26°C). Membrane voltages have not been compensated for junction potentials or residual series resistance errors. Unless otherwise noted, all measurements are reported as means ± one standard error of the mean.

Voltage-dependent capacitance was estimated from current transients elicited by small, incremental steps in the command voltage. This method,

described more fully elsewhere (Huang and Santos-Sacchi, 1993; Oliver and Fakler, 1999), relies on a simplified electrical model of the cell, under conditions where ionic currents have been blocked. The voltage protocol consisted of a stair-step series of voltage commands from -125 to 70 mV, using brief 5 mV steps 10 ms in duration. Extracellular and intracellular solutions were designed to block dominant potassium and calcium currents, resulting in a nearly linear steady-state current-voltage curve. The extracellular solution consisted of the following (in mM): 100 NaCl, 20 CsCl, 20 TEA-Cl, 1.52 $MgCl_2$, 2 CoCl2, 10 HEPES, 5 glucose, with pH adjusted to 7.2 using NaOH and osmolarity set to ~300 mOsm. The intracellular solution contained the following (in mM): 140 CsCl, 2 MgCl2, 10 HEPES, 10 EGTA, with pH adjusted to 7.2 using CsOH and osmolarity set to ~300 mOsm.

Membrane capacitance was calculated from estimates of input resistance and monoexponential fits to capacitance transients. These calculations were plotted against the voltage command eliciting the transient and fit to the derivative of the Boltzman equation describing charge movement through the membrane electric field:

$$C_m(V) = C_{lin} + \frac{Q_{\max}}{\alpha e^{((V_m - V_{1/2})/\alpha)}(1 + e^{((V_m - V_{1/2})/-\alpha)})^2} \quad (1)$$

where V_m is membrane voltage, C_{lin} is the linear, voltage-independent membrane capacitance, Q_{max} is the maximum charge moved through the membrane electric field, $V_{1/2}$ is the voltage corresponding to half-maximum charge movement, and α is the Boltzman slope factor describing voltage-sensitivity. The maximum voltage-dependent capacitance (C_{nonlin}) is equal to $C_m(V_{1/2}) – C_{lin}$.

For potassium current measurements, the bath solution was the perilymph-like saline used for dissection (see above), and the electrode solution contained (in mM): 135 NaCl, 0.1 $CaCl_2$, 3.5 $MgCl_2$, 5 HEPES, 5 EGTA, and 2.5 Na_2ATP, with pH adjusted to 7.2 with KOH and osmolarity set to 292 mOsm. Voltage commands were referenced to a holding potential of -80 mV in all cases. Tail currents were corrected off-line for a linear leak conductance and fit with a first-order Boltzman function:

$$I(V_m) = \frac{I_{\max}}{1 + e^{-(V_m - V_{1/2})/V_s}}, \quad (2)$$

where I_{max} is the maximum tail current, V_m is the membrane voltage, $V_{1/2}$ is the half-maximal activation voltage, and V_s is the Boltzman slope factor describing voltage sensitivity. In many cases, the sum of two first-order Boltzman functions was required to describe the tail currents. The F-statistic from curve fits in pClamp was used to determine whether a single or double Boltzman equation best fit the data. In some cases, the M-current blocker linopirdine (200 μM) was locally applied to selectively block KCNQ4 currents (Marcotti and Kros, 1999).

RESULTS

Altered composition of the tectorial membrane in Pit1^{dw} mutant mice

The morphological maturation of the cochlea is subject to developmental delay in many types of hypothyroid mice (Karolyi et al., 2007). We compared mid-modiolar cochlear sections of *Pit1*^{dw} mutants and wild-type littermates using light microscopy. We observed a delay in the opening of the tunnel of Corti in

Pit1^{dw} mutants at P12, but by P21 the opening was indistinguishable from wild type (Fig.3-1A). These features are similar to those described in other hypothyroid mutants. At P21 the tectorial membrane (TM) in *Pit1*^{dw} mutants clearly contains an abnormal protrusion (Fig.3-1 A). This abnormality appears to be a more prominent Hensen's stripe, and it persists through P42 (data not shown). This prominent stripe is evident in another model of secondary hypothyroidism, the *Cga* mutant that lacks pituitary TSH, but neither the underlying mechanism nor the significance has not been explored (Karolyi et al. 2007).

The tectorial membrane is comprised of collagens (*Col11a2*, *Col9a3*, and *Col9a1*) and non-collagen proteins including α-tectorin (*Tecta*) and β-tectorin (*Tectb*) and otogelin (*Otog*), all of which are critical for normal hearing (Richardson et al., 2008). We compared the concentration of TECTB in cochlear protein extracts from normal and *Pit1*^{dw} mutant mice at P21 using western blotting (Fig. 3-1 B). Two expected TECTB polypetides are detected in all mutant and wild type samples, consistent with previous reports (Knipper et al., 2001). Both isoforms of TECTB are consistently elevated in the *Pit1*^{dw} mutant samples compared to wild type (WT) littermates. Similar results were obtained at P35 (data not shown). The elevation of TECTB in *Pit1*^{dw} mutants contrasts with the significant reduction of TECTB in drug-induced hypothyroid rats (Knipper et al., 2001).

Structural changes in the TM have been reported in a variety of models with altered TH (Knipper et al., 2001; Rusch et al., 2001; Richardson et al., 2008).

Transmission electron microscopy (TEM) revealed abnormalities in the structure of the striated-sheet matrix in the TM in *Pit1*^{dw} mutants relative to wild type (Fig.3-1 C).

OHC loss in Pit1^{dw} *mutant mice*

To examine maturation of cochlear sensory cells and supporting cells we prepared whole mounts of the organ of Corti from normal and mutant mice and stained them with FITC-phalloidin, which reveals actin-containing regions of the cytoskeleton and cell-cell contacts (Fig. 3-2 A-D). At P14 and P25 the stereocilia of IHCs and OHCs and the junctions between pillar cells are clearly visible in wild type mice (Fig. 3-2 A and C). In contrast, the pillar cells do not stain with phalloidin in P14 mutants (Fig. 3-2 B). At P25 the mutant pillar cells stain with phalloidin, but the organization of the cytoskeleton is abnormal relative to normal mice, and these abnormalities persist through P42 (data not shown). Disruptions are evident in the repeated pattern of OHCs and the orientation of the OHC hair bundles in both P14 and P25 *Pit1*^{dw} mutants compared to wild type, suggesting the possibility of OHC death, followed by scar formation in the mutants (Fig. 3-2 B and D).

We performed two additional types of analyses on P42 mutant and wild type mice to examine OHC death more closely. Scanning electron microscopy (SEM) of the organ of Corti clearly confirmed the presence of scars in mutant mice in the cochlear mid turn, indicating the expansion of supporting cells into spaces created by missing OHCs (Fig.3-2 E-F). Transmission electron microscopy (TEM) analyses revealed OHCs from the mid turn of P42 *Pit1*^{dw}

mutant in an advanced stage of degeneration (Fig.3-2 G). In order to determine the location and extent of OHC death along the cochlea, we analyzed whole mounts of P42 organ of Corti by staining OHCs with FITC-phalloidin (data not shown) and antibody to the motor protein prestin (Supplemental Figure S. 3-1 A-B). Four regions of the organ of Corti were examined and quantified for OHC loss (apex, lower apex, mid turn and upper base) in 5 different animals of both *Pit1*^{dw} mutant and wild-type mice. Two-sided Student's t-tests for independent samples were conducted for differences in the mean between mutants and wild type mice. Gaps and deviations from the normal pattern of three, well-organized rows of OHCs were observed throughout the mutant organ of Corti. The most prominent hair cell loss was in the lower apical region of *Pit1*^{dw} mutants with a mean percent loss of 15±2% (mean ± one standard error of the mean) compared to wild type mice at 3±2% (Fig. 3-2 H). Mean percent OHC loss was significantly higher in the *Pit1*^{dw} mutants compared to wild type in the lower apex ($p<0.01$), mid turn ($p<0.01$), and upper base ($p<0.05$), but not significantly higher in the apex. A similar gradient of hair cell loss was described for *Barhl1* mutants (Li et al., 2002). OHC degeneration occurs in the *Pax8*$^{-/-}$ model of hypothyroidism, but *Pax8* expression in the otocyst could be a confounding factor (Christ et al., 2004). Because most *Pit1*^{dw} OHC survive and have a healthy appearance, the OHC death we observe in *Pit1*^{dw} mutants is unlikely to account for their profound hearing impairment. The remaining OHCs might be dysfunctional, however.

Adult Pit1^{dw} *mice lack DPOAE and CM*

OHCs contribute to sound processing by serving as a nonlinear cochlear amplifier. We used standard audiometric techniques to test OHC function by measuring DPOAEs and CMs because normal morphological appearance does not imply normal OHC function. Wild type 6-week-old (P42) animals had DPOAEs at low and moderate sound levels (≤80 dB SPL) at all frequencies measured (12, 24, and 48 kHz) (shown for 24 kHz, Fig. 3-3 A). Postmortem DPOAE measurements on wild type mice define the noise floor. Live, age-matched *Pit1*^{dw} mutant littermates had DPOAEs that were indistinguishable from the noise floor in mutant or wild type mice. We also recorded the magnitude and phase of the cochlear microphonic, a measure of the combined sound-driven receptor currents of both IHCs and OHCs. The CM response is dominated by the more numerous OHCs, particularly those OHCs located at the base of the cochlea close to the recording electrode (Patuzzi et al., 1989). CM amplitude was detected at all sound stimulation frequencies (4 through 30 kHz) in 6-week old (P42) wild type animals (Fig. 3-3 B). In *Pit1*^{dw} age-matched offspring CM amplitudes were indistinguishable from those recorded in postmortem normal animals, indicating compromised OHC function in the *Pit1*^{dw} mutants. The lack of a CM response was confirmed by the absence of a frequency-dependent phase shift in the mutants (Fig. 3-3 C). These data suggest that the OHCs in the *Pit1*^{dw} mutants are dysfunctional, despite their normal morphological appearance**.** Since both CM and DPOAE responses were absent in mutant mice, an OHC specific dysfunction could arise from deficits in the electrical motor response in

these cells as well as from aberrant mechanical performance, which could be associated with abnormal properties of the TM.

Maturation of prestin expression and distribution in Pit1^{dw} mice

Prestin is a member of a distinct family of anion transporters, SLC26, and it is expressed in OHCs but not in the non-motile IHCs. Prestin, officially known as SLC26A5, is presumably responsible for OHC electromotility and cochlear amplification (Zheng et al., 2000; Liberman et al., 2002). *Prestin* mutants exhibit reduced DPOAE, CM and nonlinear capacitance compared to wild type (Liberman et al., 2002; Cheatham et al., 2004; Gao et al., 2007; Dallos et al., 2008). It is not clear, however, whether abnormalities in prestin protein levels, subcellular localization, or function contribute to reduced DPOAEs and CM in *Pit1*^{dw} mice. To explore these possibilities we carried out a developmental time course of immunohistochemical staining for prestin in tissues also stained with DAPI to reveal nuclei and synpatophysin, a presynaptic marker of the efferent synapse at the base of the OHCs. In normal mice, prestin immunoreactivity is evenly distributed throughout the entire OHC membrane during the first few days after birth (shown for P8, Fig.3-4 A). Between P8 and P13, the subcellular distribution of prestin protein becomes restricted to the lateral regions of the OHC and is depleted from the basal pole of the OHC membrane (shown for P13, Fig. 3-4 A). This redistribution in prestin localization begins in the basal turn and propagates toward the apical turn of the cochlea (data not shown).

Pit1^{dw} mutants exhibit a developmental delay in prestin expression and subcellular localization. Prestin immunoreactivity is qualitatively reduced in *Pit1*^{dw} mutants at P8 compared to normal littermates (Fig.3-4 A). The level and localization of prestin expression in *Pit1*^{dw} mutants are improved at P13, resembling that of wild type mice at P8. Mutants show continued improvement at P21. By P42 the pattern of prestin expression is indistinguishable from that of 2-week-old wild type mice. This indicates a developmental delay of 3 to 4 weeks for maturation of prestin expression and localization in *Pit1*^{dw} mice.

Maturation of prestin function in Pit1^{dw} mice

If the level and subcellular localization of prestin expression is sufficient for normal OHC motor function, then the nonlinear capacitance generated by mature mutant OHCs should be similar to that of hearing mice. Membrane capacitance was estimated from current transients elicited by a stair-step voltage protocol. These data were fit to Eqn. 1 to determine the voltage-independent (linear, C_{lin}) and voltage-dependent (nonlinear, C_{nonlin}) components. Average capacitance curves are shown in Fig. 4B for wild type OHCs at 2 and 2.5 weeks of age (P13-14 and P18-19, respectively) and for *Pit1*^{dw} OHCs at 2, 4, and 6 weeks of age (P16-17, P30-32, and P43, respectively). Peak total membrane capacitance increased with age for both wild type and mutant mice. Measures of voltage-dependence ($V_{1/2}$ and a in Eqn. 1) were relatively unchanged over the age-ranges studied and across genotype (data not shown; $p > 0.01$).

For wild type mice, the increase in membrane capacitance reflected continued improvement in the nonlinear component from 2 to 2.5 weeks of age. Linear capacitance was constant over this age range (Fig. 3-4 C), suggesting that the cells had reached a mature size even while the efficacy of prestin function or density of prestin molecules continued to increase. A previous report has suggested that nonlinear capacitance reaches a plateau around 2 weeks of age in normal mice (Abe et al., 2007). This subtle difference could represent differences in mouse strain background or husbandry.

For mutant mice, the developmental increase in total membrane capacitance reflected gains in both linear and nonlinear components (Fig. 3-4 C). The gradual growth in linear capacitance from 2 to 6 weeks of age suggested a delay in the maturation of cell size in these animals compared with wild type. To address this possibility, OHCs were mechanically isolated from apical cochlear turns of P15-17 mice, and cell size was measured from captured digital images. Cell length and width for wild type OHCs were 27.9 ± 0.8 and 6.8 ± 0.3 μm (N=13), respectively, whereas these measurements in *Pit1*^{dw} OHCs were 21.3 ± 1.7 and 7.5 ± 0.5 μm (N=5), respectively. The 24% difference in cell length is statistically significant ($p < 0.01$). Mean cell surface area was estimated from average length and width measurements, considering the OHC as a simple cylinder. The mean surface area of the wild type OHCs was 1272 μm^2, whereas that for *Pit1*^{dw} OHCs was 1085 μm^2, a reduction of approximately 15%. This size difference is similar to the difference in linear capacitance between mutant and wild type cells at a similar age (18%; Fig.3-4 C). Nonlinear capacitance also

increased with age in the mutant OHCs. The developmental change in nonlinear capacitance outpaced increases in linear capacitance, suggesting that increases in the nonlinear component must be attributed, at least in part, to a greater density and/or efficacy of prestin in the OHC membrane. These physiological tests reveal a delayed maturation of prestin function in adult *Pit1*^{dw} mutants, consistent with the evidence that adult mutants eventually develop appropriate levels and subcellular localization of prestin protein. Thus, the lack of DPOAEs and CM in *Pit1*^{dw} mice are not explained by alterations in either nonlinear capacitance or prestin expression and localization. It remains possible, however, that electromotility is compromised in *Pit1*^{dw} mice through alterations in cytoskeletal structures essential to motor function or in the intrinsic electrical properties of the cell.

Reduced KCNQ4 protein expression specifically in OHC of Pit1^{dw} mutants

The voltage-dependent K^+ channel KCNQ4 is responsible for the dominant K^+ conductance, $I_{K,n}$, of mature OHCs (Marcotti and Kros, 1999). KCNQ4 sets the membrane resting potential in cochlear hair cells, and loss of KCNQ4 may cause chronic stress for the cells and lead to their degeneration (Kharkovets et al., 2006). We examined expression of KCNQ4 in the cochlear and vestibular systems using immunohistochemical staining. In normal mice the KCNQ4 immunoreactivity is distributed across the entire OHC membrane during the first few days after birth, eventually shifting from the basolateral surface to the basal pole of the cell by P12-P13 (data not shown). The level of KCNQ4

immunoreactivity in *Pit1*^{dw} mutants was reduced relative to wild type from P12 through P42 (Fig.3-5 A). The low level of KCNQ4 immunoreactivity appeared in a normal pattern. This contrasts with some rodent models of hypothyroidism that completely lack detectable KCNQ4 expression in OHCs at P12-P13 (Winter et al., 2006). We observed a developmental delay in KCNQ4 expression that followed a basal-apical gradient with expression levels in apical OHCs lagging behind those from the base (data not shown). Further examination of KCNQ4 expression within the *Pit1*^{dw} mutant inner ear revealed an expression pattern similar to that of wild type mice in the spiral ganglion and vestibular organs at all ages tested (P13, P21, P42 and P60) (Supplemental Figure S.3-3 A). This suggests that the permanent reduction in KCNQ4 expression is specific to the OHC in *Pit1*^{dw} mutants.

Reduced KCNQ4 currents in Pit1^{dw} mutants

To confirm the permanent reduction of KCNQ4 expression in mutants relative to normal OHC, we measured KCNQ4 currents during development. Voltage activation curves were constructed from tail current analysis and fit with Boltzman functions (Eqn. 2). Whole-cell currents in wild type OHCs were dominated by a low-voltage activated conductance attributed to KCNQ4 channels (Marcotti and Kros, 1999). In the presence of linopirdine, a KCNQ4 blocker, total outward current was reduced due to the elimination of $I_{K,n}$, revealing a residual high-voltage activated potassium current (Supplemental Figure S.3-2). The shapes of activation curves from *Pit1*^{dw} mutant mice were heterogeneous

suggesting large variations in the amount of KCNQ4-related conductance. While all cells from 2 week old wild type mice exhibited a dominant low-voltage activated KCNQ4 current, mutant OHCs, regardless of age, consisted of varying mixtures of low- and high-voltage activated conductances (Fig.3-5 B). Occasionally, *Pit1*^{dw} mutant OHCs were best fit by a single Boltzman with a high $V_{1/2}$ (above -20 mV), indicating the complete absence of measurable KCNQ4 current in those cells (4/17 cells in P15-17, 0/10 in P28-32, 1/18 in P40-45). To compare the amount of KCNQ4 between experimental groups, we determined the maximum tail current from Boltzman fits to the low-voltage activated components in Fig. 3-5B. This is an approximate measure of KCNQ4 current density since the sizes of all cells in this study were comparable (Fig. 3-4 C). The data are plotted for each cell and as averages in Fig. 3-5 C. Maximum KCNQ4 current was reduced in all mutant age groups compared with wild type ($p < 0.05$). In contrast to results for nonlinear capacitance, the KCNQ4 current in mutants did not steadily increase toward mature wild type levels. Instead, KCNQ4 current in the mutant animals peaked at 4 weeks of age (P28-35). Since KCNQ4 channels are active at negative membrane potentials, loss of KCNQ4 conductance would result in depolarization of the resting membrane potential. Current-clamp was used to measure resting potential in several OHCs from wild type and mutant mice. The OHCs from mutant mice at 6 weeks of age were depolarized by 10 to 15 mV compared with OHCs from 2 week old wild type mice (data not shown).

Substantially reduced endocochlear potential in Pit1^{dw} mice

The EP is the main driving force for the sensory transduction that leads to perception of sound. The potential is generated across the basal cell barrier of the stria vascularis by the K^+ channel KCNJ10, which is located in the intermediate cells (Marcus et al., 2002; Rozengurt et al., 2003; Wangemann et al., 2004). We found that the EP in 6 wk old wild type mice ranged from 105 to 113 mV (N=2), while the EP in *Pit1*^{dw} mutant mice was reduced by 45%, ranging from 48 to 50 mV (N=3) (Fig. 3-6 A). Similarly, the EP of 3 wk old mutants is 50% of wild type (data not shown). The abnormal EP contributes to the lack of DPOAE and CM and indicates that a cochlear defect of peripheral origin is involved in the deafness characteristic of the *Pit1*^{dw} mutants.

Reduced KCNJ10 protein expression in Pit1^{dw} mutants is specific to the stria vascularis

The stria vascularis contains marginal cells, intermediate cells and basal cells. Defects in any of these cells can result in hearing deficits (Jabba et al., 2006; Jin et al., 2008; Knipper et al, 2006; Rozengurt et al., 2003; Wangemann et al., 1995). To investigate the cause of the reduced EP in *Pit1*^{dw} mutant mice, we examined the expression of the K^+ channels KCNQ1 and KCNJ10 in marginal and intermediate cells, respectively, using immunohistochemical staining. The *Pit1*^{dw} mutant mice have reduced KCNJ10 immunoreactivity in both apical and basal cochlear turns compared to wild type mice at P21 (data not shown) and P42 (Fig. 3-6 B). The stria of the mutants appears smaller in width relative to

wild type at both ages, and the smaller size seemed attributable to diminished contribution of intermediate cells. KCNJ10 expression is normal in *Pit1*^{dw} mutant spiral ganglion and vestibular system at P21 and P42, revealing that the KCNJ10 deficiency is specific to the stria (Supplemental Figure S. 3-3 B). KCNQ1 is important for marginal cell function and maintenance of stria (Rivas and Francis, 2005). No obvious differences in KCNQ1 expression are noted at P21 or P42 (data not shown). Thus, reduced KCNJ10 expression is likely to be a major contributor to the lowered EP observed in *Pit1*^{dw} mutants, as observed in the KCNJ10 knockout (Marcus et al., 2002; Rozengurt et al., 2003; Wangemann et al., 2004).

Stria vascularis pathology in adult Pit1^{dw} mutants

We examined the stria vascularis at various ages in wild type and mutant mice using light microscopy of hematoxylin and eosin stained paraffin sections (data not shown) and TEM (Fig. 3-7). Ultrastructure analysis reveals evidence of abnormalities in the stria that are more obvious in mutants at P42 (N=3 per genotype and age, Fig. 3-7 A), than at P12 or P21 (data not shown). The width of the stria is consistently smaller in the mutant than the wild type. Marginal, intermediate, and basal cells all appear to be present, but there is less interdigitation of the intermediate cells with the basal aspect of the marginal cells and less infolding of the basolateral membrane. The smaller size of the mutant stria appears to come from reduced contribution of intermediate cells, consistent with reduced KCNJ10 immunostaining (Fig. 3-6). In addition, the TEM analysis

reveals prominent accumulation of dark deposits in the stria vascularis of P42 old *Pit1*^{dw} mutants with little or no deposits in wild type littermates (Fig. 3-7 B). The lipofuscin-like deposits (aging pigment) are found in all cell types of the stria, but are clearly most abundant in the central region of the stria, consistent with intermediate cells. The presence of this pathology suggests that cells in the stria vascularis of *Pit1*^{dw} mutants are undergoing deterioration.

DISCUSSION

Congenital hypothyroidism impairs multiple developmental processes within the inner ear, offering a mechanistic explanation for hypothyroidism-induced deafness. In this study we used a secondary hypothyroidism mouse model, the *Pit1*^{dw} mutant. These mice have profound congenital deafness, but normal balance. We checked for evidence of *Pit1* expression in the cochlea using RT-PCR, immunohistochemical staining, and an X-gal staining assay in the cochleae of *Pit1-lacZ* transgenic mice, and we found no evidence of *Pit1* expression in the cochlea by any of these methods (data not shown). This suggests that the hearing impairment in *Pit1* mutants is caused by the lack of *Pit1* activity in the pituitary gland. Consistent with this, the hearing impairment characteristic of *Pit1* mutants can be avoided by oral thyroid hormone supplementation in late gestation and after birth (Karolyi et al., 2007). Thus, the defects are due to thyroid hormone deficiency, rather than other problems caused by defective *Pit1*.

Here we report the use of the *Pit1* mutant to demonstrate that TH is

required for normal tectorial membrane (TM) composition and ultrastructure, ionic balance in the endolymph, outer hair cell (OHC) survival, and strial cell health. Abnormalities arising from TH deficiency contribute to the lack of distortion products (DPOAE), cochlear microphonics (CM), and the reduced endocochlear potential (EP) in *Pit1*^{dw} mutants. Deficits in these gross measures of cochlear physiology can be attributed, at least in part, to long-term defects in OHC KCNQ4 expression and strial KCNJ10 expression. The mutant OHCs eventually exhibit normal function and expression of prestin, but they exhibit permanent defects in KCNQ4 expression and function. The intermediate cells of the stria exhibit persistently low levels of KCNJ10 expression, resulting in ionic balance defects that likely contribute to the reduced EP, OHC dysfunction, and sporadic OHC death. The profound hearing impairment characteristic of *Pit1*^{dw} mutants may result from compounding effects of several TH dependent processes.

Pit1^{dw} mutants have multiple defects in the tectorial membrane

We report an increase in the size of Hensen's stripe, elevation of TECTB composition in the TM, and abnormalities in the TM ultrastructure in *Pit1*^{dw} mutants. We observed an abnormally prominent Hensen's stripe in another model of secondary hypothyroidism, but it is not clear whether this feature is commonly found in other genetic or pharmacologic models of hypothyroidism (Karolyi et al., 2007). The *Tectb* knockout mice lack Hensen's stripe, suggesting that TECTB is required to develop this structure (Russell *et al.*, 2007). Thus, the increased TECTB in *Pit1*^{dw} mutants could be a contributing factor to the

development of a more prominent Hensen's stripe. It is somewhat surprising that the *Pit1* mouse model of hypothyroidism causes increased composition of TECTB in the TM while the pharmacological rat model has obviously decreased TECTB (Knipper et al. 2001). The composition of the TM has not been assessed quantitatively in other models of hypothyroidism, but ultrastructural abnormalities of the TM are a consistent feature (Richardson et al., 2008) (Rusch et al., 2001). The significance of altered TM composition and ultrastructural features for OHC function is not entirely clear in *Pit1* mutants or other animal models that are completely deaf and have multiple abnormalities of the organ of Corti. There are clues, however, from humans and mice with mutations in individual TM components such as *Tecta, Tectb,* and *Otog* (Legan et al., 2000; Simmler et al., 2000; Legan et al., 2005; Russell et al., 2007). Loss of function in any of these individual components affects hearing, although none causes profound, congenital deafness characteristic of the *Pit1* mutant. *Otog* mutants have severe balance defects and variable hearing problems (Simmler et al., 2000). *Tecta* mutants have high frequency hearing deficits of 60 to 80 dB, and OHC dysfunction (Simmler et al., 2000). *Tectb* mutants are less sensitive to low frequency tones, while the high frequency resolution is enhanced (Russell et al., 2007). These results reveal the importance of tectorial membrane composition for cochlear frequency resolution. Thus, we expect that the TM alterations in *Pit1* mutants could contribute to the hearing deficits and OHC dysfunction we observe.

TH is not required for prestin expression or function

Prestin is a motor protein that underlies OHC motility. TH regulates its transcription, and studies in other hypothyroid rodents showed that the level of expression and subcellular distribution of prestin is abnormal (Weber et al., 2002; Winter et al., 2006). Here we show that these abnormalities in prestin expression and function in *Pit1*^{dw} mutants are transient, representing a developmental delay that reaches maturity by about 6 weeks of age. Although it is possible that OHC motility is compromised by defects in cytoskeletal specializations that support motor movement, it seems unlikely that deficits in OHC motor function could account completely for the absence of DPOAEs and CM in 6 week old mutants.

Pharmacological models of hypothyroidism demonstrated that the absence of TH for more than 3 weeks causes abnormal subcellular distribution of prestin within the hair cell along the lateral membrane (Weber et al., 2002). Physiological studies suggest that prestin function is also abnormal in TR double mutants at P8 (Rusch et al., 2001). While data on prestin protein distribution and function in older drug treated and TR mutant animals are not provided, we predict that prestin activity will mature functionally in pharmacologically treated animals as it does in *Pit1* mutants.

Altered potassium channel expression and function in Pit1^{dw} mutants

Pit1^{dw} mutants exhibit detectable expression of KCNQ4 in the OHC throughout adulthood, but the levels are consistently reduced, and the KCNQ4 currents are persistently lower than in normal 2 week old mice. In the mutants

maximum tail current for KCNQ4 peaked at 4 weeks of age, suggesting that the developmental profile for KCNQ4 function in the mutants is qualitatively similar to that described previously for normal mice (Beisel et al., 2005), despite the consistent deficiency relative to hearing animals. The persistently reduced KCNQ4 expression and function in *Pit1*^{dw} mice contrast with the eventual maturation of prestin expression and function in these mutants.

Abnormal KCNQ4 expression results in chronic depolarization of *Pit1*^{dw} OHCs, which may lead to the untimely demise of OHCs that we observed in 6 week old *Pit1*^{dw} mice. The level of depolarization we observed in *Pit1*^{dw} OHCs was similar to that of mice with disrupted or dominant negative forms of KCNQ4 (Kharkovets et al., 2006). Mice with altered KCNQ4 conductance, through pharmacological block or genetic disruption, exhibit progressive OHC loss (Nouvian et al., 2003). Taken together these data support the idea that sporadic OHC loss occurs concomitant with reduced KCNQ4 conductance and a depolarized resting potential.

Normal EP is required for OHC function including the generation of DPOAE and CM. *Pit1*^{dw} have approximately half the EP of wild type animals. A reduction in EP of the magnitude we observed in *Pit1*^{dw} mutants would be expected to reduce, but not eliminate, DPOAE and ABR responses, based on the precedent set by the *Claudin11* mutants (Gow et al., 2004). Although it is possible that differing genetic backgrounds could be an important influence, it is likely that the absence of distortion products in *Pit1*^{dw} mice arises from a combination of several deficits (Karolyi et al., 2007).

We report persistently reduced expression of KCNJ10 in the stria vascularis *Pit1*^{dw} mutants, which probably contributes to the low EP in *Pit1*^{dw} mutants. This conclusion is supported by the observation that *Kcnj10* mutant mice lack EP and have compromised hearing (Marcus et al., 2002), and *Slc26a4* deficient mice, a euthyroid model of Pendred syndrome, lack both EP and KCNJ10 (Rusch et al., 2001; Wangemann et al., 2004). We predict that KCNJ10 expression is reduced in the stria vascularis of other hypothyroid animals and the thyroid hormone receptor *Thra, Thrb* double mutants, which are unable to respond to TH (Rusch et al., 2001).

Many genetic defects affect the development and function of both the vestibular apparatus and the cochlea. It is intriguing that hypothyroidism does not appear to affect the vestibular system. The basis for the cochlear specificity of TH action is not known. It may be relevant that the alteration in KCNQ4 and KCNJ10 expression in *Pit1*^{dw} mutants is confined to OHCs and stria, respectively. Normal expression of both genes was detected in *Pit1*^{dw} mutant spiral ganglion and vestibular system at all ages tested. This cell type specific dysregulation of *Kcnq4* and *Kcnj10* expression in response to hypothyroidism suggests that the same genes have different requirements for TH in different cell types within the same organ. Differential sensitivity to TH deficiency could be achieved by many mechanisms, such as utilization of different cell type specific transcription factors; these could be co-regulators, and/or deiodinases. Alternatively variation in the critical timing for TH exposure could underlie differences in TH sensitivity, where early differentiation of one cell type may benefit from the mother's TH during

gestation, while cell types differentiating later would not have this benefit.

TH is required for maintenance of healthy cells in the organ of Corti and stria vascularis

Sporadic OHC death in *Pit1*^{dw} mice occurs concomitant with reduced KCNQ4 conductance and a depolarized resting potential. The progressive OHC loss is probably caused by the chronic depolarization. This idea is supported by the observation that mice with altered KCNQ4 conductance through pharmacological block (Nouvian et al., 2003) or genetic disruption (Kharkovets et al., 2006) exhibit progressive OHC loss. The percentage of OHC loss that we observe in *Pit1*^{dw} mice, however, is unlikely to account for their profound deafness (Bohne et al., 1990). Dysfunction of the stria vascularis is likely to be an important contributor to the hearing deficit. We observed abnormally low expression of KCNJ10 in the stria and abnormalities in ultrastructure including accumulation of lipofuscin-like deposits. Lipofuscin accumulation accelerates in aging cochleae of humans and other model organisms (Nadol, 1979; Bohne et al., 1990; Schuknecht and Gacek, 1993; Kazee and West, 1999; Scholtz et al., 2001; Konig et al., 2007). In addition, lipofuscin accumulates in the aging and diseased brains of Alzheimer's and Parkinson's patients (Eichhoff et al., 2008) and in the eyes of patients with atrophic age-related macular degeneration (Holz et al., 1999; Schmitz-Valckenberg et al., 2004; Abeywickrama et al., 2007). Thus, the pathological appearance of cells in the stria vascularis suggests that the *Pit1*^{dw} mutant stria are undergoing changes associated with physiological

stress or premature aging.

The low level of KCNJ10 in *Pit1*^{dw} mice is unlikely to account for the small size of the stria because neither *Kcnj10* nor *Slc26a4* mutant mice exhibit obvious cellular defects in the stria at the light microscopy level, despite the complete absence of KCNJ10 protein in both cases (Marcus et al., 2002; Wangemann et al., 2004). Taken together, these data suggest that thyroid hormone has a critical role in development and maintenance of strial cells, in addition to its role in enhancing KCNJ10 expression.

Why are Pit1^{dw} mice profoundly deaf?

Thyroid hormone regulates many processes in the developing cochlea. TM, DPOAE, CM and EP defects, as well as mutations in prestin, *Kcnq4* and *Kcnj10,* are consistent with progressive and/or moderate to severe hearing impairment of peripheral origin when present singly. The profound hearing impairment observed in *Pit1*^{dw} mutants could either be explained by a compounding effect of these genes that individually have moderate effects or it could mean that there are additional processes involved. Given the broad effects of TH on gene expression, it seems likely that other processes, such as IHC function, neurotransmission, and innervation, may also be compromised (Brandt et al., 2007; Sendin et al., 2007).

Advantages of the Pit1^{dw} model for studying the role of thyroid hormone in hearing

The advantages of studying *Pit1*^{dw} mutants are their viability, simple, autosomal recessive inheritance of hypothyroidism, responsiveness to TH supplementation, and availability of normal littermate controls. The viability of this model makes it possible to distinguish the aspects of TH deficiency that lead to permanent hearing defects from those that cause a delay in maturation of hearing. For example, this model allowed us to conclude that the developmental delay in prestin expression is not permanent, but the alterations in the TM and defective KCNJ10 and KCNQ4 expression and function are. In addition, the *Pit1*^{dw} mutants reveal the importance of TH for stria vascularis and OHC function and to avoid pathological changes and cell death. The prominence of hypothyroidism and presbycusis in older individuals suggests that our studies may be important for understanding the mechanisms contributing to age related hearing impairment.

Is hypothyroidism a risk factor for sensory and strial presbycusis?

There are several lines of evidence that suggest hypothyroidism may be a risk factor for presbycusis. Some of pathological features the *Pit1*^{dw} hypothyroid mice are also found in cases of age-related and environmentally-induced hearing loss. These include OHC loss and defects in the strial cell structure and function. In addition, the *Pit1*^{dw} hypothyroid mice exhibit reduced expression of *Kcnq4,* a gene mutated in cases of autosomal dominant hearing loss that have recently been found to be associated with presbycusis (Van Eyken et al., 2006).

Hypothyroidism is common in older individuals. The disorder occurs in about 30% of people over 60 years of age (Fransen et al., 2003). Since TH is apparently necessary for strial function and hair cell survival in young mice, it is possible that reduced thyroid function in adults is a risk factor for age related hearing loss, or that individuals born from mothers with hypothyroidism during pregnancy could be predisposed to age related hearing loss. While this is speculative, the mouse could be an excellent tool to investigate genetic and environmental modifiers of age related hearing loss (Johnson and Zheng, 2002; Nemoto et al., 2004).

ACKNOWLEDGEMENTS

The immunohistochemical analyses by whole mount and sectioning, and animal colony maintenance were done by M.M. and Q.F. DPOAE, CM, and EP were done by D.F.D. T.-W.G. contributed to the study of OHC loss. Y.R. analyzed the TEM. Nonlinear capacitance and KCNQ4 current measurements were done by R.K.D. Conceptualization of the experimental design and preparation of this manuscript was done by M.M., S.A.C., and R.K.D. We thank the following individuals for their important contributions to this work: Margaret I. Lomax for intellectual contributions and financial support, Alicia Giordimaina and Albert Chow for statistical analysis, Lisa A. Beyer for TEM and scanning electron microscopy, Karin Halsey and Jennifer Benson for physiological tests (DPOAE, CM and EP), Dr. Hassan Chaib for Western blot analysis, Dr. Guy Richardson for the β-tectorin antibody, and Dr. Jentsch for the KCNQ4 antibody.

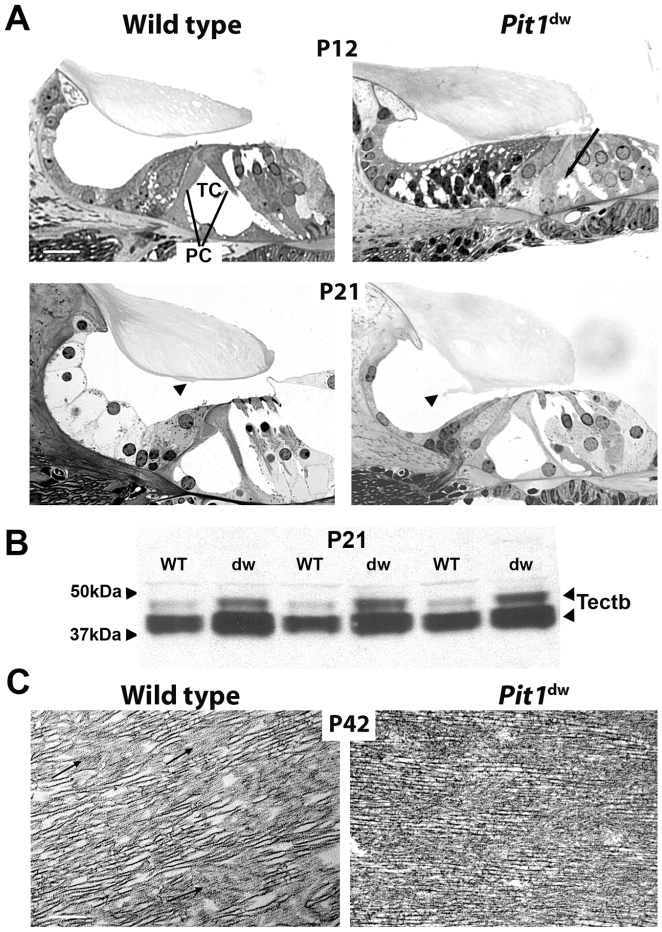

Figure 3-1. Tectorial membrane abnormalities in *Pit1*^{dw} mice. ***A***, Plastic sections of the organ of Corti taken from wild-type and *Pit1*^{dw} mutant mice at P12 and P21 were visualized by light microscopy. The arrow indicates the unopened tunnel of Corti (TC) in the P12 old mutant. OHCs, IHCs, and pillar cells (PC) are indicated. Scale bars: 10 μm. ***B***, Analysis of TECTB content in the tectorial membrane of P21 animals using Western blotting. Two polypeptide bands of TECTB are present at 43 and 47 kDa. The blot was reprobed with a GAPDH antibody, and equivalent amounts of immunoreactive 36 kDa protein were detected, indicating equivalent amounts of proteins were loaded (data not shown). ***C***, Transmission electron micrographs illustrate the ultrastructure of the tectorial membrane in P42 old animals. Regions shown are from the central core of the tectorial membrane overlying the organ of Corti. Fine diameter filaments (arrows) forming the striated sheet matrix are different in the wild-type mice and the mutants. Scale bars: 2 μm.

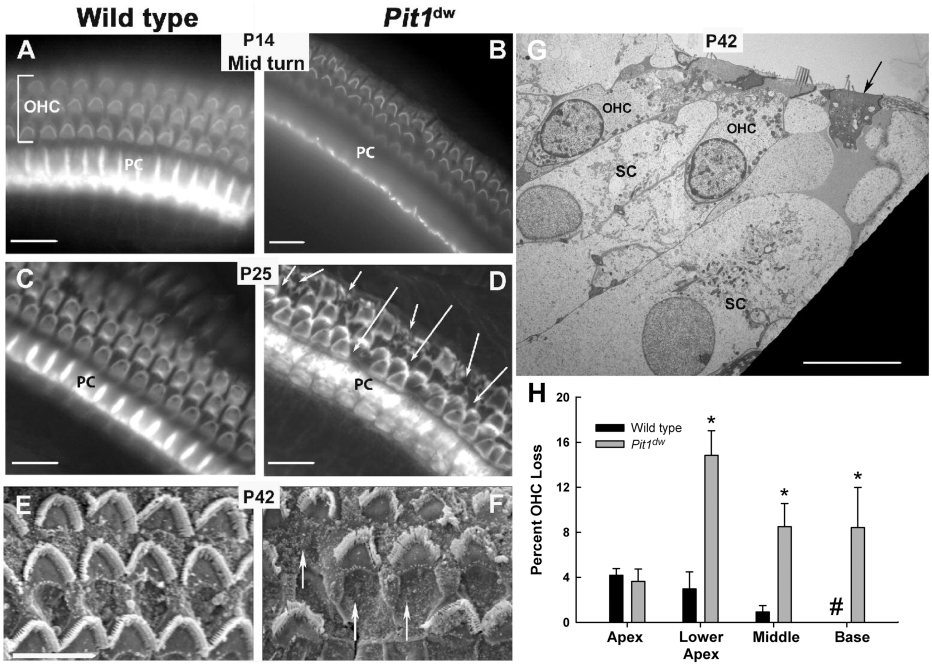

Figure 3-2. *Pit1*^{dw} mutants undergo significant OHC loss compared with wild-type mice. ***A–D***, Whole mounts of the organ of Corti of mice ages P14 and P25 were stained with FITC-phalloidin to reveal actin-rich structures and visualized by light microscopy. ***E–G***, Scanning electron microscopy (***E***, ***F***) and TEM (***G***) were used to examine the organ of Corti from P42 mice. The TEM reveals that the width of supporting cells (SC) that neighbor degenerating OHCs (arrow) are larger than SC neighboring healthy OHC. Pillar cells (PC). Arrows indicate OHC degeneration and scar formation. Scale bars: 10 μm. ***H***, Outer hair cell loss was quantified by region (apex, lower apex, mid and upper base turns) in five different animals of both *Pit1*^{dw} mutant and wild-type mice. The length of each region was 100 μm, encompassing 166–181 OHCs per region. Mean percentage outer hair cell loss was significantly higher in the *Pit1*^{dw} mutants compared with the wild-type mice (*) in the lower apex ($p < 0.01$), mid turn ($p < 0.01$), and upper base ($p < 0.05$). No OHC loss was observed in wild-type cochlea at the upper base (#). All statistical tests were conducted in SPSS 15.0.1.1 [EC] . Error bars represent one SEM.

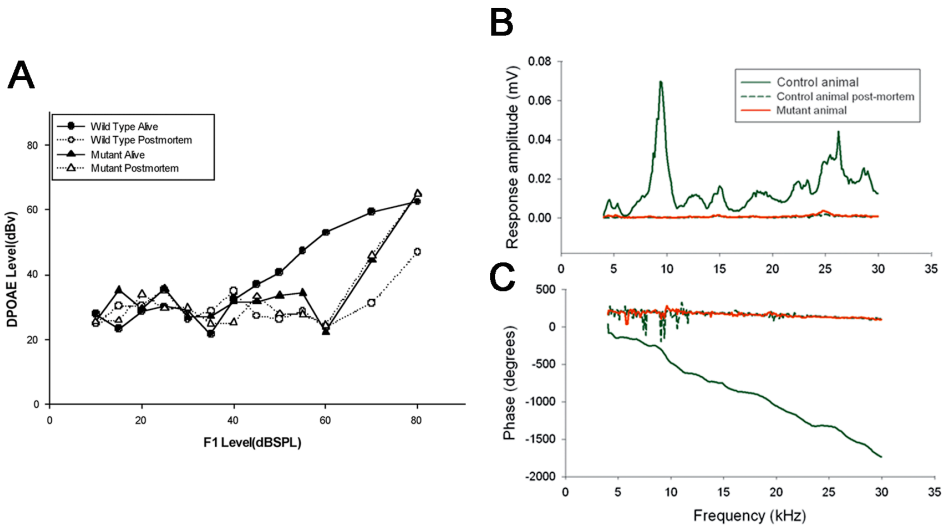

Figure 3-3. Pit1^{dw} mutant mice lack DPOAE and CM responses. ***A***, DPOAEs were measured in alive wild-type and mutant mice at P42 (black circles and black triangles, respectively) and compared with DPOAEs of postmortem animals (white circles and triangles). Data are shown for the 24 kHz frequency only. Error bars indicate ±1 SEM. ***B***, ***C***, CM potentials were tested at various sound stimulation frequencies (4 through 30 kHz) in P42 wild-type animals (green line), in *Pit1*^{dw} mutant mice (red line) and in postmortem animals (green dashed line) of age-matched offspring (***B***). CM amplitudes were confirmed by the phase shift data (***C***).

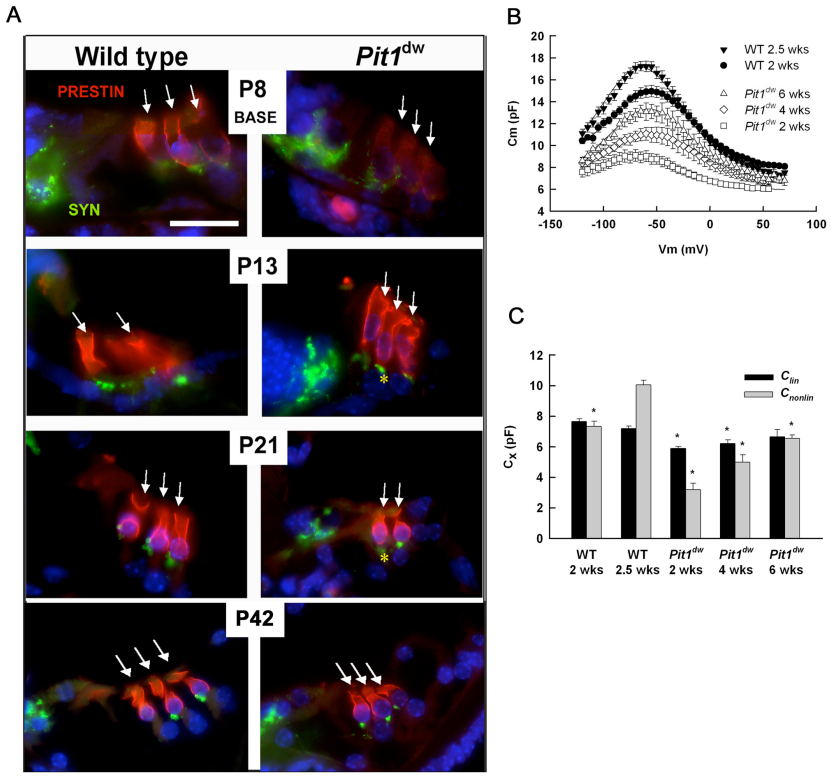

Figure 3-4. Prestin protein expression and function mature in adult *Pit1*^{dw} mutant mice. ***A***, Prestin expression and localization was analyzed by staining paraffin-embedded sections from wild-type and *Pit1*^{dw} mutants at P8, P14, P21, and P42 with prestin-specific antibodies (red). Sections were visualized with light microscopy. Synaptophysin (Syn) staining (green) identifies the basal poles of OHC. Nuclei were labeled using DAPI (blue). Asterisks (*) mark prestin labeling detected at the basal pole of the hair cell. Arrows identify rows of outer hair cells. Scale bars: 10 μm. ***B***, Average capacitance-voltage curves were generated for OHCs from wild-type mice at 2 and 2.5 weeks and for mutants at 2, 4, and 6 weeks of age (respectively, N = 5, 6, 5, 6, 4). Curves were fit to Eq. 1 to estimate linear and nonlinear capacitance components. Fit parameters: WT: 2 weeks, C_{lin} = 7.7 pF, Q_{max} = 0.82 pC, = 28.2 mV, $V_{1/2}$ = –56.3 mV; 2.5 weeks, C_{lin} = 7.2 pF, Q_{max} = 1.07 pC, = 26.9 mV, $V_{1/2}$ = –65.0 mV; *Pit1*^{dw}: 2 weeks, C_{lin} = 5.9 pF, Q_{max} = 0.36 pC, = 28.6 mV, $V_{1/2}$ = –70.2 mV; 4 weeks, C_{lin} = 6.2 pF, Q_{max} = 0.61 pC, = 31.6 mV, $V_{1/2}$ = –57.5 mV; 6 weeks, C_{lin} = 6.7 pF, Q_{max} = 0.69 pC, = 26.8 mV, $V_{1/2}$ = –56.8 mV. ***C***, Average values for linear and maximum nonlinear capacitance are shown for each experimental group. Error bars represent one SEM. *p < 0.01 with respect to data from 2.5-week-old wild-type OHCs.

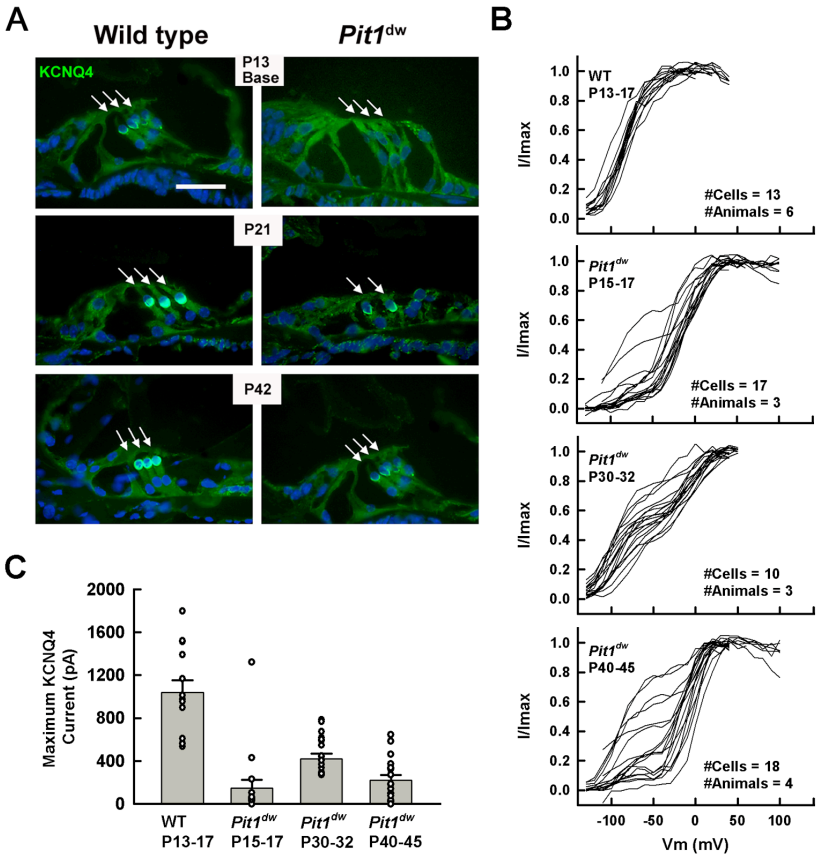

Figure 3-5. KCNQ4 protein expression and function are permanently reduced in the cochlear OHC of *Pit1*^{dw} mutant mice. ***A***, KCNQ4 immunoreactivity is reduced in OHCs (arrows) of mutant mice relative to wild type. Frozen sections obtained from P13, P21, and P42 wild-type and mutant mice were stained for KCNQ4 (green). Nuclei were stained with DAPI (blue). Outer hair cells from *Pit1*^{dw} mice exhibit a nonmonotonic developmental increase in KCNQ4 currents. ***B***, Normalized tail-currents are shown for 2-week wild-type mice and 2-, 4-, and 6-week-old mutants. Wild-type OHCs uniformly exhibited a dominant low-voltage activated potassium conductance attributed to KCNQ4 function. Mutant OHCs were heterogeneous, regardless of age, in that some cells had KCNQ4 while others did not. ***C***, Average maximum tail-current for low-voltage activated components of the Boltzman fits is shown for wild-type and mutant OHCs. Average currents were lower in mutants than wild type ($p < 0.05$). Also, there was a statistically reliable effect of age on average KCNQ4 current using a one-way ANOVA ($p < 0.01$).

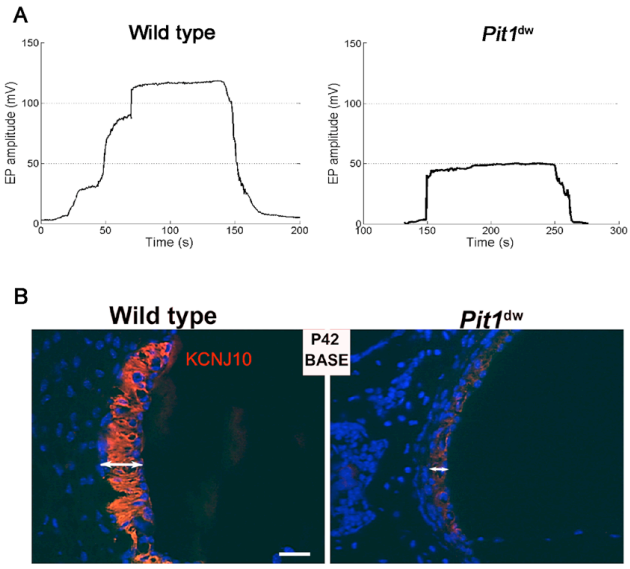

Figure 3-6. Endocochlear potential and KCNJ10 expression are lower in *Pit1*^{dw} mutants than wild type. ***A***, EP were measured in P42 wild-type and age-matched mutant animals. Representative plots of endocochlear potential (in mV) for littermate control and *Pit1*^{dw} mutant animals are shown. The time depicted includes electrode insertion into and withdrawal from the endolymph. ***B***, Frozen sections of the organ of Corti of wild-type and mutant mice collected at P21 and P42 were stained for KCNJ10 (red) (data shown for P42 only). Nuclei (blue). KCNJ10 immunoreactivity is detected in the intermediate cells of the stria vascularis of these mice.

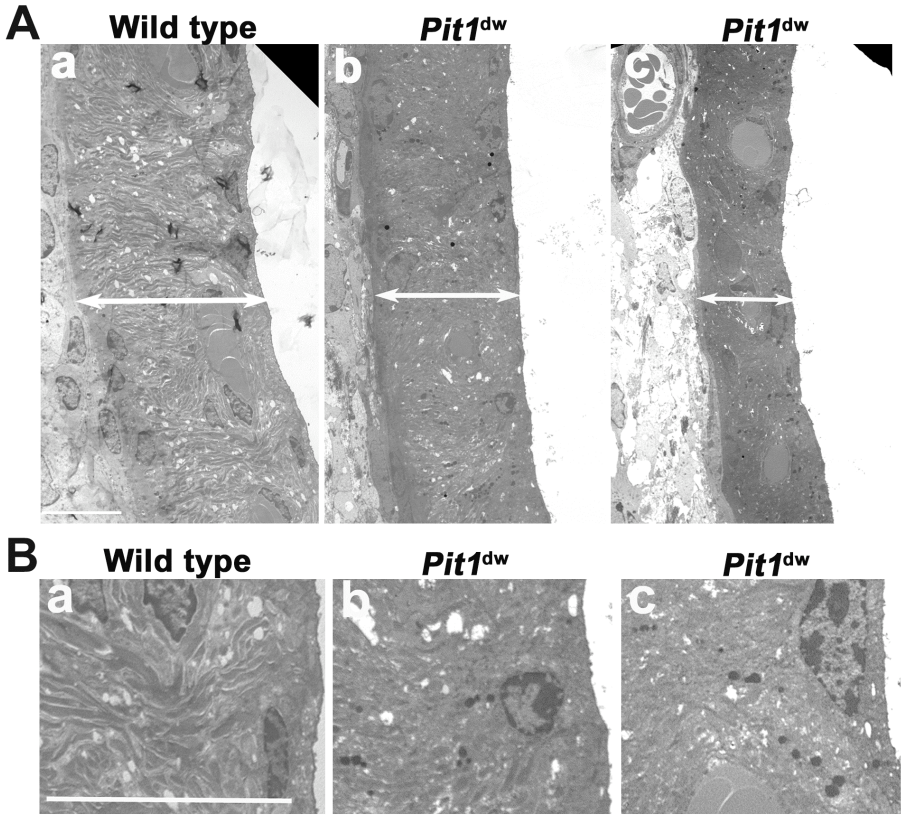

Figure 3-7. Stria vascularis pathology in adult *Pit1* mutants. ***A***, Stria vascularis prepared from P42 wild-type mice (***a***) and mutant mice (***b***, ***c***) were analyzed by TEM. Double-headed arrow bars define the width of the stria vascularis. ***B***, Lipofuscin granules are more abundant in the intermediate cells of *Pit1*^{dw} mutant mice, suggesting that the mutant cells are exhibiting signs of aging. The ultrastructure of wild-type (***a***) stria vascularis animals was compared with *Pit1*^{dw} mutants (***b***, ***c***). Lipofuscin-like granules are more abundant in the mutants. Sections shown are from the basal turns of the cochlea, which were more prominently affected than the apex. Scale bars: 10 μm.

SUPPLEMENTAL FIGURES

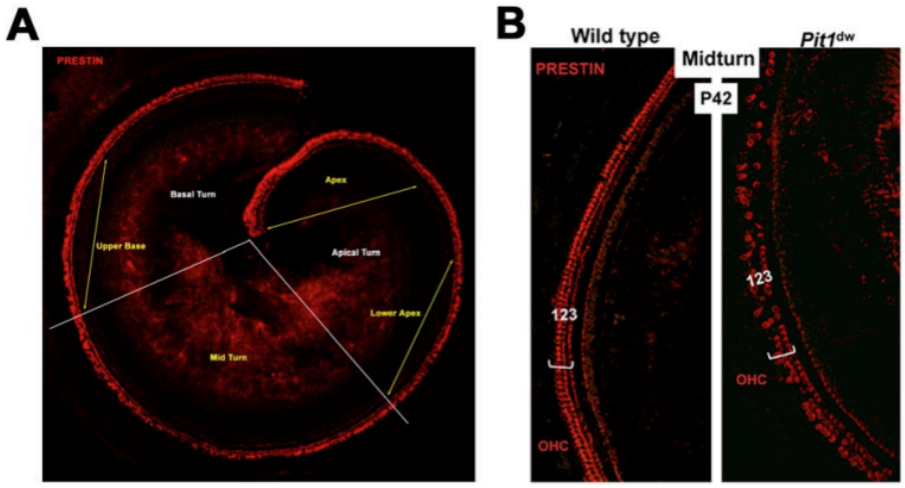

Figure S-1
(A) Definition of cochlear regions.
Whole mounts of P42 organ of Corti were stained with OHC motor protein prestin, then analyzed by confocal microscopy (Zeiss laser scanning microscope LSM-510). The four different regions of the organ of Corti that are considered in our study are labeled in yellow as: apex, lower apex, mid turn and upper base.
(B) Outer hair cell loss in *Pit1*dw mutants.
Whole mounts of P42 organ of Corti were stained with prestin, then analyzed by confocal microscopy. Gaps and deviations from the normal pattern of three, well-organized rows of outer hair cells were observed throughout the mutant organ of Corti.

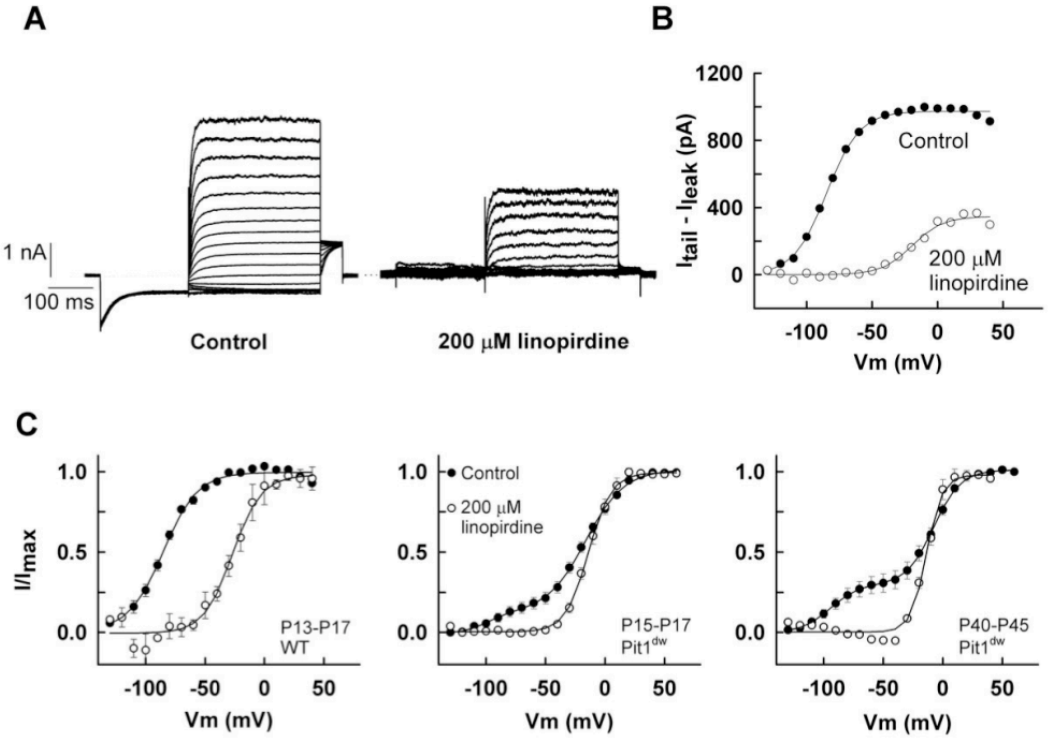

Figure S-2
KCNQ4 currents in mouse OHCs are blocked by 200 μM linopirdine.
Whole-cell patch-clamp recordings were obtained from OHCs in apical regions of the cochlea. **(A)** Membrane voltage was initially stepped to -120 mV from a holding potential of -80 mV. This pre-pulse was followed by a series of voltage steps from -130 mV to 40 mV. Tail currents were elicited by a final step to -40 mV. Currents are shown with leak subtraction but without series resistance compensation. Linopirdine blocked the majority of the outward current activated at negative membrane potentials. **(B)** Tail currents in control saline and in the presence of linopirdine were fit with single first-order Boltzman functions. Fit parameters: Control, Imax = 972 pA, V1/2 = -84.8 mV, Vs = 12.5 mV; linopirdine, Imax = 348 pA, V1/2 = -19.3 mV, Vs = 11.7 mV. Data in (A) and (B) are from an OHC from a P17 wild-type mouse. **(C)** Average normalized tail-currents are shown for wild-type mice (left), 2 week old *Pit1*dw mice (middle), and 6 week old *Pit1*dw mice (right) in the presence of control saline or 200 μM linopirdine. Mutant mice displayed two outward potassium currents, easily separable by their negative or positive voltage dependence. In these cases, double Boltzman functions were required to properly fit the data. For all animals, linopirdine was effective in eliminating the negative conductance, presumably through block of KCNQ4 channels. Fit parameters and number of cells per group (N): WT, P13-P17, control, V1/2 = -85.5 mV, Vs = 14.9 mV, linopirdine, V1/2 = -25.9 mV, Vs = 12.6 mV, N = 4; *Pit1*dw, P15-P17, control, V1/2(1) = -96.1 mV, Vs(1) = 7.5 mV,

V1/2(2) = -15.8 mV, Vs(2) = 14.0 mV, linopirdine, V1/2 = -13.5 mV, Vs = 9.8 mV, N = 7; *Pit1*dw, P40-P45, control, V1/2(1) = -95.1 mV, Vs(1) = 10.8 mV, V1/2(2) = -7.4 mV, Vs(2) = 9.6 mV, linopirdine, V1/2 = -12.5 mV,
Vs = 7.1 mV, N = 7.

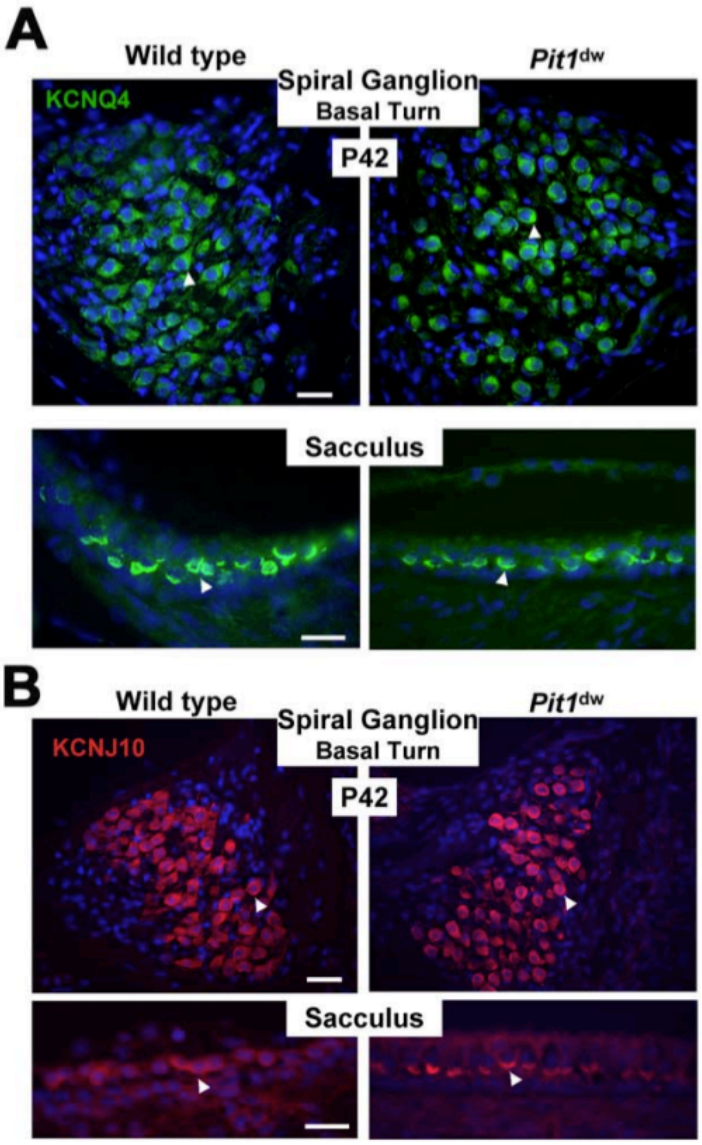

Figure S-3.
Normal KCNQ4 and KCNJ10 expression in spiral ganglion cells and in vestibular hair cells of *Pit1*^{dw} mutants.
Frozen sections from the basal turn of the cochlea of wild-type and mutant mice were collected at P42 and stained for **(A)** KCNQ4 (green) and for **(B)** KCNJ10 (red). Nuclei (blue). **(A)** KCNQ4 expression in vestibular hair cells and in spiral

ganglion cells (arrowheads) is evident in both wild-type and *Pit1*dw mutant mice**. (B)** KCNJ10 expression is readily detected in vestibular hair cells and in spiral ganglion cells (arrowheads). Scale Bars: 10μm. Similar results for KCNQ4 and KCNJ10 were obtained at P13, P21, and P60 (data not shown).

REFERENCES

Abe S, Katagiri T, Saito-Hisaminato A, Usami S, Inoue Y, Tsunoda T, Nakamura Y (2003) Identification of CRYM as a candidate responsible for nonsyndromic deafness, through cDNA microarray analysis of human cochlear and vestibular tissues. Am J Hum Genet 72:73-82.

Abe T, Kakehata S, Kitani R, Maruya S, Navaratnam D, Santos-Sacchi J, Shinkawa H (2007) Developmental expression of the outer hair cell motor prestin in the mouse. J Membr Biol 215:49-56.

Abeywickrama C, Matsuda H, Jockusch S, Zhou J, Jang YP, Chen BX, Itagaki Y, Erlanger BF, Nakanishi K, Turro NJ, Sparrow JR (2007) Immunochemical recognition of A2E, a pigment in the lipofuscin of retinal pigment epithelial cells. Proc Natl Acad Sci U S A 104:14610-14615.

Beyer LA, Odeh H, Probst FJ, Lambert EH, Dolan DF, Camper SA, Kohrman DC, Raphael Y (2000) Hair cells in the inner ear of the pirouette and shaker 2 mutant mice. J Neurocytol 29:227-239.

Bohne BA, Gruner MM, Harding GW (1990) Morphological correlates of aging in the chinchilla cochlea. Hear Res 48:79-91.

Brandt N, Kuhn S, Munkner S, Braig C, Winter H, Blin N, Vonthein R, Knipper M, Engel J (2007) Thyroid hormone deficiency affects postnatal spiking activity and expression of Ca2+ and K+ channels in rodent inner hair cells. J Neurosci 27:3174-3186.

Brown-Borg HM, Borg KE, Meliska CJ, Bartke A (1996) Dwarf mice and the ageing process. Nature 384:33.

Camper SA, Saunders TL, Katz RW, Reeves RH (1990) The *Pit-1* transcription factor gene is a candidate for the Snell dwarf mutation. Genomics 8:586-590.

Cantos R, Lopez DE, Merchan JA, Rueda J (2003) Olivocochlear efferent innervation of the organ of corti in hypothyroid rats. J Comp Neurol 459:454-467.

Cheatham MA, Huynh KH, Gao J, Zuo J, Dallos P (2004) Cochlear function in Prestin knockout mice. J Physiol 560:821-830.

Dallos P, Wu X, Cheatham MA, Gao J, Zheng J, Anderson CT, Jia S, Wang X, Cheng WH, Sengupta S, He DZ, Zuo J (2008) Prestin-based outer hair cell motility is necessary for mammalian cochlear amplification. Neuron 58:333-339.

Deol MS (1973) Congenital deafness and hypothyroidism. Lancet 2:105-106.

Eichhoff G, Busche MA, Garaschuk O (2008) In vivo calcium imaging of the aging and diseased brain. Eur J Nucl Med Mol Imaging.

Fransen E, Lemkens N, Van Laer L, Van Camp G (2003) Age-related hearing impairment (ARHI): environmental risk factors and genetic prospects. Exp Gerontol 38:353-359.

Gage PJ, Brinkmeier ML, Scarlett LM, Knapp LT, Camper SA, Mahon KA (1996) The Ames dwarf gene, *df*, is required early in pituitary ontogeny for the extinction of *Rpx* transcription and initiation of lineage specific cell proliferation. Molecular Endocrinology 10:1570-1581.

Gao J, Wang X, Wu X, Aguinaga S, Huynh K, Jia S, Matsuda K, Patel M, Zheng J, Cheatham M, He DZ, Dallos P, Zuo J (2007) Prestin-based outer hair cell electromotility in knockin mice does not appear to adjust the operating point of a cilia-based amplifier. Proc Natl Acad Sci U S A 104:12542-12547.

Gow A, Davies C, Southwood CM, Frolenkov G, Chrustowski M, Ng L, Yamauchi D, Marcus DC, Kachar B (2004) Deafness in Claudin 11-null mice reveals the critical contribution of basal cell tight junctions to stria vascularis function. J Neurosci 24:7051-7062.

Holz FG, Schutt F, Kopitz J, Volcker HE (1999) [Introduction of the lipofuscin-fluorophor A2E into the lysosomal compartment of human retinal pigment epithelial cells by coupling to LDL particles. An in vitro model of retinal pigment epithelium cell aging]. Ophthalmologe 96:781-785.

Huang G, Santos-Sacchi J (1993) Mapping the distribution of the outer hair cell motility voltage sensor by electrical amputation. Biophys J 65:2228-2236.

Johnson KR, Zheng QY (2002) Ahl2, a second locus affecting age-related hearing loss in mice. Genomics 80:461-464.

Karolyi IJ, Dootz GA, Halsey K, Beyer L, Probst FJ, Johnson KR, Parlow AF, Raphael Y, Dolan DF, Camper SA (2007) Dietary thyroid hormone replacement ameliorates hearing deficits in hypothyroid mice. Mamm Genome 18:596-608.

Kazee AM, West NR (1999) Preservation of synapses on principal cells of the central nucleus of the inferior colliculus with aging in the CBA mouse. Hear Res 133:98-106.

Kharkovets T, Dedek K, Maier H, Schweizer M, Khimich D, Nouvian R, Vardanyan V, Leuwer R, Moser T, Jentsch TJ (2006) Mice with altered KCNQ4 K+ channels implicate sensory outer hair cells in human progressive deafness. Embo J 25:642-652.

Knipper M, Zinn C, Maier H, Praetorius M, Rohbock K, Kopschall I, Zimmermann U (2000) Thyroid hormone deficiency before the onset of hearing causes irreversible damage to peripheral and central auditory systems. J Neurophysiol 83:3101-3112.

Knipper M, Bandtlow C, Gestwa L, Kopschall I, Rohbock K, Wiechers B, Zenner HP, Zimmermann U (1998) Thyroid hormone affects Schwann cell and oligodendrocyte gene expression at the glial transition zone of the VIIIth nerve prior to cochlea function. Development 125:3709-3718.

Knipper M, Richardson G, Mack A, Muller M, Goodyear R, Limberger A, Rohbock K, Kopschall I, Zenner HP, Zimmermann U (2001) Thyroid hormone-deficient period prior to the onset of hearing is associated with reduced levels of beta-tectorin protein in the tectorial membrane: implication for hearing loss. J Biol Chem 276:39046-39052.

Konig O, Ruttiger L, Muller M, Zimmermann U, Erdmann B, Kalbacher H, Gross M, Knipper M (2007) Estrogen and the inner ear: megalin knockout mice suffer progressive hearing loss. Faseb J.

Legan PK, Lukashkina VA, Goodyear RJ, Kossi M, Russell IJ, Richardson GP (2000) A targeted deletion in alpha-tectorin reveals that the tectorial membrane is required for the gain and timing of cochlear feedback. Neuron 28:273-285.

Legan PK, Lukashkina VA, Goodyear RJ, Lukashkin AN, Verhoeven K, Van Camp G, Russell IJ, Richardson GP (2005) A deafness mutation isolates a second role for the tectorial membrane in hearing. Nat Neurosci 8:1035-1042.

Li S, Crenshaw EB, 3rd, Rawson EJ, Simmons DM, Swanson LW, Rosenfeld MG (1990) Dwarf locus mutants lacking three pituitary cell types result from mutations in the POU-domain gene pit-1. Nature 347:528-533.

Li S, Price SM, Cahill H, Ryugo DK, Shen MM, Xiang M (2002) Hearing loss caused by progressive degeneration of cochlear hair cells in mice deficient for the Barhl1 homeobox gene. Development 129:3523-3532.

Liberman MC, Gao J, He DZ, Wu X, Jia S, Zuo J (2002) Prestin is required for electromotility of the outer hair cell and for the cochlear amplifier. Nature 419:300-304.

Marcotti W, Kros CJ (1999) Developmental expression of the potassium current IK,n contributes to maturation of mouse outer hair cells. J Physiol 520 Pt 3:653-660.

Marcus DC, Wu T, Wangemann P, Kofuji P (2002) KCNJ10 (Kir4.1) potassium channel knockout abolishes endocochlear potential. Am J Physiol Cell Physiol 282:C403-407.

Mustapha M, Beyer LA, Izumikawa M, Swiderski DL, Dolan DF, Raphael Y, Camper SA (2007) Whirler mutant hair cells have less severe pathology than shaker 2 or double mutants. J Assoc Res Otolaryngol 8:329-337.

Nadol JB, Jr. (1979) Electron microscopic findings in presbycusic degeneration of the basal turn of the human cochlea. Otolaryngol Head Neck Surg 87:818-836.

Nemoto M, Morita Y, Mishima Y, Takahashi S, Nomura T, Ushiki T, Shiroishi T, Kikkawa Y, Yonekawa H, Kominami R (2004) Ahl3, a third locus on mouse chromosome 17 affecting age-related hearing loss. Biochem Biophys Res Commun 324:1283-1288.

Nouvian R, Ruel J, Wang J, Guitton MJ, Pujol R, Puel JL (2003) Degeneration of sensory outer hair cells following pharmacological blockade of cochlear KCNQ channels in the adult guinea pig. Eur J Neurosci 17:2553-2562.

Oliver D, Fakler B (1999) Expression density and functional characteristics of the outer hair cell motor protein are regulated during postnatal development in rat. J Physiol 519 Pt 3:791-800.

Richardson GP, Lukashkin AN, Russell IJ (2008) The tectorial membrane: one slice of a complex cochlear sandwich. Curr Opin Otolaryngol Head Neck Surg 16:458-464.

Rozengurt N, Lopez I, Chiu CS, Kofuji P, Lester HA, Neusch C (2003) Time course of inner ear degeneration and deafness in mice lacking the Kir4.1 potassium channel subunit. Hear Res 177:71-80.

Rueda J, Prieto JJ, Cantos R, Sala ML, Merchan JA (2003) Hypothyroidism prevents developmental neuronal loss during auditory organ development. Neurosci Res 45:401-408.

Rusch A, Erway LC, Oliver D, Vennstrom B, Forrest D (1998) Thyroid hormone receptor beta-dependent expression of a potassium conductance in inner hair cells at the onset of hearing. Proc Natl Acad Sci U S A 95:15758-15762.

Rusch A, Ng L, Goodyear R, Oliver D, Lisoukov I, Vennstrom B, Richardson G, Kelley MW, Forrest D (2001) Retardation of cochlear maturation and impaired hair cell function caused by deletion of all known thyroid hormone receptors. J Neurosci 21:9792-9800.

Russell IJ, Legan PK, Lukashkina VA, Lukashkin AN, Goodyear RJ, Richardson GP (2007) Sharpened cochlear tuning in a mouse with a genetically modified tectorial membrane. Nat Neurosci 10:215-223.

Schmitz-Valckenberg S, Bultmann S, Dreyhaupt J, Bindewald A, Holz FG, Rohrschneider K (2004) Fundus autofluorescence and fundus perimetry in the junctional zone of geographic atrophy in patients with age-related macular degeneration. Invest Ophthalmol Vis Sci 45:4470-4476.

Scholtz AW, Kammen-Jolly K, Felder E, Hussl B, Rask-Andersen H, Schrott-Fischer A (2001) Selective aspects of human pathology in high-tone hearing loss of the aging inner ear. Hear Res 157:77-86.

Schuknecht HF, Gacek MR (1993) Cochlear pathology in presbycusis. Ann Otol Rhinol Laryngol 102:1-16.

Sendin G, Bulankina AV, Riedel D, Moser T (2007) Maturation of ribbon synapses in hair cells is driven by thyroid hormone. J Neurosci 27:3163-3173.

Simmler MC, Cohen-Salmon M, El-Amraoui A, Guillaud L, Benichou JC, Petit C, Panthier JJ (2000) Targeted disruption of otog results in deafness and severe imbalance. Nat Genet 24:139-143.

Uziel A (1986) Periods of sensitivity to thyroid hormone during the development of the organ of Corti. Acta Otolaryngol Suppl 429:23-27.

Uziel A, Legrand C, Ohresser M, Marot M (1983) Maturational and degenerative processes in the organ of Corti after neonatal hypothyroidism. Hear Res 11:203-218.

Van Eyken E, Van Laer L, Fransen E, Topsakal V, Lemkens N, Laureys W, Nelissen N, Vandevelde A, Wienker T, Van De Heyning P, Van Camp G (2006) KCNQ4: a gene for age-related hearing impairment? Hum Mutat 27:1007-1016.

Van't Hoff W, Stuart DW (1979) Deafness in myxoedema. Q J Med 48:361-367.

Vanderschueren-Lodeweyckx M, Debruyne F, Dooms L, Eggermont E, Eeckels R (1983) Sensorineural hearing loss in sporadic congenital hypothyroidism. Arch Dis Child 58:419-422.

Wangemann P, Itza EM, Albrecht B, Wu T, Jabba SV, Maganti RJ, Lee JH, Everett LA, Wall SM, Royaux IE, Green ED, Marcus DC (2004) Loss of KCNJ10 protein expression abolishes endocochlear potential and causes deafness in Pendred syndrome mouse model. BMC Med 2:30.

Weber T, Zimmermann U, Winter H, Mack A, Kopschall I, Rohbock K, Zenner HP, Knipper M (2002) Thyroid hormone is a critical determinant for the regulation of the cochlear motor protein prestin. Proc Natl Acad Sci U S A 99:2901-2906.

Winter H, Braig C, Zimmermann U, Geisler HS, Franzer JT, Weber T, Ley M, Engel J, Knirsch M, Bauer K, Christ S, Walsh EJ, McGee J, Kopschall I, Rohbock K, Knipper M (2006) Thyroid hormone receptors TRalpha1 and TRbeta differentially regulate gene expression of Kcnq4 and prestin during final differentiation of outer hair cells. J Cell Sci 119:2975-2984.

Zheng J, Shen W, He DZ, Long KB, Madison LD, Dallos P (2000) Prestin is the motor protein of cochlear outer hair cells. Nature 405:149-155.

CHAPTER 4

Genetic background of *Prop1*^{df} mutants provides remarkable protection against hypothyroidism induced hearing impairment

ABSTRACT

Hypothyroidism is a cause of genetic and environmentally induced deafness. The sensitivity of cochlear development and function to thyroid hormone (TH) mandates understanding TH action in this sensory organ. *Prop1*^{df} and *Pou1f1*^{dw} mutant mice carry mutations in different pituitary transcription factors, each resulting in the inability to produce pituitary thyrotropin. Despite the same lack of detectable serum TH, these mutants have very different hearing abilities: *Prop1*^{df} mutants are mildly affected, while *Pou1f1*^{dw} mutants are completely deaf. Genetic studies show that this difference is attributable to the genetic backgrounds. Using embryo transfer we discovered that factors intrinsic to the fetus are the major contributor to this difference, not maternal effects. We analyzed *Prop1*^{df} mutants to identify processes in cochlear development that are disrupted in *Pou1f1*^{dw} mutants but protected in *Prop1*^{df} mutants by the genetic background. Although outer hair cell (OHC) function develops slowly, Prestin

* Both Alicia Giordimaina and I are major contributors to this project. Alicia worked on it for her undergradute honors thesis, and I was her supervisor.

and KCNQ4 expression are normal in mature *Prop1*^{df} mutants. The endocochlear potential and KCNJ10 expression in the stria vascularis are also normal, and no differences in neurofilament or synaptophysin staining are evident in *Prop1*^{df} mutants. The synaptic vesicle protein otoferlin normally shifts expression from OHC to IHC as temporary afferent fibers beneath the OHC regress postnatally. *Prop1*^{df} mutants exhibit persistent, abnormal expression of otoferlin in apical OHC, suggesting incomplete regression of afferent fibers. Thus, the genetic background of *Prop1*^{df} mutants is remarkably protective for most functions except otoferlin expression in the cochlear apex. The *Prop1*^{df} mutant is an attractive model for identifying the genes that protect against deafness.

INTRODUCTION

Congenital hypothyroidism (CH) occurs in about 1/4000 live births. Low TH levels can affect a child's neural development and auditory function to cause severe cognitive dysfunction and deafness (Debruyne et al., 1983; Rovet et al., 1996). However, the extent of hearing impairment varies among patients with CH, and the cause of this variability is not clear.

The etiology of CH includes dysgenesis of thyroid gland (primary), failure of pituitary gland or hypothalamus (secondary), and maternal iodine deficiency. Animal models simulating different hypothyroid conditions have been utilized to discover defects in the cochlear development (Uziel et al., 1983; Uziel et al.,

1985b; Uziel et al., 1985a; O'Malley et al., 1995; Li et al., 1999; Knipper et al., 2001; Christ et al., 2004; Mustapha et al., 2009). The Ames dwarf (*Prop1*$^{df/df}$) and Snell dwarf (*Pouf1*$^{dw/dw}$, also known as *Pit1*$^{dw/dw}$) mice are models of recessive, secondary hypothyroidism (Karolyi et al., 2007). These mice carry inactivating, missense mutations in the genes encoding paired-like homeodomain transcription factors Prophet of Pit-1 (*Prop1*), and *Pou1f1*, respectively. These genes are expressed in the pituitary gland, with no detectable expression in the cochlea (Gage et al., 1996; Sornson et al., 1996). *Prop1*$^{df/df}$ mutants fail to activate expression of *Pou1f1*, which results in the failure of initial determination of the lineage of cell types required for production of growth hormone (GH), prolactin (PRL), and thyroid-stimulating hormone (TSH) (Sornson et al., 1996). Thus, both *Prop1* and *Pou1f1* mutants lack TSH and TH due to failure of the pituitary TSH cells to develop.

Despite the fact that *Prop1* and *Pou1f1* encode pituitary transcription factors in the same developmental pathway and induce indistinguishable TH deficiencies, the degrees of hearing impairment in the two mutants are very different (Karolyi et al., 2007). At six weeks of age, *Prop1*$^{df/df}$ mice exhibit hearing thresholds of about 40 dB SPL (sound pressure level), representing a deficit of 13~17 dB SPL threshold shift relative to normal mice of the DF strain at 4, 10, and 20 kHz, while *Pou1f1*$^{dw/dw}$ mice have severe deafness with thresholds >100 dB, representing a 38~81 dB shift relative to normal mice on the DW strain. To determine the basis for this difference, Karolyi et al. (2007) performed an intercross between the two strains. The mixed DF and DW genetic background

results in F2 *Pou1f1* mutants with improved hearing and *Prop1* mutants with worse hearing than observed on the original DW and DF backgrounds, respectively. This indicates that genetic background, or genomic variation, accounts for the differences in hearing between *Prop1*$^{df/df}$ and *Pou1f1*$^{dw/dw}$ mutants (Karolyi et al., 2007).

Maternal thyroid function can also affect the hearing abilities of humans and other animals. In areas with endemic cretinism, deafness is equally prevalent in euthyroid and hypothyroid patients, suggesting the maternal hypothyroidism may cause a low TH level in utero which results in auditory dysfunction in the euthyroid children (Boyages and Halpern, 1993; Chan et al., 2009). A thyroid ablation study in sheep demonstrated that maternal and fetal hypothyroxinemia combine to cause neurological damage (McIntosh et al., 1983). Goitrogen treatment of pregnant and lactating rodents between the onset of fetal thyroid gland function (*E17~18*) and the onset of hearing at *postnatal day 12* (P12) can lead to permanent hearing defects in the offspring (Deol, 1973; Knipper et al., 2000). In addition, elevated maternal thyroid peroxidase autoantibodies during the third trimester are also associated with hearing deficits in children (Wasserman et al., 2008). Taken together, maternal effects including maternal TH level, gestation time, and maturity of the fetus at birth, could affect the sensitivity of genetically predisposed hypothyroid animals to hearing impairment.

Pleiotropic effects of hypothyroidism on cochlear development have been demonstrated in several different TH-deficient animal models (O'Malley et al., 1995; Knipper et al., 1998; Li et al., 1999; Knipper et al., 2000; Knipper et al.,

2001; Ng et al., 2001; Griffith et al., 2002; Brandt et al., 2007; Sendin et al., 2007; Mustapha et al., 2009; Wangemann et al., 2009; Winter et al., 2009). The *Pou1f1*$^{dw/dw}$ mutants exhibit immature cochlear morphology, tectorial membrane abnormalities, reduced expression and function of potassium channels, hair cell loss, and strial cell deterioration (Mustapha et al., 2009). Several of these features have been reported in hypothyroid rodent models induced by thyro-toxic drugs or other genetic lesions, suggesting that there are common effects of TH deficiency. Because of the diversity of effects, TH likely regulates multiple, critical processes of inner ear development. It still remains to be determined which processes are most sensitive to TH deficiency and to what degree the observed effects contribute to the hearing problems in the hypothyroid animals.

We explored the maternal contribution to the genetic background effects on *Prop1* and *Pou1f1* mutants by transferring fertilized *Prop1*$^{df/df}$ and *Pou1f1*$^{dw/dw}$ eggs to common surrogate mothers for gestation and nursing, and found no significant effects. This suggests that factors intrinsic to the fetus play the major roles in the varying responses of *Prop1*^{df} and *Pou1f1*^{dw} mutant cochlea to hypothyroidism. Most studies have focused on hypothyroid rodent models with severe hearing impairment. We examined the mildly affected *Prop1*^{df} mutants to determine which developmental processes are rescued by the genetic background, and which functions remain defective. We determined that many aspects of cochlear development are initially delayed in *Prop1* mutants, but they eventually mature to become indistinguishable from wild type. The only persistent abnormality we observed was immature otoferlin expression. This suggests that

a mild exocytosis defect may account for the mild hearing problems in *Prop1*$^{df/df}$ mutants. Overall, with its mild hearing deficit despite the severe hypothyroidism, *Prop1*^{df} mice provide a valuable tool for us to explore the cause of variation in hearing impairment in hypothyroid mice and humans and to identify the potential modifiers that protect against hearing loss due to hypothyroidism.

METHODS AND MATERIALS

Mice

All experiments were approved by the University Committee on the Use and Care of Animals and conducted in accord with the principles and procedures outlined in the National Institutes of Health Guidelines.

DF/B-*p/+, Prop1*^{df} mice were obtained from Dr. Andrzej Bartke in 1988 and maintained at the University of Michigan. This stock is not inbred but has gone through population constriction. DW/J-*Mlph*$^{ln/ln}$*, Pou1f1*^{dw} mice were obtained from The Jackson Laboratory (Bar Harbor, ME). The DW/J stock is inbred, but not defined. B6/D2 mice are the F1 hybrids produced by breeding C57BL/6J and DBA/2J mouse strains. These hybrids were purchased from The Jackson Laboratory.

Previously described procedures for animal care and genotyping were used, including feeding mice a higher fat chow designed for breeding (PMI5020), delaying weaning of mutants until 35 d, and housing mutants with normal

littermates to provide warmth (Karolyi et al., 2007). Mice were in a specific pathogen free facility with automatic watering and ventilated cages. In all experiments, at least 3 animals of each genotype were analyzed for each age group studied unless stated otherwise. Embryonic days gestation are counted from the time of conception with e0.5 denoting the morning after mating. Postnatal day zero (P0) is designated as the day of birth.

Embryo transfer experiments

Three to four week old *Prop1*$^{df/+}$ or *Pou1f1*$^{dw/+}$ females were superovulated by intraperitoneal injection of 5 U each of pregnant mare serum gonadotropin (PMSG) followed by human chorionic gonadotropin (HCG) 46 ~ 50 hours later. Females were placed with heterozygous males of the same genotype, i.e. *Prop1*$^{df/+}$ or *Pou1f1*$^{dw/+}$, for overnight mating. *E0.5* embryos (1-cell stage) were collected from fallopian tubes of the plugged females and cultured in M16 medium (Sigma) with penicillin and streptomycin at 37^{o}C incubator overnight. Eight 2-cell stage embryos were put into one oviduct of each pseudo-pregnant B6/D2 female, which were generated by mating with vasectomized B6/D2 males. Wild type 2-cell stage B6/D2 embryos were placed in the oviduct on the opposite side of the same pseudo-pregnant female. Pups born and weaned from surrogate mothers were genotyped and evaluated for hearing. Wild type mice with the same coat color as the mutants were used as controls. For simplicity, "_S" is added to genotype symbols to represent mice born from surrogate mother in this article.

Auditory physiology

Auditory brainstem response (ABR*),* distortion product otoacoustic emissions (DPOAEs) and endocochlear potential (EP) were measured as previously described (Karolyi et al., 2007).

Antibodies

The antibodies used to detect prestin (1:200), KCNJ10 (1:300), KCNJ4 (1:300) synaptophysin (1:400), TRITC-labeled secondary antibodies (1:200) and Alexa Fluor 488 conjugated secondary antibodies (1:200) have been previously described (Mustapha et al., 2009). The rabbit polyclonal anti-Neurofilament 200 antibody (1:500, Sigma) is commercially available. The rabbit polyclonal anti-otoferlin antibody (1:500) was kindly provided by Dr. Christine Petit (Roux et al., 2006).

Immunohistofluorescence

Preparation of cochlear cryosections and the procedures for immunostaining those sections have been previously described (Mustapha et al., 2009).

Whole mount immunofluorescence

Mouse inner ears were rapidly dissected from the temporal bones in phosphate-buffered saline (PBS). The temporal bones were immersed in 4% paraformaldehyde (PFA) for fixation. Under stereoscopic magnification, the round and oval windows were opened, and the bone from the apical tip of the

cochleae was removed to allow fixative to flow throughout the tissue. One hour later, the stria vascularis and tectorial membrane were removed and the organ of Corti was exposed. After two washes in PBS, the tissue was incubated in 5% normal goat serum with 0.3% triton for 1 hour, and then with the primary antibody at 4°C overnight. After three washes in PBS, samples were incubated with the secondary antibody for 2 hours at room temperature, washed again three times in PBS and mounted in ProLong Gold Antifade Reagent (Invitrogen). All fluorescent microscopy was performed on a Leica Leitz DMRB compound microscope with Leica Fiber Optic Illumination. Images were captured using a QImaging Retiga 2000R Fast 1394 camera and QCapture Pro 5.1.1.14 software. Images were processed using Adobe® Photoshop® CS2 9.0.

Statistical Analysis

All statistical analyses were performed with SPSS 15.0. The *p* values reported for ABR were generated by independent samples t-tests or Tukey's multiple comparisons following oneway ANOVA. Error bars represent standard deviation for means.

RESULTS

Prop1$^{df/df}$ mutants have a mild hearing deficit

ABR tests were used to determine the hearing proficiency of *Prop1*$^{df/df}$ mutants as well as wild type controls. At 4 weeks old the ABR thresholds of

Prop1$^{df/df}$ mutants are elevated relative to controls by 21 dB SPL and 34 dB SPL at 4 kHz and 20 kHz, respectively (Fig. 4-1, P<0.05). When the mice are 6~7 weeks old, mutant hearing has improved but is still worse than normal, with elevations of 11 and 14 dB SPL at 4 and 20 kHz, respectively (Fig. 4-1, P<0.001). This indicates that the cochlear development of *Prop1*$^{df/df}$ mutants undergoes maturation between 4 and 7 weeks of age, but it does not achieve wild type function. This is consistent with previous reports that measured different ages of conventionally housed mice at different frequencies (Karolyi et al., 2007).

Gestational and neonatal environments do not account for variant responses to hypothyroidism in *Prop1*$^{df/df}$ and *Pou1f1*$^{dw/dw}$ mutants

To determine the degree to which maternal effects contribute to the different degrees of hearing impairment in *Prop1*$^{df/df}$ and *Pou1f1*$^{dw/dw}$ mutants, the fertilized eggs from all genotypes from both strains were transplanted into the uteri of B6/D2 surrogate mothers, which would provide common gestation and lactation environments for both mutants. We chose the mothers of the B6/D2 strain as surrogates because they have hybrid vigor and exhibit good mothering instincts. The hearing ability of the progeny born to the surrogates was tested by ABR at four weeks of age, including *Prop1*$^{df/df}$_S and *Pou1f1*$^{dw/dw}$_S mutants as well as wild types from each strain. The hearing deficits of *Prop1*$^{df/df}$_S and *Pou1f1*$^{dw/dw}$_S mutants are significantly different from their normal littermates and

from each other, but they are indistinguishable from the *Prop1*$^{df/df}$ and *Pou1f1*$^{dw/dw}$ mice born to mothers from their own backgrounds (Fig. 4-2, P<0.001 at both 4 kHz and 20 kHz). Thus, factors intrinsic to the fetus play the major roles in the different responses of *Prop1*$^{df/df}$ and *Pou1f1*$^{dw/dw}$ mutant cochlea to hypothyroidism, and maternal effects are minimal in this context.

Mild outer hair cell (OHC) dysfunction with normal expression of KCNQ4 and prestin in *Prop1*^{dfdf} mutants

Cochlear OHCs are unique in their electromotility and work as a cochlear amplifier in sound processing (Ospeck et al., 2003). DPOAE is used as a standard audiometric technique to measure OHC function of amplification. At four weeks of age, *Prop1*$^{df/df}$ mutants have DPOAE responses at 12 or 24 kHz that are indistinguishable from the noise floor in postmortem mutant or wild type mice (Fig. 4-3 A). By seven weeks old, *Prop1*$^{df/df}$ mutants and wild types have similar DPOAE levels at 12 kHz frequency, but the mutants have only 50% of normal cochlear sensitivity at 24 kHz (Fig. 4-3 A). The maturation process of DPOAE in mice begins from lower frequencies at P11 and obtains the adult-like pattern at higher frequencies by P28 (Narui et al., 2009). This demonstrates that *Prop1*$^{df/df}$ mutant cochlea have delayed development of OHC function. ABR measurements also improve between four and seven weeks of age (Fig. 4-1), suggesting that the OHC dysfunction could be the major contributor to the mild hearing impairment in *Prop1*$^{df/df}$ mutants.

KCNQ4 is an M-type K+ channel localized exclusively to the basal pole of the hair cells, and it is responsible for the dominant K+ conductance in mature OHCs (Marcotti and Kros, 1999; Kharkovets et al., 2000). Mutations in KCNQ4 cause progressive deafness in both human and mice (Kubisch et al., 1999; Kharkovets et al., 2006). *Pou1f1*$^{dw/dw}$ mutant mice have permanently reduced expression and function of KCNQ4 in OHCs (Mustapha et al., 2009). We examined KCNQ4 expression in *Prop1*$^{df/df}$ mutant cochlea at four weeks. Normal levels and localization of KCNQ4 immunoreactivity are present in *Prop1*$^{df/df}$ mutants relative to wild types (Fig. 4-3 B and C). The normal expression pattern exists in seven-week old mutants (data not shown), despite the permanent hearing deficit shown by ABR and DPOAE at this age. The DF/B genetic background supports normal KCNQ4 expression despite the severe hypothyroidism.

Prestin (SLC26A5) is a member of the sulfate transporter family proteins (Lohi et al., 2000) and is expressed along the basolateral membrane of OHCs (Adler et al., 2003; Yu et al., 2006), conferring electromotility to the OHCs (Zheng et al., 2000). Prestin is transcriptionally regulated by TH during final differentiation of outer hair cells (Weber et al., 2002; Winter et al., 2006). Prestin is required for normal OHC length (Liberman et al., 2002). We examined prestin expression in *Prop1*$^{df/df}$ mutants by immunohistochemistry. There is no significant difference in prestin expression levels in OHCs of mutants and wild types at 4 weeks of age (Fig. 4-3 D and E). Prestin localizes at the lateral wall of *Prop1*$^{df/df}$ mutant OHCs, which is the expected mature pattern (Fig. 4-3 D and E).

OHC length is not apparently affected in *Prop1*$^{df/df}$ mutants either. Thus, the DF/B genetic background of the *Prop1* mutants supports the development of prestin expression and localization.

Developmentally delayed expression of KCNJ10 in the stria vascularis and normal EP in *Prop1*$^{df/df}$ mutants

Endocochlear potential (EP) is the driving force for the transduction of ions through the channels in hair cell stereocilia. An EP level of +80mV is essential for normal hearing. Since EP affects the amplitude of DPOAE, EP was also examined in the present study. The EP of 7-week-old *Prop1*$^{df/df}$ mutants ranges from 81 to 93 mV (N=3), which is indistinguishable from the EP levels (88 to 92 mV, N=2) in wild types (Fig. 4-4). Thus, the poor DPOAE in *Prop1*$^{df/df}$ mutants likely results from defective OHCs, not abnormal EP.

KCNJ10 (Kir4.1) K^+ channels in the intermediate cells of the stria vascularis are required for generation of a normal EP (Marcus et al., 2002). Permanent reduction of KCNJ10 expression was observed in *Pou1f1*$^{dw/dw}$ mutants, which accounts for the substantially reduced EP in those mice (Mustapha et al., 2009). We examined the KCNJ10 expression in 4 and 6 week old *Prop1*$^{df/df}$ mutants by immunohistochemical staining. At 4 weeks of age, the KCNJ10 fluorescence levels are lower in mutants than wild types (Fig. 4-4B). By 6 weeks of age, the KCNJ10 fluorescence levels in the mutant are indistinguishable from the wild types (Fig. 4-4B). The subcellular localization of

KCNJ10 is normal in both the 4-week-old mutant and 6-week-old mutant. This is consistent with the normal EP observed. Thus, the DF/B-*Prop1*^{df} genetic background protects against permanent reduction of KCNJ10 in the absence of TH.

Gross neurite outgrowth and synaptogenesis of OHCs are unaffected in *Prop1*$^{df/df}$ mutant cochlea

The maturation of the nervous system in the rodent cochlea takes place during the first two postnatal weeks of life, which overlaps with the critical time window of TH function (Knipper et al., 2000). TH deprivation causes abnormalities in cochlear innervation and synaptogenesis in multiple hypothyroid animal models (Uziel et al., 1983; Brandt et al., 2007; Sendin et al., 2007). Neuronal marker proteins are usually used for examination of the innervation patterns. We used antibodies that recognize the neurofilament protein NF-200, which stains both afferent and efferent fibers, to detect the neurite outgrowth in *Prop1*$^{df/df}$ mutant cochlea at 4 and 7 weeks. No significant differences were observed between mutants and wild types in terms of gross number and patterning of neuronal fibers at 4 weeks (Fig. 4-5 B) or 7 weeks (data not shown). Synaptophysin is a presynaptic marker of efferent fibers, which comprise 95% of the fibers innervating OHCs. A strong and normally organized pattern of synaptophysin staining was observed in both *Prop1*$^{df/df}$ mutants (Fig. 4-5 A). Thus, neither the gross neurite outgrowth nor the efferent synaptogenesis of OHCs are affected by low TH levels in DF/B-*Prop1*$^{df/df}$ mice.

Prolonged presence of otoferlin in apical OHCs of *Prop1*$^{df/df}$ mutants

Otoferlin is thought to be the major calcium sensor and essential for exocytosis at both inner hair cell (IHC) and immature OHC ribbon synapses (Roux et al., 2006; Beurg et al., 2008). Expression of otoferlin begins prenatally in both IHCs and OHCs and vanishes from OHCs by P6 (Roux et al., 2006). The absence of otoferlin in OHCs parallels the retraction of afferent fibers from OHCs, which is an important event for OHC maturation (Beurg et al., 2008). Together with myosin VI, otoferlin is involved in the maintenance of the basolateral synaptic structure of IHCs (Heidrych et al., 2009). We examined the expression of otoferlin by immunostaining whole-mount and cryosectioned tissues. Similar expression levels of otoferlin were seen in IHCs of *Prop1*$^{df/df}$ mutant cochlea as the wild type. Abnormally strong otoferlin staining persists in the OHCs in the apical coil of 6-week-old *Prop1*^{df} mutant cochlea (Fig. 4-6 C and D). Weak otoferlin immunostaining is expected in the OHCs in the apical region of mature cochlea in wild type animals (Roux et al., 2006), but none was observed in the *Prop1* wild types (Fig. 4-6), which may be due to strain differences or sensitivity of detection. Thus, the prolonged existence of otoferlin expression in apical OHCs of mutant cochlea may reflect the immaturity of the cells.

DISCUSSION

Maternal effects are minimal for variation of hearing deficits between *Prop1*$^{df/df}$ and *Pou1f1*$^{dw/dw}$ mutants

Maternal effects are defined as the causal influence of the maternal genotype or phenotype on the phenotype of the offspring (Wolf and Wade, 2009). Based on this definition, maternal effects may include direct or indirect consequences of maternal traits, such as nesting behavior, gene transcription, hormone levels, antibodies, placental permeability, and the particular environments in which mothers lay eggs (Rhees et al., 1999; Wolf and Wade, 2009). In mammals, the role of maternal effects exist at two distinct maternal stages---prenatal uterine and postnatal nursing and nurturing. By transferring embryos between two inbred mouse strains with large body size (C3H) and small body size (SWR), both uterine and postnatal maternal effects were proven to contribute to the prenatal and early postnatal development of offspring, and no obvious donor genotype effects were observed (Cowley et al., 1989; Pomp et al., 1989; Rhees et al., 1999).

The hearing abilities of progeny are substantially affected by maternal TH levels in both human and rodents (Boyages and Halpern, 1993; Knipper et al., 2001). In our breeding scheme the mothers of *Prop1*$^{df/df}$ and *Pou1f1*$^{dw/dw}$ mutants are heterozygous for the recessive *Prop1* and *Pou1f1* mutations, respectively. Thus, maternal TH levels are in the normal range. We expected that strain differences in normal basal TH levels transferred to the fetus or neonate through the placenta or milk, respectively, could contribute to the different levels of hearing impairment characteristic of *Prop1*$^{df/df}$ and *Pou1f1*$^{dw/dw}$ mutant mice. In addition, it is possible that strain differences in gestation time or maturity at birth that are controlled by the mother could influence the effects of fetal

hypothyroidism on hearing deficit. For example, longer gestation time might allow a hypothyroid fetus to benefit from maternal TH long enough to protect it during the critical period for TH dependent cochlear development.

Our embryo transfer experiments demonstrated that a consistent mothering environment does not significantly change the hearing deficits in *Prop1*$^{df/df}$ and *Pou1f1*$^{dw/dw}$ mutants from the ones they exhibit when born from mothers on the original backgrounds. From this striking result we conclude that the strain differences intrinsic to the fetus play the major role in inducing different hearing deficits between *Prop1*$^{df/df}$ and *Pou1f1*$^{dw/dw}$ mutants. Other strain combinations might reveal strong maternal effects, however, because there are compelling data to support the importance of maternal thyroid hormone for development (Deol, 1973; Knipper et al., 2000). Future genetic studies with DF/B-*Prop1* and DW/J-*Pou1f1* mutants may identify loci that enhance or suppress the ability of hypothyroid mice to develop normal hearing, and the results of the embryo transfer studies direct the focus to factors intrinsic to the fetus and/or neonate.

The effects of genetic background on hearing ability in mice are noted in many inbred strains. The most familiar example is that C57BL/6J mice carry a mutation in cadherin 23 (*Cdh23*) known as *Age-related hearing locus (Ahl)* and develop progressive deafness after 10 months. QTL analysis has identified several modifiers of hearing impairments (Ikeda et al., 1999; Ikeda et al., 2002; Drayton and Noben-Trauth, 2006; Mashimo et al., 2006; Noguchi et al., 2006; Van Eyken et al., 2006; Ohlemiller et al., 2010). We expect that QTL analysis of

DF/B and/or DW/J strains could identify the protective and susceptibility genes for hypothyroidism induced hearing impairment. These modifiers could also be genes involved in Mendelian hearing defects, as mutations in *Cdh23* also account for nonsyndromic autosomal recessive deafness *DFNB12*.

Delayed maturation of innervation may account for the mild hearing impairment in *Prop1*$^{df/df}$ mutants

The only permanent abnormality we observed in *Prop1*$^{df/df}$ mutant cochlea is prolonged existence of otoferlin in OHCs and reduced expression in IHC at the apical turn of the sensory epithelium. This indicates that maturation of cochlear innervation is not completely protected by *Prop1*^{df} genetic background. During normal neurodevelopment in the cochlea, otoferlin initially is expressed in IHCs and immature OHCs. By P6, the disappearance of otoferlin from OHCs parallels the retraction of afferent dendrites and formation of efferent synapses (Roux et al., 2006). Thus, abnormal persistence of otoferlin in *Prop1*$^{df/df}$ mutant OHCs implies an immature innervation pattern at the level of OHCs. The effects of hypothyroidism on the cochlear nervous system are expected to be mostly associated with OHC wiring (Uziel et al., 1983) because maturation of synaptogenesis at the IHC is achieved at birth while the pattern of synapses at OHC exhibit drastic changes within the first two postnatal weeks. The perinatal period is the critical time window of TH functioning for normal hearing, and it could influence both IHC and OHC synapse remodeling. In *Prop1*$^{df/df}$ mutant

cochlear the prolonged persistence of otoferlin staining in OHCs was only observed at apical turn. The order of cochlear maturation is from the basal turn to the apical turn. The delayed maturation of innervation pattern in the apical OHCs is consistent with the mild degree of hearing impairment in *Prop1*$^{df/df}$ mutants.

Usually IHC dysfunction corresponds to severe hearing loss because IHCs are the master sound sensors within the cochlea. The maturation of ribbon synapses in IHCs are affected by hypothyroidism in rodents mice (Brandt et al., 2007; Sendin et al., 2007). In those studies, the expression of otoferlin in IHCs was completely absent or substantially reduced in drug-treated rats and *Pax8* knockout mice, respectively. We observed reduced otoferlin expression in the IHCs of *Pou1f1*$^{dw/dw}$ mutants also (data not shown). This is quite different from the *Prop1*$^{df/df}$ mutants, which preserved almost normal otoferlin expression level in IHCs. The regulator(s) of otoferlin expression in IHCs would be candidates for the modifier(s) in the *Prop1*^{df} genetic background that protect hearing against hypothyroidism.

Gene regulation by TH is complicated during cochlear development and could be substantially affected by genetic background

We examined expression of several cochlear genes that are affected in other hypothyroid animal models. In *Pou1f1*$^{dw/dw}$ mutants, prestin expression and localization are developmentally delayed, but they become indistinguishable from

normal littermates by 6 weeks (Mustapha et al., 2009). The capacitance levels in mutants this age are compatible with levels in young hearing mice, consistent with normal prestin function. In *Prop1*$^{df/df}$ mutants, however, both expression and localization of prestin are not affected by the absence of TH, suggesting prestin function is not strictly TH-dependent. TH response elements (TREs) exist within prestin gene and are transactivated by TH receptor (TR), retinoid X receptor (RXR) heterodimers (Weber et al., 2002). The *Prop1*^{df} genetic background may support either RXR or an as yet uncharacterized heterodimer partner of TRs interacting with TREs to compensate the absence of TH to activate prestin gene. Alternatively, completely independent transcriptional controls elements or factors may compensate.

KCNQ4 expression is permanently reduced in *Pou1f1*$^{dw/dw}$ mutants (Mustapha et al., 2009), but *Prop1*$^{df/df}$ mutants have normal KCNQ4 expression. TRalpha1 receptors regulate KCNQ4 expression during final differentiation of OHCs (Winter et al., 2006). TRalpha1 knockout mice, however, do not exhibit hearing impairment, which implies that the activation of KCNQ4 gene cannot solely depend on TH/TR pathway (Rusch et al., 1998). A novel TH-signaling pathway can bypass TRs to mediate TH regulation (Shibusawa et al., 2003). It will be interesting to determine which TR and TH independent pathway activates KCNQ4 on the *Prop1*^{df} mutant background.

Permanently reduced KCNJ10 expression in the stria vascularis contributes to the reduction of EP level in *Pou1f1*$^{dw/dw}$ mutants (Mustapha et al., 2009). In the *Prop1*$^{df/df}$ mutants, EP level is normal and expression of KCNJ10 is

developmentally delayed but reaches normal level by 6 weeks old. It is not known whether TH directly regulates *Kcnj10* transcription in susceptible strains or whether it influences the stability of the protein. Differences in scaffolding protein expression can have profound, pleiotropic effects on protein stability (Heydemann and McNally, 2007).

The roles of the TH, TR complex in gene regulation have been widely documented in many physiological fields including development, homeostasis, cell proliferation and differentiation, etc. The downstream effects of TH/TRs on gene expression can be either activation or repression. A comparison of the cochlea gene expression profiles from *Pou1f1*$^{dw/dw}$ mutants and wild types revealed that half of the genes are up-regulated and half are down-regulated in *Pou1f1*$^{dw/dw}$ mutants (Tzy-wen Gong, unpublished data). This proves the complexity of gene regulation by TH. It is intriguing that the genetic background of *Prop1* mice can rescue expression of so many genes in the absence of TH. We favor a model involving genetic variation in a TH responsive transcription factor in the cochlea or alteration that boosts the effective level of thyroid hormone in the cochlea (van der Deure et al., 2010). This could account for improvement in many TH dependent processes in the presence of the DF/B background. Alternatively, there could be a complex set of genes that contribute to the protective effects. Sorting out this difference could be very important for us to identify the genes and pathways that are the most sensitive to TH regulation in inner ear development.

In conclusion, the *Prop1*$^{df/df}$ mutant mice lack TH, yet they exhibit only a mild hearing deficit. This mild hearing impairment may due to the immature innervation pattern of apical OHCs in the cochlea. The genetic background of *Prop1* mice can compensate for many cochlear developmental processes that are apparently dependent on TH in other strains. Identification of the protective factor(s) for hypothyroidism-induced hearing loss would help us understand the mechanism of gene regulation by TH in the inner ear and potentially identify novel genes involved in the normal auditory function.

ACKNOWLEDGEMENTS

We would like to thank Maggie Van Keuren, Ph.D. and the Transgenic Animal Model Core of the University of Michigan for performing the embryo transfer, Dr. David Dolan's lab at Kresge Hearing Research Institute for ABR tests and Dr. Mirna Mustapha for intellectual contributions.

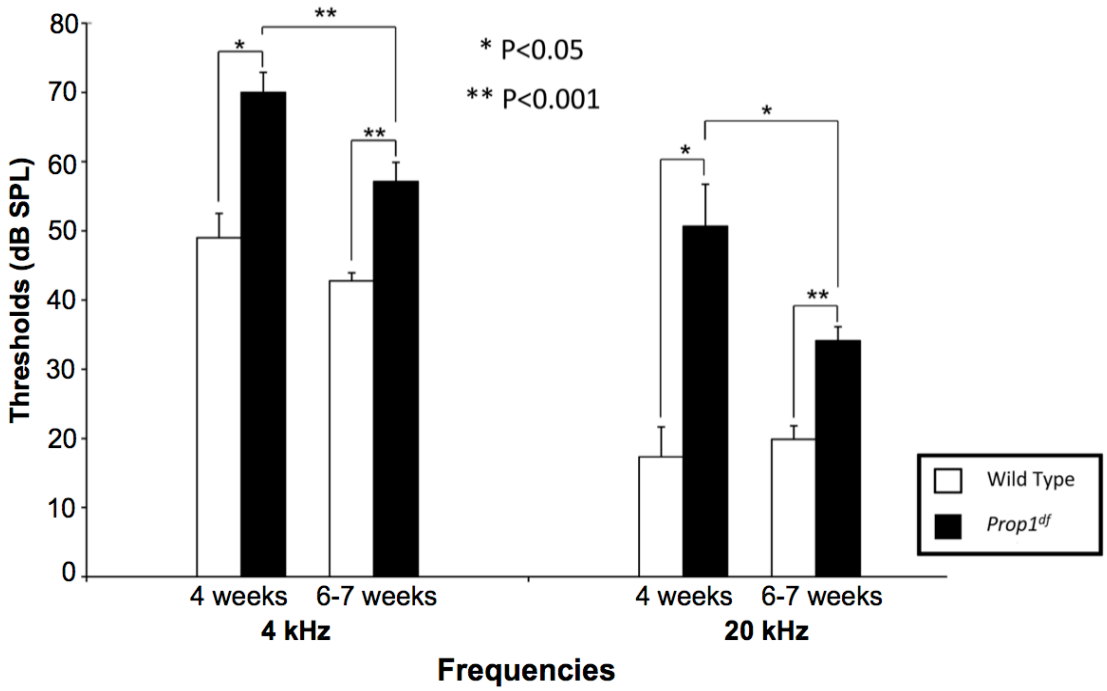

Figure 4-1. *Prop1*^{df} mutants have a mild hearing deficit.

ABR tests were performed on sets of normal mice (white bars) and mutant mice (black bars) at ages of 4 weeks and 6-7 weeks. N=3 per genotype at 4 wk, n=9 for 6-7 wk old wild type, and n=8 for 6-7 wk old mutant.

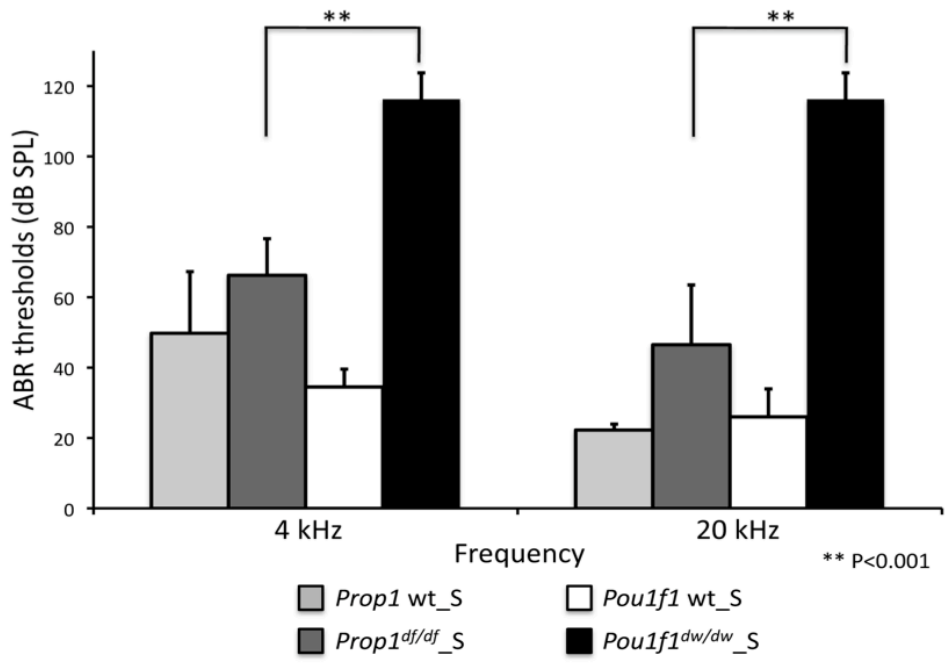

Figure 4-2. Gestational and neonatal environments do not account for different hearing abilities of *Prop1*^{df} and *Pou1f1*^{dw} mutants.

Pups born from surrogate mothers (designated as "Genotype_S") were tested by ABR. The hearing deficits of *Prop1*$^{df/df}$_S and *Pou1f1*$^{dw/dw}$_S are significantly different (P<0.001). For each group, four mice were tested (n=4).

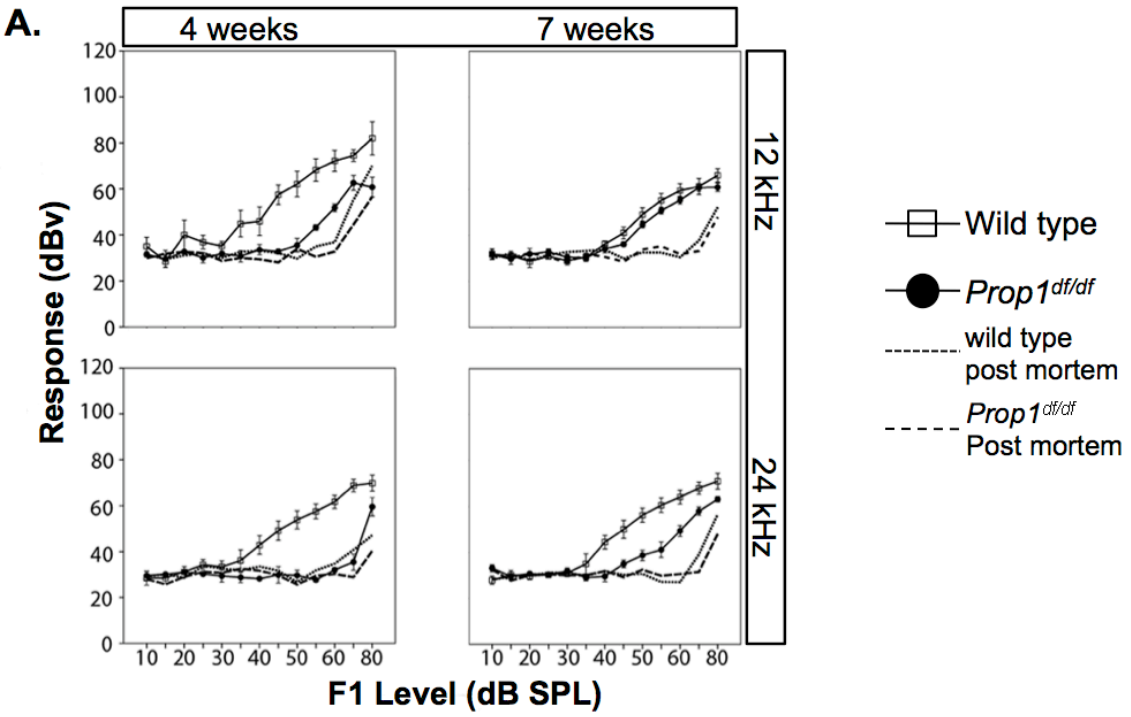
A.
4 weeks
7 weeks
12 kHz
24 kHz
Response (dBv)
F1 Level (dB SPL)
Wild type
Prop1df/df
wild type post mortem
Prop1df/df Post mortem

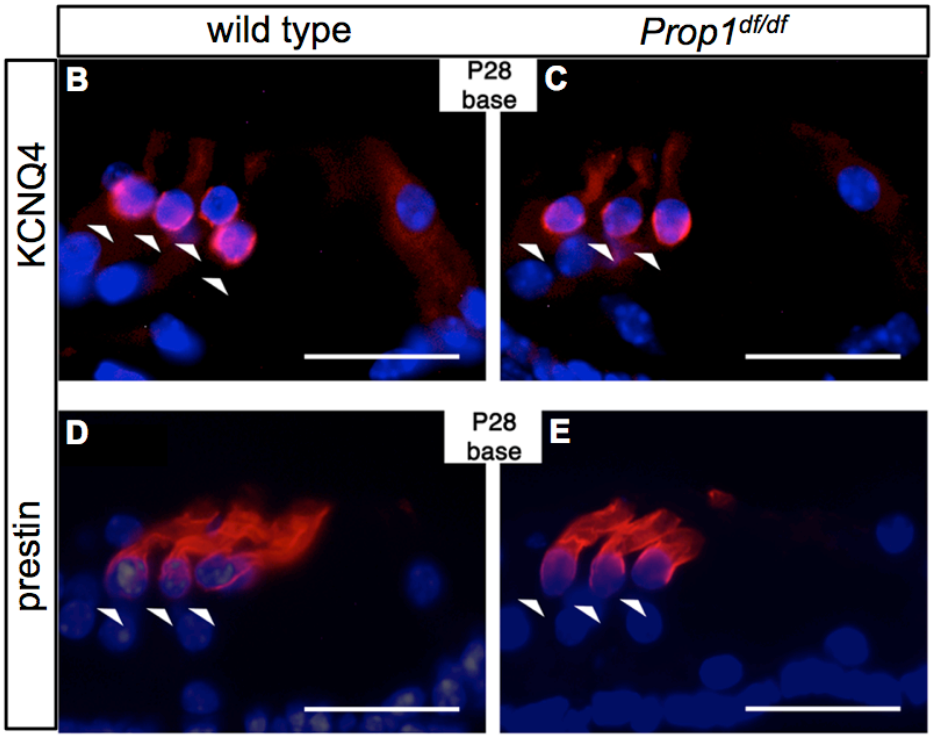
wild type
Prop1df/df
KCNQ4
prestin
B
C
D
E
P28 base
P28 base

Figure 4-3. *Prop1*^{df} mutants exhibit mild OHC dysfunction with normal expression of KCNQ4 and prestin.

A. DPOAEs were measured in live 4 wk and 7 wk old wild type and *Prop1*^{df} mutant mice (black circles and white squares, respectively), and compared with DPOAEs of postmortem animals (dotted and dashed line). Data are shown for the 12 and 24 kHz frequencies. N=3 for each genotype group of 4 wk old mice and n=6 for 7 wk. **(*B,C*).** KCNQ4 immunoreactivity is normal in OHCs (arrows) of mutant mice relative to wild type. Frozen sections obtained from P28 wild type and mutant mice were stained for KCNQ4 (red). Nuclei were stained with DAPI (blue). **(*D,E*).** Prestin expression and localization was analyzed by staining frozen sections from wild type and *Prop1*^{df} mutants at P28 with prestin-specific antibodies (red). Nuclei were labeled using DAPI (blue). Arrows identify rows of outer hair cells. Scale bars: 10 μm.

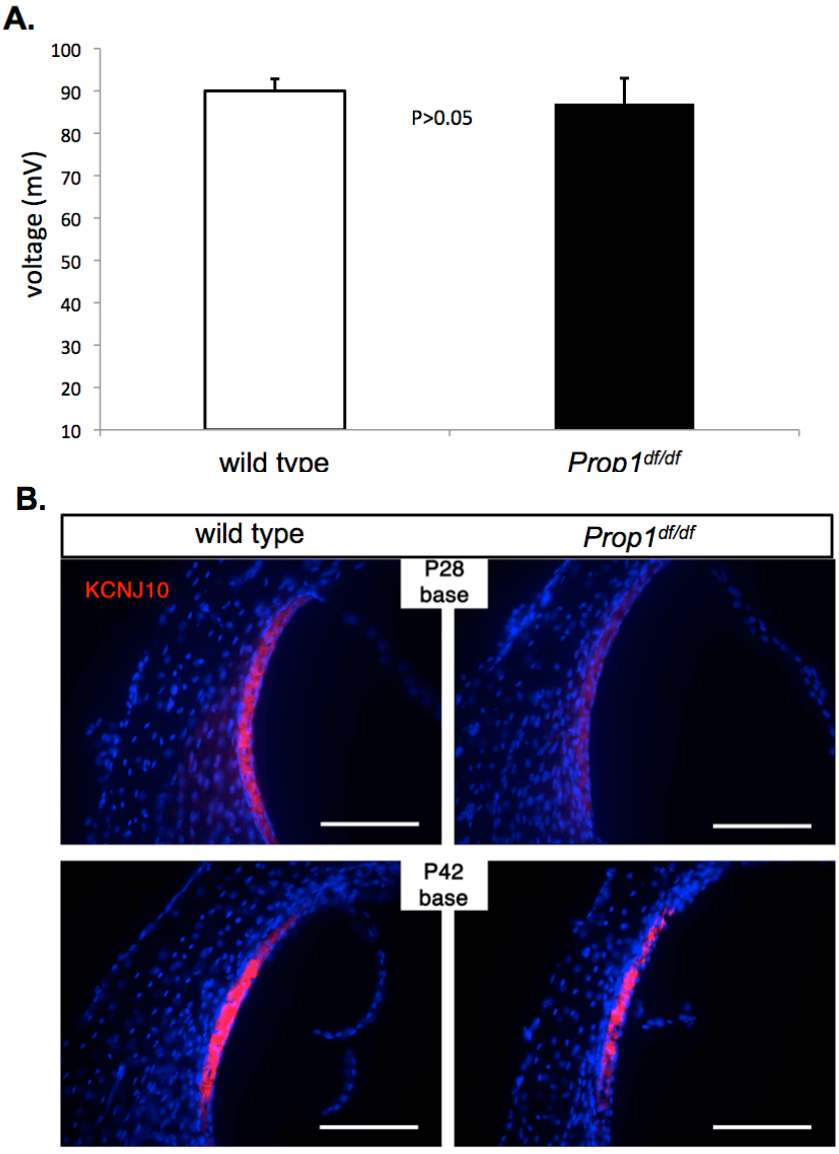

Figure 4-4. Endocochlear potential (EP) is normal and KCNJ10 expression is developmentally delayed in *Prop1*^{df} mutants.

A. EP was measured in P42 wild type and age-matched mutant animals. Levels of EP (in mV) for littermate control and *Prop1*^{df} mutants are shown. ***B.*** Frozen sections of the organ of Corti of wild type and mutant mice collected at P28 and P42 were stained for KCNJ10 (red). Nuclei are marked by DAPI (blue). KCNJ10 expression is detected in the intermediate cells of the stria vascularis**.**

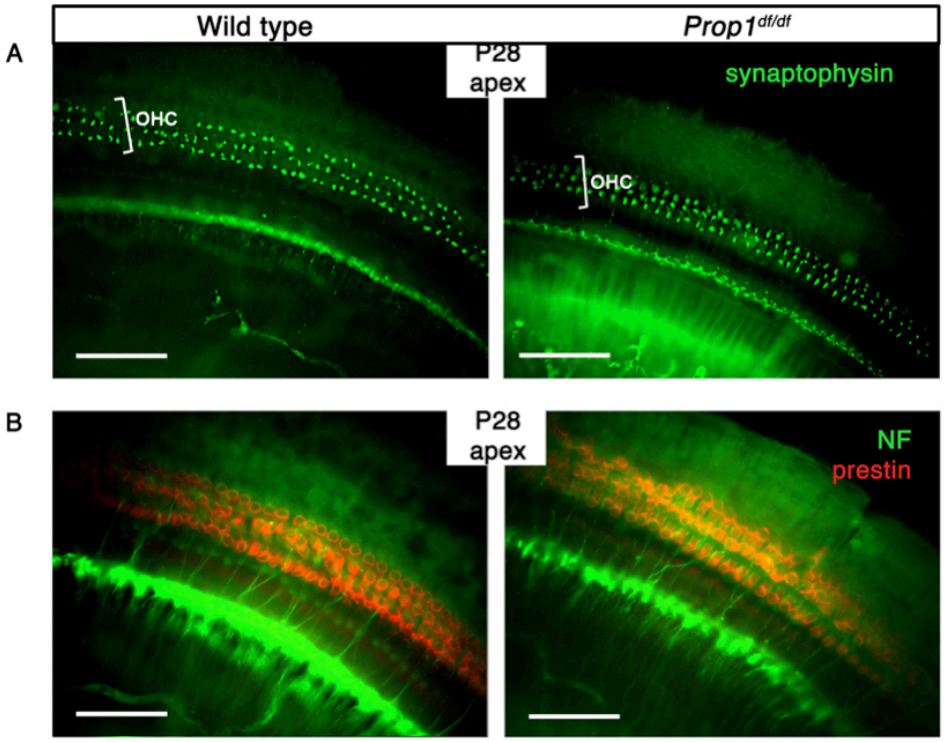

Figure 4-5. Neurite growth and synaptogenesis of OHCs are grossly unaffected in *Prop1*^{df} mutants.

A. Synaptophysin, a presynaptic marker of efferent fibers, is stained on whole mount preparations of cochlear epithelia with an anti-synaptophysin antibody (green). ***B.*** Neurofilament protein (NF-200) immunostaining was used to detect the neurite outgrowth in cochlea whole-mounts of P28 mutants as well as wild type controls. Prestin immunostaining was used to indicate the position of OHCs (red).

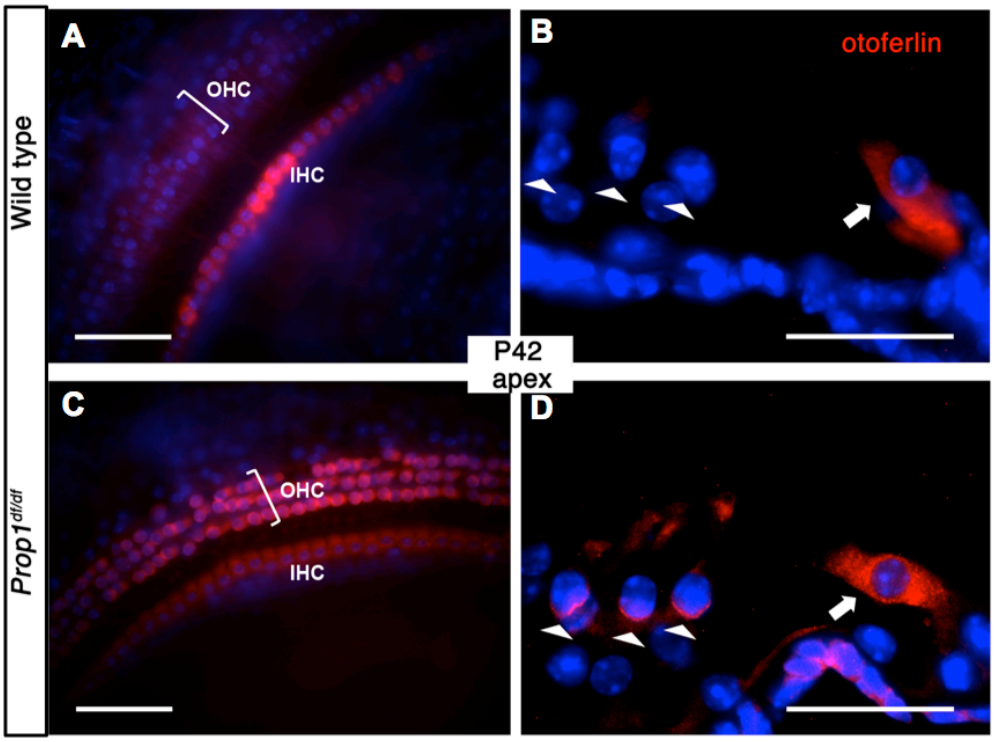

Figure 4-6. Prolonged presence of otoferlin at apical OHCs in *Prop1*^{df} mutants.

(A,C). Otoferlin immunostaining (red) was done on whole mount preparations of sensory epithelia from the apical turn of *Prop1*^{df} mutants and wild type. ***(B,D).*** Frozen sections of organ of Corti were collected and stained by anti-otoferlin antibody (red). Arrowheads indicate the rows of OHCs. Arrows point to the IHCs. Nuclei are blue in all stainings.

REFERENCES

Adler HJ, Belyantseva IA, Merritt RC, Jr., Frolenkov GI, Dougherty GW, Kachar B (2003) Expression of prestin, a membrane motor protein, in the mammalian auditory and vestibular periphery. Hear Res 184:27-40.

Beurg M, Safieddine S, Roux I, Bouleau Y, Petit C, Dulon D (2008) Calcium- and otoferlin-dependent exocytosis by immature outer hair cells. J Neurosci 28:1798-1803.

Boyages SC, Halpern JP (1993) Endemic cretinism: toward a unifying hypothesis. Thyroid 3:59-69.

Brandt N, Kuhn S, Munkner S, Braig C, Winter H, Blin N, Vonthein R, Knipper M, Engel J (2007) Thyroid hormone deficiency affects postnatal spiking activity and expression of Ca2+ and K+ channels in rodent inner hair cells. J Neurosci 27:3174-3186.

Chan SY, Vasilopoulou E, Kilby MD (2009) The role of the placenta in thyroid hormone delivery to the fetus. Nat Clin Pract Endocrinol Metab 5:45-54.

Christ S, Biebel UW, Hoidis S, Friedrichsen S, Bauer K, Smolders JW (2004) Hearing loss in athyroid pax8 knockout mice and effects of thyroxine substitution. Audiol Neurootol 9:88-106.

Cowley DE, Pomp D, Atchley WR, Eisen EJ, Hawkins-Brown D (1989) The impact of maternal uterine genotype on postnatal growth and adult body size in mice. Genetics 122:193-203.

Debruyne F, Vanderschueren-Lodeweyckx M, Bastijns P (1983) Hearing in congenital hypothyroidism. Audiology 22:404-409.

Deol MS (1973) Congenital deafness and hypothyroidism. Lancet 2:105-106.

Drayton M, Noben-Trauth K (2006) Mapping quantitative trait loci for hearing loss in Black Swiss mice. Hear Res 212:128-139.

Gage PJ, Roller ML, Saunders TL, Scarlett LM, Camper SA (1996) Anterior pituitary cells defective in the cell-autonomous factor, df, undergo cell lineage specification but not expansion. Development 122:151-160.

Griffith AJ, Szymko YM, Kaneshige M, Quinonez RE, Kaneshige K, Heintz KA, Mastroianni MA, Kelley MW, Cheng SY (2002) Knock-in mouse model for resistance to thyroid hormone (RTH): an RTH mutation in the thyroid hormone receptor beta gene disrupts cochlear morphogenesis. J Assoc Res Otolaryngol 3:279-288.

Heidrych P, Zimmermann U, Kuhn S, Franz C, Engel J, Duncker SV, Hirt B, Pusch CM, Ruth P, Pfister M, Marcotti W, Blin N, Knipper M (2009) Otoferlin interacts with myosin VI: implications for maintenance of the basolateral synaptic structure of the inner hair cell. Hum Mol Genet 18:2779-2790.

Heydemann A, McNally EM (2007) Consequences of disrupting the dystrophin-sarcoglycan complex in cardiac and skeletal myopathy. Trends Cardiovasc Med 17:55-59.

Ikeda A, Zheng QY, Zuberi AR, Johnson KR, Naggert JK, Nishina PM (2002) Microtubule-associated protein 1A is a modifier of tubby hearing (moth1). Nat Genet 30:401-405.

Ikeda A, Zheng QY, Rosenstiel P, Maddatu T, Zuberi AR, Roopenian DC, North MA, Naggert JK, Johnson KR, Nishina PM (1999) Genetic modification of hearing in tubby mice: evidence for the existence of a major gene (moth1) which protects tubby mice from hearing loss. Hum Mol Genet 8:1761-1767.

Karolyi IJ, Dootz GA, Halsey K, Beyer L, Probst FJ, Johnson KR, Parlow AF, Raphael Y, Dolan DF, Camper SA (2007) Dietary thyroid hormone replacement ameliorates hearing deficits in hypothyroid mice. Mamm Genome 18:596-608.

Kharkovets T, Hardelin JP, Safieddine S, Schweizer M, El-Amraoui A, Petit C, Jentsch TJ (2000) KCNQ4, a K+ channel mutated in a form of dominant deafness, is expressed in the inner ear and the central auditory pathway. Proc Natl Acad Sci U S A 97:4333-4338.

Kharkovets T, Dedek K, Maier H, Schweizer M, Khimich D, Nouvian R, Vardanyan V, Leuwer R, Moser T, Jentsch TJ (2006) Mice with altered KCNQ4 K+ channels implicate sensory outer hair cells in human progressive deafness. EMBO J 25:642-652.

Knipper M, Zinn C, Maier H, Praetorius M, Rohbock K, Kopschall I, Zimmermann U (2000) Thyroid hormone deficiency before the onset of hearing causes irreversible damage to peripheral and central auditory systems. J Neurophysiol 83:3101-3112.

Knipper M, Bandtlow C, Gestwa L, Kopschall I, Rohbock K, Wiechers B, Zenner HP, Zimmermann U (1998) Thyroid hormone affects Schwann cell and oligodendrocyte gene expression at the glial transition zone of the VIIIth nerve prior to cochlea function. Development 125:3709-3718.

Knipper M, Richardson G, Mack A, Muller M, Goodyear R, Limberger A, Rohbock K, Kopschall I, Zenner HP, Zimmermann U (2001) Thyroid hormone-deficient period prior to the onset of hearing is associated with reduced levels of beta-tectorin protein in the tectorial membrane: implication for hearing loss. J Biol Chem 276:39046-39052.

Kubisch C, Schroeder BC, Friedrich T, Lutjohann B, El-Amraoui A, Marlin S, Petit C, Jentsch TJ (1999) KCNQ4, a novel potassium channel expressed in sensory outer hair cells, is mutated in dominant deafness. Cell 96:437-446.

Li D, Henley CM, O'Malley BW, Jr. (1999) Distortion product otoacoustic emissions and outer hair cell defects in the hyt/hyt mutant mouse. Hear Res 138:65-72.

Liberman MC, Gao J, He DZ, Wu X, Jia S, Zuo J (2002) Prestin is required for electromotility of the outer hair cell and for the cochlear amplifier. Nature 419:300-304.

Lohi H, Kujala M, Kerkela E, Saarialho-Kere U, Kestila M, Kere J (2000) Mapping of five new putative anion transporter genes in human and

characterization of SLC26A6, a candidate gene for pancreatic anion exchanger. Genomics 70:102-112.
Marcotti W, Kros CJ (1999) Developmental expression of the potassium current IK,n contributes to maturation of mouse outer hair cells. J Physiol 520 Pt 3:653-660.
Marcus DC, Wu T, Wangemann P, Kofuji P (2002) KCNJ10 (Kir4.1) potassium channel knockout abolishes endocochlear potential. Am J Physiol Cell Physiol 282:C403-407.
Mashimo T, Erven AE, Spiden SL, Guenet JL, Steel KP (2006) Two quantitative trait loci affecting progressive hearing loss in 101/H mice. Mamm Genome 17:841-850.
McIntosh GH, Potter BJ, Mano MT, Hua CH, Cragg BG, Hetzel BS (1983) The effect of maternal and fetal thyroidectomy on fetal brain development in the sheep. Neuropathol Appl Neurobiol 9:215-223.
Mustapha M, Fang Q, Gong TW, Dolan DF, Raphael Y, Camper SA, Duncan RK (2009) Deafness and permanently reduced potassium channel gene expression and function in hypothyroid Pit1dw mutants. J Neurosci 29:1212-1223.
Narui Y, Minekawa A, Iizuka T, Furukawa M, Kusunoki T, Koike T, Ikeda K (2009) Development of distortion product otoacoustic emissions in C57BL/6J mice. Int J Audiol 48:576-581.
Ng L, Rusch A, Amma LL, Nordstrom K, Erway LC, Vennstrom B, Forrest D (2001) Suppression of the deafness and thyroid dysfunction in Thrb-null mice by an independent mutation in the Thra thyroid hormone receptor alpha gene. Hum Mol Genet 10:2701-2708.
Noguchi Y, Kurima K, Makishima T, de Angelis MH, Fuchs H, Frolenkov G, Kitamura K, Griffith AJ (2006) Multiple quantitative trait loci modify cochlear hair cell degeneration in the Beethoven (Tmc1Bth) mouse model of progressive hearing loss DFNA36. Genetics 173:2111-2119.
O'Malley BW, Jr., Li D, Turner DS (1995) Hearing loss and cochlear abnormalities in the congenital hypothyroid (hyt/hyt) mouse. Hear Res 88:181-189.
Ohlemiller KK, Rosen AD, Gagnon PM (2010) A major effect QTL on chromosome 18 for noise injury to the mouse cochlear lateral wall. Hear Res 260:47-53.
Ospeck M, Dong XX, Iwasa KH (2003) Limiting frequency of the cochlear amplifier based on electromotility of outer hair cells. Biophys J 84:739-749.
Pomp D, Cowley DE, Eisen EJ, Atchley WR, Hawkins-Brown D (1989) Donor and recipient genotype and heterosis effects on survival and prenatal growth of transferred mouse embryos. J Reprod Fertil 86:493-500.
Rhees BK, Ernst CA, Miao CH, Atchley WR (1999) Uterine and postnatal maternal effects in mice selected for differential rate of early development. Genetics 153:905-917.
Roux I, Safieddine S, Nouvian R, Grati M, Simmler MC, Bahloul A, Perfettini I, Le Gall M, Rostaing P, Hamard G, Triller A, Avan P, Moser T, Petit C (2006)

Otoferlin, defective in a human deafness form, is essential for exocytosis at the auditory ribbon synapse. Cell 127:277-289.
Rovet J, Walker W, Bliss B, Buchanan L, Ehrlich R (1996) Long-term sequelae of hearing impairment in congenital hypothyroidism. J Pediatr 128:776-783.
Rusch A, Erway LC, Oliver D, Vennstrom B, Forrest D (1998) Thyroid hormone receptor beta-dependent expression of a potassium conductance in inner hair cells at the onset of hearing. Proc Natl Acad Sci U S A 95:15758-15762.
Sendin G, Bulankina AV, Riedel D, Moser T (2007) Maturation of ribbon synapses in hair cells is driven by thyroid hormone. J Neurosci 27:3163-3173.
Shibusawa N, Hashimoto K, Nikrodhanond AA, Liberman MC, Applebury ML, Liao XH, Robbins JT, Refetoff S, Cohen RN, Wondisford FE (2003) Thyroid hormone action in the absence of thyroid hormone receptor DNA-binding in vivo. J Clin Invest 112:588-597.
Sornson MW, Wu W, Dasen JS, Flynn SE, Norman DJ, O'Connell SM, Gukovsky I, Carriere C, Ryan AK, Miller AP, Zuo L, Gleiberman AS, Andersen B, Beamer WG, Rosenfeld MG (1996) Pituitary lineage determination by the Prophet of Pit-1 homeodomain factor defective in Ames dwarfism. Nature 384:327-333.
Uziel A, Marot M, Rabie A (1985a) Corrective effects of thyroxine on cochlear abnormalities induced by congenital hypothyroidism in the rat. II. Electrophysiological study. Brain Res 351:123-127.
Uziel A, Legrand C, Rabie A (1985b) Corrective effects of thyroxine on cochlear abnormalities induced by congenital hypothyroidism in the rat. I. Morphological study. Brain Res 351:111-122.
Uziel A, Pujol R, Legrand C, Legrand J (1983) Cochlear synaptogenesis in the hypothyroid rat. Brain Res 283:295-301.
van der Deure WM, Peeters RP, Visser TJ (2010) Molecular aspects of thyroid hormone transporters, including MCT8, MCT10, and OATPs, and the effects of genetic variation in these transporters. J Mol Endocrinol 44:1-11.
Van Eyken E, Van Laer L, Fransen E, Topsakal V, Lemkens N, Laureys W, Nelissen N, Vandevelde A, Wienker T, Van De Heyning P, Van Camp G (2006) KCNQ4: a gene for age-related hearing impairment? Hum Mutat 27:1007-1016.
Wangemann P, Kim HM, Billings S, Nakaya K, Li X, Singh R, Sharlin DS, Forrest D, Marcus DC, Fong P (2009) Developmental delays consistent with cochlear hypothyroidism contribute to failure to develop hearing in mice lacking Slc26a4/pendrin expression. Am J Physiol Renal Physiol 297:F1435-1447.
Wasserman EE, Nelson K, Rose NR, Eaton W, Pillion JP, Seaberg E, Talor MV, Burek L, Duggan A, Yolken RH (2008) Maternal thyroid autoantibodies during the third trimester and hearing deficits in children: an epidemiologic assessment. Am J Epidemiol 167:701-710.
Weber T, Zimmermann U, Winter H, Mack A, Kopschall I, Rohbock K, Zenner HP, Knipper M (2002) Thyroid hormone is a critical determinant for the

regulation of the cochlear motor protein prestin. Proc Natl Acad Sci U S A 99:2901-2906.
Winter H, Braig C, Zimmermann U, Geisler HS, Franzer JT, Weber T, Ley M, Engel J, Knirsch M, Bauer K, Christ S, Walsh EJ, McGee J, Kopschall I, Rohbock K, Knipper M (2006) Thyroid hormone receptors TRalpha1 and TRbeta differentially regulate gene expression of Kcnq4 and prestin during final differentiation of outer hair cells. J Cell Sci 119:2975-2984.
Winter H, Ruttiger L, Muller M, Kuhn S, Brandt N, Zimmermann U, Hirt B, Bress A, Sausbier M, Conscience A, Flamant F, Tian Y, Zuo J, Pfister M, Ruth P, Lowenheim H, Samarut J, Engel J, Knipper M (2009) Deafness in TRbeta mutants is caused by malformation of the tectorial membrane. J Neurosci 29:2581-2587.
Wolf JB, Wade MJ (2009) What are maternal effects (and what are they not)? Philos Trans R Soc Lond B Biol Sci 364:1107-1115.
Yu N, Zhu ML, Zhao HB (2006) Prestin is expressed on the whole outer hair cell basolateral surface. Brain Res 1095:51-58.
Zheng J, Shen W, He DZ, Long KB, Madison LD, Dallos P (2000) Prestin is the motor protein of cochlear outer hair cells. Nature 405:149-155.

CHAPTER 5

A locus on Chromosome 2 modifies the severity of hearing impairment in hypothyroid *Pou1f1*^{dw} dwarf mice

ABSTRACT

Thyroid hormone (TH) has pleiotropic effects on cochlear development, and genomic variation influences the severity of associated hearing deficits. *Prop1*^{df} and *Pou1f1*^{dw} mutant mice lack pituitary thyrotropin, which causes severe TH deficiency and variable hearing impairment, depending on the genetic background (Karolyi et al., 2007). DW-*Pou1f1*^{dw} mutants are profoundly deaf and exhibit delayed development of the organ of Corti, permanently reduced potassium channel gene expression and function, and other abnormalities (Mustapha et al., 2009). In contrast, DF-*Prop1*^{df} mutants have very mild hearing impairment. To assess the genetic complexity of protective effects, an F1 intercross was generated between DW-*Pou1f1*^{dw} carriers and an inbred strain with excellent hearing, CAST/EiJ, derived from a wild population of *Mus castaneus*. Approximately 16% of the *dw/dw* F2 progeny had normal hearing. A genome scan of these individuals revealed a locus on Chromosome 2, named

* I set up the breeding colonies of (DW-*Pou1f1* X CAST) and (DW-*Pou1f1* X AKR) in the Camper lab, arranged the ABR tests for all the F2 *dw/dw* mutants and genotyped the polymorphic alleles of *Mtap1a* gene on all the individual mice. I participated in writing the manuscript.

modifier of *dw* hearing, *Mdwh*, that rescues hearing despite persistent hypothyroidism. This chromosomal region contains the modifier of tubby hearing 1 (*Moth1*) locus that encodes a protective allele of the microtubule-associated protein *Mtap1a* (Ikeda et al., 2002). We crossed DW-*Pou1f1*^{dw} carriers with the AKR strain, which carries a protective allele of *Mtap1a,* and found that AKR is not protective for hearing in the DW-*Pou1f1*$^{dw/dw}$ F2 progeny. Thus, protective alleles of *Mtap1a* are not sufficient to rescue DW-*Pou1f1*$^{dw/dw}$ hearing. Microarray analysis identified cochlear gene expression changes associated with hypothyroidism in *Pou1f1*^{dw} mice. Some of these are positional candidates for the modifier gene. We expect that identification of protective modifiers will enhance our understanding of the mechanisms of hypothyroidism-induced hearing impairment.

INTRODUCTION

Thyroid hormone (TH) is an important regulator of many processes in mammalian development including body growth (Cabello and Wrutniak, 1989) and central nervous system maturation (Bernal, 2005). Auditory function is particularly sensitive to the effects of TH, which is required for the complex development and physiology of the cochlea (Deol, 1973; Uziel, 1986; Sohmer and Freeman, 1996). Mutations in several different genes can prevent or interfere with the TH signaling pathway that is required for normal auditory development and function. In addition to gene mutations that cause hypothyroidism, mutations of genes encoding thyroid hormone receptors (THRs)

(Forrest et al., 1996; Rusch et al., 2001) and iodothyronine deiodinases (Ng et al., 2004; Ng et al., 2008) can diminish the developing cochlea's response to TH and exhibit similar auditory phenotypes. Cases of congenital hypothyroidism are classified as primary if caused by thyroid gland dysfunction and secondary if caused by pituitary gland abnormalities. Mouse models of primary hypothyroidism include the hypothyroid mutation (*hyt*) of the *Tshr* gene, which has residual activity and mild to negligible hearing deficit (O'Malley et al., 1995; Sprenkle et al., 2001; Karolyi et al., 2007), and the thyroid dyshormonogenesis mutation (*thyd*) of the *Duox2* gene, which causes severe to profound deafness in mice (Johnson et al., 2007). *Pax8* knockout mice are athyroid, exhibit ear abnormalities, and lack an auditory brainstem response (ABR) to sound. The utility of this model is limited because the mice survive only to postnatal day 21 (P21), and the expression of *Pax8* in the otic placode makes it difficult to distinguish the influence of thyroid and direct cochlear effects (Christ et al., 2004).

Hearing impairment has been examined in three mouse models of secondary hypothyroidism: the Snell dwarf (*dw*) mutation of the *Pou1f1* gene (formerly *Pit1*), the Ames dwarf (*df*) mutation of the *Prop1* gene, and a targeted knockout mutation of the *Cga* gene, which encodes an essential subunit of thyrotropin (Karolyi et al., 2007). *Pou1f1* and *Prop1* both encode transcription factors in the same pathway of pituitary gland development. Mice with null mutations in *Prop1*, *Pou1f1*, or *Cga* lack pituitary thyrotropin and have no measurable TH in the serum. In spite of these similarities, the hearing defects in

Pou1f1^{dw} and *Cga* mutant mice are profound, whereas *Prop1*^{df} mutants have only a mild hearing impairment. The *Pou1f1*^{dw} and *Prop1*^{df} mutations are on different strain backgrounds, and analysis of a small cross between *Pou1f1*^{dw} and *Prop1*^{df} mice showed that genetic background is likely responsible for the different hearing phenotypes (Karolyi et al., 2007).

Advances in understanding how TH signaling affects the development and function of the cochlea will help to illuminate the molecular mechanisms that underlie development of normal auditory functions. We chose the *Pou1f1*^{dw} mutant mice because of the severity of their hearing impairment, their responsiveness to TH replacement, and their well-characterized cochlear pathologies (Mustapha et al., 2009). Detailed morphological, physiological, and gene expression analyses of *Pou1f1*^{dw} mutants during the course of cochlear development revealed tectorial membrane abnormalities, loss of outer hair cells (OHCs) preceded by their compromised function (as evidenced by an absence of distortion product otoacoustic emissions, DPOAE, and cochlear microphonics, CM), reduced endocochlear potential, and reduced expression of potassium channel proteins (KCNJ10 in the stria vascularis and KCNQ4 in OHCs), all of which are likely contributors to the severe hearing impairment of these mutant mice (Mustapha et al., 2009). Similar features, including lack of DPOAE, reduced endocochlear potential, and tectorial membrane abnormalities, are characteristic of the *Cga* knockout mice (Karolyi et al., 2007).

Although insights have been gained from studies of existing hypothyroid mouse models, our understanding of the molecular mechanisms underlying the

hearing impairment associated with hypothyroidism is still incomplete. The observed influence of genetic background on the severity of hearing impairment in hypothyroid mice offers an opportunity to identify modifier genes and pathways that could enhance our understanding of these mechanisms. Here we describe results from a large linkage cross that was designed to map loci that modify the hearing of hypothyroid *Pou1f1* dwarf mice. Heterozygous *Pou1f1*^{dw} mice were intercrossed with wild derived, inbred strain CAST/EiJ, which have good hearing. F2 mutant progeny (*dw/dw*) from this intercross ranged from normal hearing to completely deaf, despite the fact that they were all profoundly hypothyroid and equally growth impaired. By analysis of this cross, we identified a locus on Chromosome (Chr) 2 that had a highly significant linkage association (LOD=10) with the ABR threshold variation exhibited by the mutant intercross mice. This quantitative trait locus (QTL) was given the symbol *Mdwh* (modifier of *dw* hearing). The *Mdwh* interval contains *Moth1*, the modifier of tubby hearing, which varies among strains by the length of an alanine-proline amino acid repeat in *Mtap1a*, microtubule associated protein 1a (Ikeda et al., 2002). DW/J has a susceptible allele of *Mtap1a*, while CAST/EiJ and AKR have protective alleles. *dw/dw* mutants born from an intercross of F1 (AKR x *Pou1f1*^{dw}) mice are all deaf, suggesting that *Mdwh* is not *Moth1*, but represents a novel locus that protects against hearing impairment in hypothyroid *Pou1f1*^{dw} mutants.

MATERIALS & METHODS

Mice

Mice of the C3H/HeJ-*Pou1f1*$^{dw\text{-}J}$/J, DW/J- *Pou1f1*^{dw} and CAST/EiJ inbred strains and their derivative F1 and F2 hybrids were housed in the Research Animal Facility of The Jackson Laboratory. AKR mice were obtained from The Jackson Laboratory. A stock of DW/J-*Pou1f1*^{dw} and CAST/EiJ F2 hybrids were also generated at University of Michigan. All procedures were approved by the Institutional Animal Care and Use Committees of each institution. The Jackson Laboratory and the University of Michigan are both accredited by the American Association for the Accreditation of Laboratory Animal Care (AAALAC) and are registered with the United States Department of Agriculture as research facilities. Genotyping processes for *dw* and *dw-J* alleles were previously described (Eicher and Beamer, 1980; Karolyi et al., 2007).

Assessment of hearing by ABR threshold analysis

The inbred strain, F1 hybrid, and F2 intercross mice were assessed for hearing by auditory-evoked brainstem response (ABR) thresholds at the Jackson Laboratory as previously described (Zheng et al., 1999). Briefly, mice are anesthetized and body temperature is maintained at 37-38°C by placing them on an isothermal pad in a sound-attenuating chamber. Sub-dermal needles are used as electrodes, inserted at the vertex, and ventro-laterally to each ear. Stimulus presentation, ABR acquisition, equipment control and data management were coordinated using the computerized Intelligent Hearing Hearing Systems (IHS; Miami, Florida). A pair of high frequency transducers is coupled with the IHS system to generate specific acoustic stimuli. Broadband

clicks, and 8, 16, and 32 kHz tone-bursts are respectively channeled into the animal's ear canals. The amplified brainstem responses are averaged by a computer and displayed on the computer screen. Auditory thresholds are obtained for each stimulus by reducing the sound pressure level (SPL) at 10 dB steps and finally at 5 dB steps up and down to identify the lowest level at which an ABR pattern can be recognized. Samples of CBA/CaJ mice are tested periodically as references for normal hearing, and for monitoring the reliability of the equipment and testing procedures. ABR tests at the University of Michigan were done as previously described (Karolyi et al., 2007).

Linkage intercross mapping

Individual DNA samples from linkage intercross mice were genotyped by PCR amplification with primer pairs designed to amplify specific microsatellite markers purchased from Integrated DNA Technologies (Coralville, IA, USA). PCR reactions and PCR product visualization methods were as previously described (Gagnon et al., 2006). ABR thresholds for click, 8 kHz, 16 kHz, and 32 kHz stimuli were evaluated as quantitative traits and QTL linkage analysis was performed using the computer program Map Manager QTX (version b20), which uses a fast regression method to detect and localize quantitative trait loci within intervals defined by genetic markers and can perform pair-wise locus analysis to search for QTL interactive effects. It reports the resulting regression coefficients and a likelihood ratio statistic that is based on natural logarithms, but can be converted to conventional LOD scores by dividing by 4.61.

Candidate gene analysis

PCR for comparative DNA sequence analysis was performed according to the same conditions as described above for linkage mapping. DNA sequences of the PCR primers used to amplify the polymorphic repeat sequence GCTCCA of *Mtap1a* were 5'-TCTGGGACCTCACTCCTCTG (forward) and 5'-GTTTCTCCTGGGCCATTAGC (reverse). PCR products from genomic DNA were purified with the QIAquick PCR Purification Kit (Qiagen Inc., Valencia, CA). DNA sequencing was performed using the same primers as for DNA amplification, then run on an Applied Biosystems 3700 DNA Sequencer with an optimized Big Dye Terminator Cycle Sequencing method.

RESULTS

We reported strain background effects on hearing in hypothyroid mice that were produced from an intercross of *Prop1*^{df} and *Pou1f1*^{dw} strains (Karolyi et al., 2007). There were insufficient F2 progeny, however, to assess the heterogeneity of effects among them (≤ 6 for each genotype group). The unique nature of each stock (DW/J and DF/B), and the fact that DF/B are not inbred, compelled us to extend this analysis of modifier effects by comparing thresholds of mice with different *Pou1f1* mutant genotypes on multiple genetic backgrounds (Fig. 5-1). As previously reported, *dw/dw* mice on the DW/J strain background are nearly deaf at 4 weeks of age, whereas *+/dw* heterozygotes have normal hearing thresholds. On a C3H/HeJ strain background, mice homozygous for a different

null mutation of *Pou1f1,* the dw^J allele, show a hearing impairment greater than that of the parental C3H/HeJ strain mice but not nearly as severe as that of *dw* mutants on the DW/J strain background. Both the *dw* and dw^J alleles are recessive, complete loss of function alleles that result from a missense mutation in the homeodomain that abolishes DNA binding and an intra-genic rearrangement, respectively (Camper et al., 1990; Li et al., 1990). Compound heterozygotes (DW/J x C3H/HeJ) F1 hybrids (dw/dw^J) exhibit a hearing impairment that is intermediate between that of DW/J-*dw/dw* and C3H/HeJ-dw^J/dw^J mutants. Mutant *dw/dw* mice of the B6.DW-$Pou1f1^{dw}$/*J* congenic strain exhibit severe hearing impairment like that of *dw/dw* mutants on the DW/J strain background. The congenic strain was constructed by transferring the *dw* mutation from the DW/J strain onto an otherwise C57BL/6J strain background by multiple rounds of backcrossing and selection. All of these results support the idea that the genetic background affects the degree of hearing loss of hypothyroid *Pou1f1* mutants.

To investigate the genetic complexity of the strain-related hearing loss variation of $Pou1f1^{dw}$ mutant mice and to map the putative modifier genes, we produced a linkage intercross between (DW/J-$Pou1f1^{dw}$ x CAST/EiJ) F1 hybrids. We chose the CAST/EiJ strain because mice of this strain retain good hearing at old ages and because of the increased likelihood of genetic marker polymorphisms with the DW/J strain (Zheng et al., 1999). *Pou1f1* mutant (*dw/dw*) F2 progeny from this intercross represented about 25% of the total, as expected, and these mutants were tested for hearing and analyzed for genetic linkage.

ABR thresholds for click, 8 kHz, 16 kHz, and 32 kHz stimuli were measured at 1-2 months of age (average 40 days) for each of 196 F2 mutant mice. The *dw/dw* F2 mice exhibited a wide range of ABR thresholds that were distributed in a skewed bimodal fashion, suggesting a major influence of one or a few genes (Fig. 5-2). A bell-shaped distribution with a single mode would have suggested that many genes with small effects contribute to the hearing differences among the mutant mice. A substantial portion, 16% (N=31), of the mutant F2 mice exhibited normal hearing thresholds (< 35 dB SPL). The body weights of the mutant *dw/dw* F2 mice were about three-fold smaller than normal mice, consistent with profound hypothyroidism and growth deficiency. There was no significant correlation between body weight and ABR thresholds (Table 5-1). This suggests that the rescue of hearing does not occur concomitantly with a growth rescue.

As a first approach for mapping modifier loci for hearing, we performed a genome-wide scan for linkage by limiting our analysis to F2 mice with the most extreme ABR thresholds, 30 with the lowest (15-30 dB SPL) and 11 with the highest (95-100 dB SPL) thresholds. Selecting mice with extreme phenotypes maximizes information for more efficient linkage scanning without sacrificing detection capability (Darvasi, 1997). We typed 90 microsatellite markers spaced at 15 cM intervals on all 20 mouse chromosomes, which covered >90% of the genome. We used the Map Manager QTX computer program (Manly et al., 2001) to analyze quantitative trait loci (QTLs) associated with ABR threshold variation. We evaluated intercross linkage using a free model (2 degrees of

freedom), without prior assumptions of dominant, recessive, or additive effects. The LOD scores for associations of 16 kHz thresholds with the 90 markers are shown in Fig. 5-3. With this model, a LOD score of 4.3 is considered a significant intercross linkage value, corresponding to a genome-wide type I error of 0.05 (Lander and Kruglyak, 1995). The highest and only statistically significant linkage associations were found with markers on Chr 2, and additional Chr 2 markers were then analyzed (Fig. 5-4 A). The maximum LOD score was 7.9 for the linkage associations of *D2Mit134* and *D2Mit304* with 16 kHz ABR thresholds (LOD scores were 7.0, 6.7, and 7.4 for click, 8 kHz, and 32 kHz thresholds, respectively). Given that a LOD score of 4.3 is considered significant, the Chr 2 linkage with a LOD score of 7.9 validated designation of this new QTL as "modifier of *dw* hearing", with the symbol *Mdwh*.

In order to confirm the significance of this linkage and to clarify the additive and dominance components of the phenotypic variance, we extended the linkage studies by genotyping the remaining 155 *dw/dw* F2 mice from the intercross for Chr 2 markers surrounding the *Mdwh* locus. The most likely map position for the *Mdwh* QTL is the same when determined from all 196 $Pit1^{dw/dw}$ F2 mice as from the 41 *dw/dw* mice with the most extreme hearing phenotypes (Fig. 5-4 B). Both analyses gave peak associations with *D2Mit304* (which was non-recombinant with *D2Mit134* in the 41 extreme mice). The 1.5-LOD support interval, which provides 95% confidence of coverage (Dupuis and Siegmund, 1999), for both analyses is the 118-138 Mb region of Chr 2 (NCBI Build m37). Because of the increased sample size, the LOD scores for linkage associations were higher

when all 196 mice were analyzed, with a peak score of 10.1 for marker *D2Mit304* (Fig. 5-4 B).

The effects of *Mdwh* on the hearing thresholds of dwarf intercross mice are highly significant and vary little in response to the different auditory stimuli (LOD 9.0-10.1; Table 5-2). The LOD scores shown in Fig. 5-4 and Table 5-2 are for an additive inheritance model. These values were essentially the same as those calculated for a free model (no inheritance assumptions) and larger than those of recessive and dominant models, indicating that the effects of *Mdwh* are primarily additive. The fact that ABR thresholds of mice heterozygous for *D2Mit304* marker (DC) are intermediate between those of homozygotes (DD or CC) also supports an additive model of inheritance (Table 5-2).

The genetic interval containing *Mdwh* was estimated to span about 20 Mb, between the 118 and 138 Mb positions of Chr 2 (Fig. 5-4). An interesting candidate gene within this interval is *Mtap1a*, the gene encoding microtubule-associated protein 1 A. *Mtap1a*, located at 121.1 Mb on Chr 2, is particularly intriguing because it has been reported to modify the hearing of mice with the tubby (*tub*) mutation in a strain-specific manner (Ikeda et al., 2002). The wild type *Mtap1a* alleles from strains AKR/J, CAST/Ei and 129P2/OlaHsd protect tubby mice from hearing deficits, whereas a sequence variant in the C57BL/6J strain conferred susceptibility to hearing impairment. We examined the *Mtap1* gene in the DW/J strain and found that it is the same allelic form as that of the C57BL/6J strain (Fig. 5-5), consistent with the possibility that this allele confers hearing loss susceptibility to *Pou1f1*$^{dw/dw}$ mutants as it does for *tub/tub* mutant

mice. Both DW/J-*Pou1f1*$^{dw/J}$ and C57BL/6J strains contain five repeats of a 6 bp sequence in the large exon 5 of *Mtap1a*, whereas all other strains we examined (AKR/J, CAST/EiJ, 129P2/OlaHsd, C3H/HeJ, BALB/cByJ and DF/B-*Prop1*^{df}/J) contain 15 repeats of this sequence.

To assess the likelihood that the *Moth1* allele of *Mtap1a* is identical to *Mdwh*, we created F1 intercrosses between DW/J-*Pou1f1*$^{dw/+}$ and each of the two strains CAST/EiJ and AKR/J and assessed the segregation of non-DW/J *Mtap1a* alleles with the ability of F2 *Pou1f1*$^{dw/dw}$ mutants to hear. Among 68 *Pou1f1*$^{dw/dw}$ (DW/J-*Pou1f1*$^{+/dw}$ x CAST/EiJ) F2 mice, 23.5% of them had ABR thresholds less than 35 dB SPL, which we designated as normal hearing. There is an enrichment of CAST/EiJ *Mtap1a* alleles among the hearing F2 mutants, but homozygosity for CAST/EiJ alleles is not sufficient for normal hearing ability (indicated by open arrow in Fig. 5-6 A). An F2 *Pou1f1*$^{dw/dw}$ mouse homozygous for DW/J *Mtap1a* alleles exhibits good hearing (37 dB SPL) (indicated by black arrow in Fig. 5-6 A), suggesting that CAST/EiJ *Mtap1a* alleles are not necessary for hearing either. Average ABR thresholds of each *Mtap1a* genotype group were calculated and shown in Fig. 5-6 B. The mice carrying heterozygous *Mtap1a* alleles from DW/J and CAST/EiJ backgrounds showed ABR threshold levels intermediate between those of the mice carrying homozygous alleles from DW/J or CAST/EiJ, respectively. This result is consistent with our hypothesis that the *Mdwh* locus shows an additive effect on the protection of hearing in *dw/dw* mutants. Sixty-two F2 *Pou1f1*$^{dw/dw}$ mice were collected from an intercross between (DW/J-*Pou1f1*$^{dw/+}$ x AKR/J) F1 mice, and none of the progeny had good

hearing (Fig. 5-7). Thus, the AKR/J genetic background cannot protect against hypothyroidism-induced hearing loss in *Pou1f1*$^{dw/dw}$ mutants even though AKR/J mice have the same *Mtap1a* allele as CAST/EiJ.

DISCUSSION

TH deficiency can have major effects on neuronal development, body growth and cochlear development resulting in cretinism, dwarfism and deafness if not treated promptly. It is intriguing that the consequences of severe thyroid hormone deficiency can be highly variable in mouse and man. Mutations in the pituitary transcription factor *Pou1f1* result in severe hypothyroidism, dwarfism and profound deafness on the DW/J genetic background, but the hearing deficit is milder when crossed to a good hearing, but genetically undefined, strain, DF/B. Because the critical period for TH replacement is late gestation and early neonatal life, we assessed the contribution of the maternal environment to the differential hearing impairments between DW/J and DF/B strains (data shown in Chapter 4). Our results prove that this particular genetic background effect is intrinsic to the fetus, rather than an influence of maternal TH during gestation or lactation.

In this study, we examined the effects of the CAST/EiJ genetic background on the hearing of *Pou1f1* mutants and show that strain-specific alleles of the *Mdwh* locus on Chr 2 have a major influence on the hearing of hypothyroid *Pou1f1* dwarf mice (*dw/dw*). This locus showed a highly significant association (LOD score of 10) with hearing ability and could explain about 20% of the ABR

threshold variation of dwarf F2 mice from a DW/J-*Pou1f1*^{dw} x CAST/EiJ intercross. Given the pleiotropic effects of TH on the inner ear development, it is very surprising that the *Mdwh* appears simple and genetically tractable.

The *Mdwh* modifier locus does not appear to affect the basal level of TH in *Pou1f1* mutant mice, which lack thyroid stimulating hormone (TSH). If the modifier had a general effect on thyroid hormone levels, then the dwarf mice with good hearing would be expected to be larger than the deaf dwarfs. We have detected such generalized effects in other models with partial restoration of TSH production (Cushman et al., 2001). Because the weights of hearing and deaf dwarfs are indistinguishable and only ABR thresholds are variable (Table 5-1), it is likely that *Mdwh* is modifying processes that affect cochlear development or function even in the absence of systemic thyroid hormone stimulation. We cannot rule out a local effect on cochlear TH production or transport, however.

The *Mdwh* gene may modify the degree of hearing impairment due to hypothyroidism by altering the basal expression levels of critical gene(s) without enhancing TH production. This model is drawn from a similar case of genetic background effects in which the viability of *Prop1* mutant newborn mice correlated with higher basal levels of surfactant B gene expression in the lung at birth than mutants that exhibited lethality (Nasonkin et al., 2004). The transcription factor *Nkx2.1* is necessary for surfactant B expression in the lung, and *Nkx2.1* transcription is up regulated by thyroid hormone. The mutant mice that were cyanotic and died had lower basal levels of *Nkx2.1* expression than those that were viable, suggesting that genetic background affected the basal

level of *Nkx2.1* expression in the absence of TH. In the case of *Mdwh*, the DW/J hearing loss susceptibility allele may have a less active basal state (in the absence of TH) than the CAST/Ei protective allele. If cochlear development and function were sensitive either directly or indirectly to slight variations in the level of *Mdwh* gene activity, then the lower basal levels in hypothyroid F2 mice with the DW/J allele could explain their more severe hearing impairment, whereas the higher basal level of *Mdwh* gene activity associated with the CAST/EiJ allele would protect from severe hearing loss and could explain the additive nature of *Mdwh* allele effects on ABR thresholds.

We considered the *Mtap1a* gene as a particularly intriguing candidate gene for *Mdwh*. It maps within the 20 Mb candidate interval on Chr 2 and is the gene responsible for the strain-specific modification of hearing in tubby (*tub*) mutant mice (Ikeda et al., 2002). The underlying mechanism proposed for this modification is an altered protein-protein interaction between MTAP1A (a microtubule-associated protein) and a protein localized to the post-synaptic density in hair cells, PSD95, a protein critical for the cyto-architecture at the synapse. Another hearing-related QTL on Chr 2, which could be equivalent to *Mtap1a* or *Mdwh*, modifies the degree of hearing loss in Beethoven mutant mice, which carry a mutation in *Tmc1* (Noguchi et al., 2006). Intriguingly, the phenotype of these mice is outer hair cell loss and reduced DPOAE, the same as that observed in *Pou1f1*^{dw} mutants (Mustapha et al., 2009).

Evidence implicating *Mtap1a* as the gene underlying the modifier effects of the *Mdwh* locus include the following. First, the DW/J strain has the same

Mtap1a allele as C57BL/6J (Fig. 5-5), which was shown to confer susceptibility to hearing loss in *tub* mutant mice (Ikeda et al., 2002). The DW/J and C57BL/6J strain backgrounds both confer an increased susceptibility to hearing impairment in *Pou1f1*^{dw} mutant mice (Fig. 5-1), and both have the same *Mtap1a* allele. Second, the expression of *Mtap1a* is altered by TH in the cerebellum of hypothyroid rats (Benjamin et al., 1988) and in the sensory motor cortex of hypothyroid (*hyt*) mutant mice (Biesiada et al., 1996). Third, MTAP1A interacts directly with the calcium-activated potassium channel BKCa (Park et al., 2004), and defects in *Kcnma1*, which encodes one of the BKCa subunits, cause progressive hearing loss and loss of KCNQ4 (Ruttiger et al., 2004). Fourth, KCNQ4 is regulated by thyroid hormone receptors THRalpha1 and THRbeta in outer hair cells (Winter et al., 2006), and its expression is reduced in *Pou1f1*^{dw} mutant outer hair cells (Ikeda et al., 2002). Finally, recent studies demonstrate that TH is essential for morphological and functional maturation of inner hair cell (IHC) ribbon synapses (Brandt et al., 2007; Sendin et al., 2007). These studies suggest that presynaptic dysfunction of IHCs, which could be proven by demonstrating reduced exocytosis efficiency, is a mechanism in congenital hypothyroid deafness, and MTAP1A has been proposed to be involved in synaptic function (Ikeda et al., 2002). Although these lines of evidence seem compelling when taken together, our study on segregation of CAST/EiJ and AKR/J *Mtap1a* alleles in F2 *Pou1f1*^{dw} mutants showed CAST/EiJ and AKR/J *Mtap1a* alleles are neither sufficient nor necessary for good hearing in those mice. We observed the same result in F2 mutants from an intercross between

the DW/J strain and the 129P2/OlaHsd strain (129P2), which contains the same *Mtap1a* allele as CAST/EiJ and AKR/J (data not shown). We conclude that either *Mdwh* is not *Mtap1a*, that *Mtap1a* is not the sole component of *Mdwh*, or that additional modifiers obscure the effects of *Mtap1* on hearing.

Given the pleiotropic effects that thyroid hormone has on cochlear development (Mustapha et al., 2009), *Mdwh* could consist of multiple genes, possibly including *Mtap1a*, whose combined actions protect against hypothyroidism-induced hearing impairment in *Pou1f1*^{dw} mutants. Future directions to identify the protective genes could include refining the critical interval by generating more animals and genotyping more markers on Chr 2, and creating a congenic mouse line with CAST/EiJ alleles of *Mdwh* and DW/J alleles at other loci to determine if the CAST/EiJ *Mdwh* is sufficient to protect against hearing loss. Another strategy would be to directly sequence the candidate genes within the *Mdwh* locus from the DW/J strain and compare them with the C3H/HeJ, CAST/EiJ, and other inbred strain sequences generated by the Mouse Genomes Project (http://www.sanger.ac.uk/resources/mouse/genomes/). There are more than 1,000 genes within the *Mdwh* locus. Among this set there are 10 genes that are differentially expressed in the cochlea of *Pou1f1*$^{dw/dw}$ mutant and wild type mice (Tzywen Gong, unpublished data), and 4 hearing-associated genes. These genes are the highest priority for exon sequencing. A successful application of the candidate gene sequencing approach was the identification of a stop codon in sodium channel modifier 1 (SCNM1) on the genetic background

of the C57BL/6J strain that intensifies the severity of inherited movement disease caused by a mutation in the sodium channel gene *Scn8a* (Buchner et al., 2003).

In conclusion, Identifying the gene(s) that modify the expression of mutant auditory phenotypes related to congenital hypothyroidism will be important for determining the molecular mechanisms that underlie thyroid hormone's influence on cochlear development and function. In addition, it is likely that a mechanistic understanding of modifier gene action will provide a conceptual framework for understanding the multifactorial basis for hearing loss.

ACKNOWLEDGEMENTS

I would like to thank Dr. Kenneth R. Johnson at The Jackson Laboratory and his associates, Chantal Longo-Guess and Leona H. Gagnon, for mapping of the *Mdwh* locus, contributions to the manuscripts and Figures 5-1 to 5-5. Thanks also go to Dr. David Dolan and Jennifer Benson in the Dolan Lab at Kresge Hearing Research Institute for ABR tests on the mice in Fig. 5-6 and 5-7.

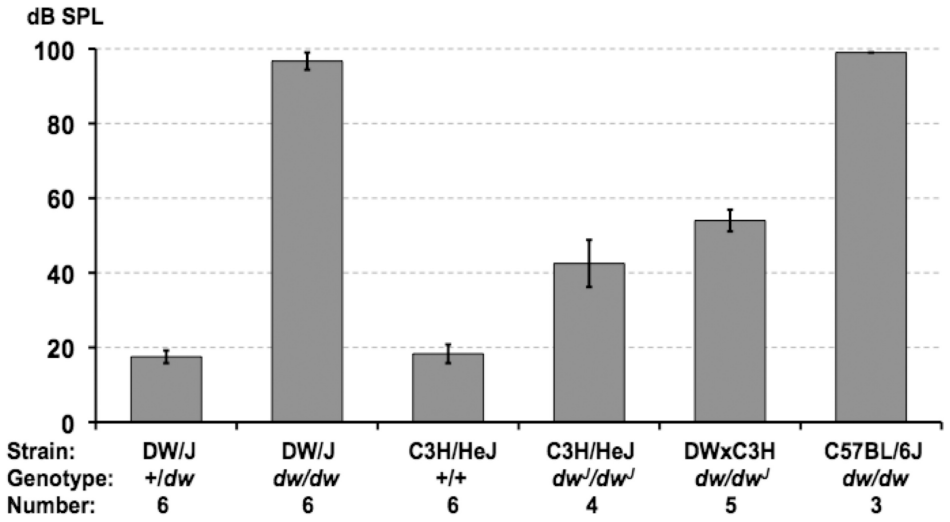

Figure 5-1. Genetic background modifies severity of hearing impairment in *Pou1f1*$^{dw/dw}$ mice.
Average 16 kHz ABR thresholds (with standard error bars) are shown for mice with different *Pou1f1* genotypes on different strain backgrounds. Note that *dwarf* mutant mice on the DW/J and C57BL/6J strain backgrounds have a much more severe hearing impairment than mutant mice on the C3H/HeJ background.

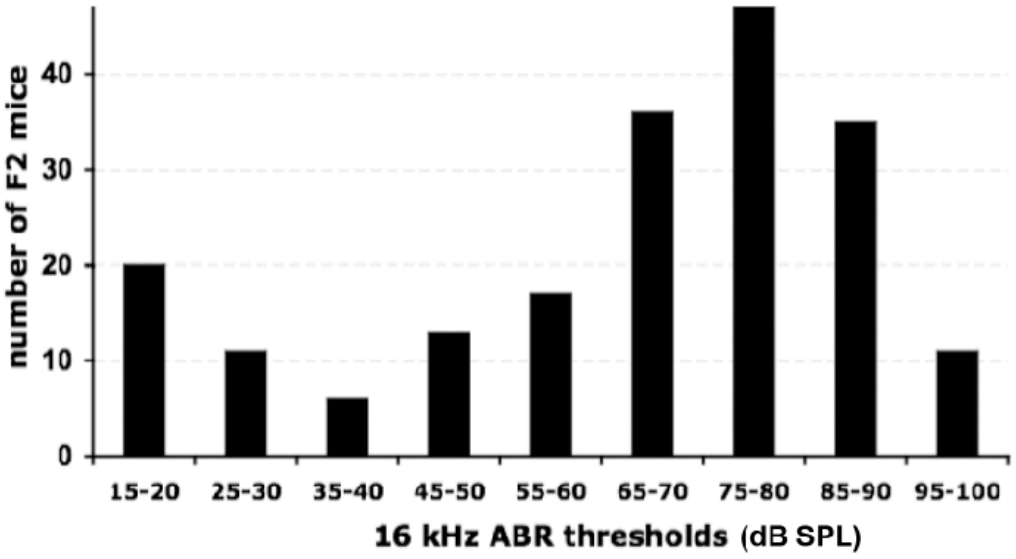

Figure 5-2. Degree of hearing impairment varies among F2 *dw/dw* progeny of the (DW-*Pou1f1*$^{dw/+}$ x CAST) intercross.
A frequency distribution is shown for 196 *dw/dw* F2 mice sorted according to their 16 kHz ABR thresholds. All mice were tested at 4-8 weeks of age. Note the bimodal shape of the distribution with peaks at 15-20 and 75-80 dB SPL.

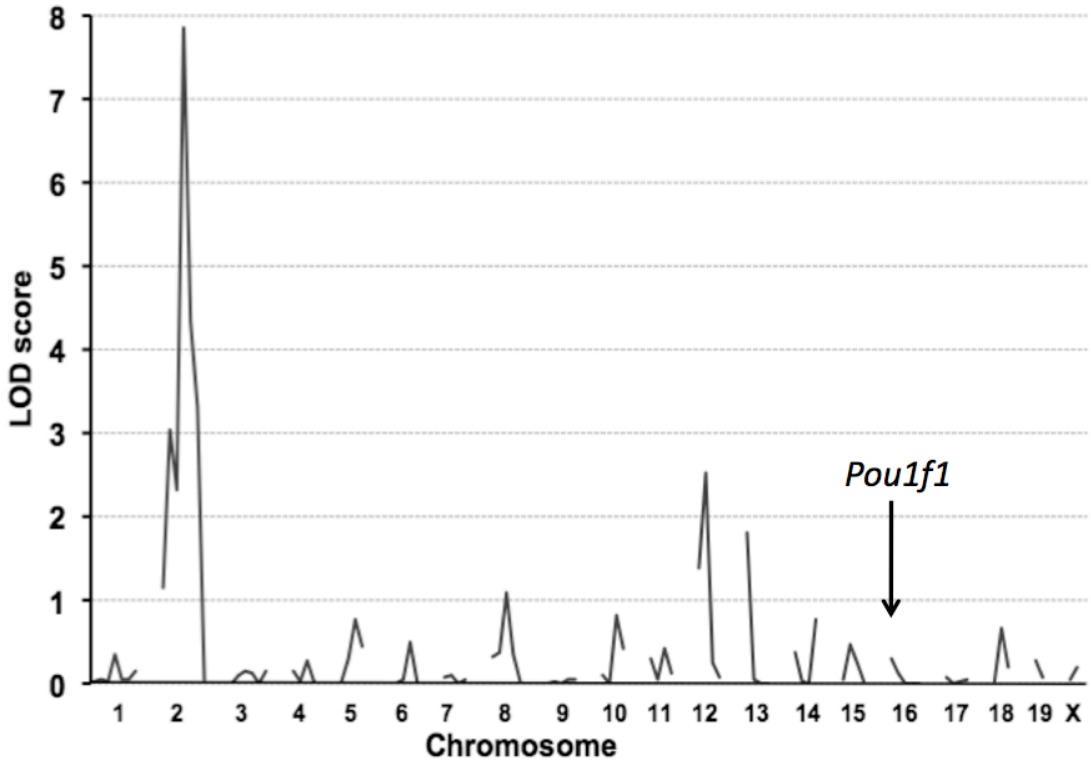

Figure 5-3. Genome-wide linkage analysis of (DW-*Pou1f1*$^{dw/+}$ x CAST) F2 mice identifies a hearing modifier locus on Chr 2.
The 41 *dw/dw* F2 mice with the most extreme ABR thresholds were analyzed, and LOD scores are shown for the linkage associations of these threshold values with each of 90 chromosomal markers. Only markers on Chr 2 showed statistically significant linkage. The *Pou1f1* gene is located on Chr 16.

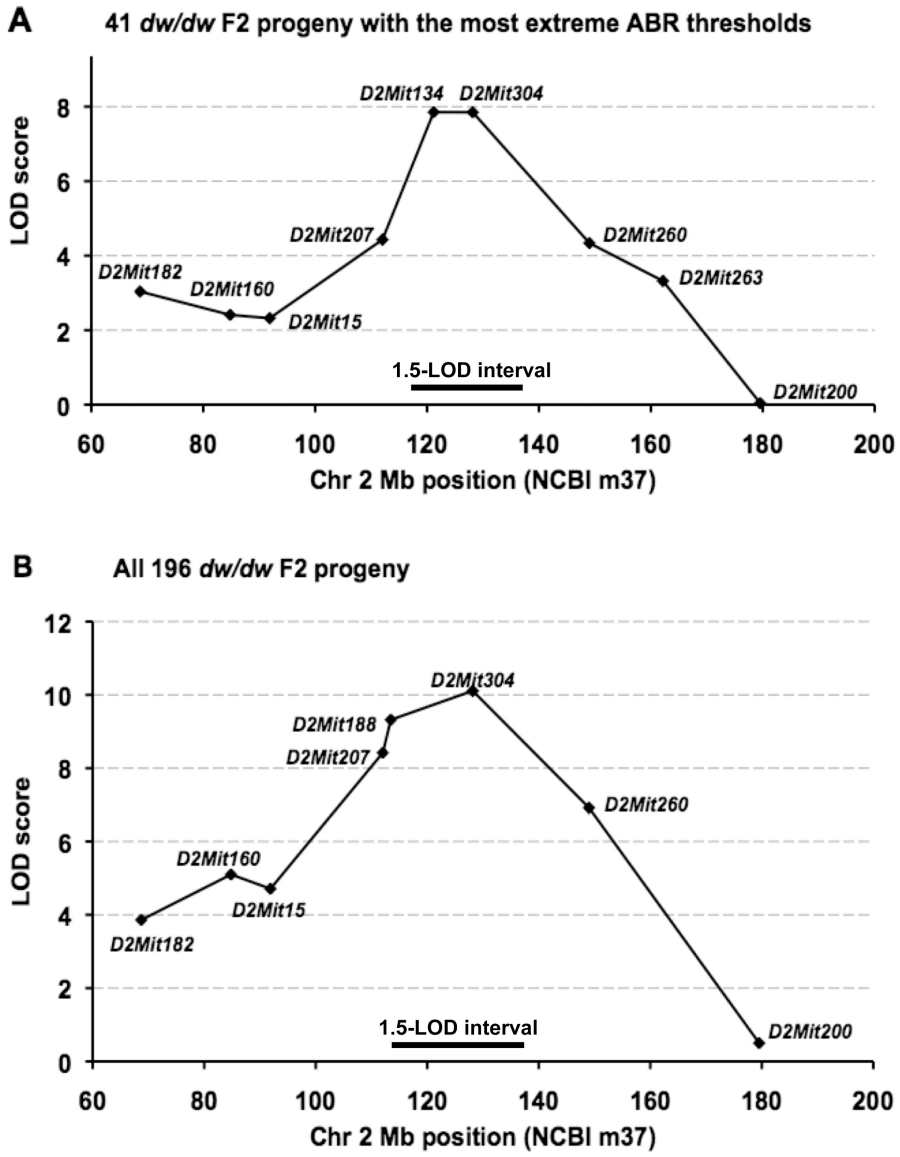

Figure 5-4. Additional mice and markers refined the map position of *Mdwh* on Chr 2.

A. Map position as determined from the 41 *dw/dw* F2 mice with the most extreme thresholds. The peak LOD scores (7.9) were for *D2Mit134* at the 121 Mb position and *D2Mit304* at the 128 Mb position. ***B.*** Map position as determined from all 196 *dw/dw* F2 mice. The peak LOD score (10.1) was for *D2Mit304* at the 128 Mb position. The 1.5-LOD support intervals for both analyses show that *Mdwh* is most likely located within the 116-136 Mb region of Chr 2.

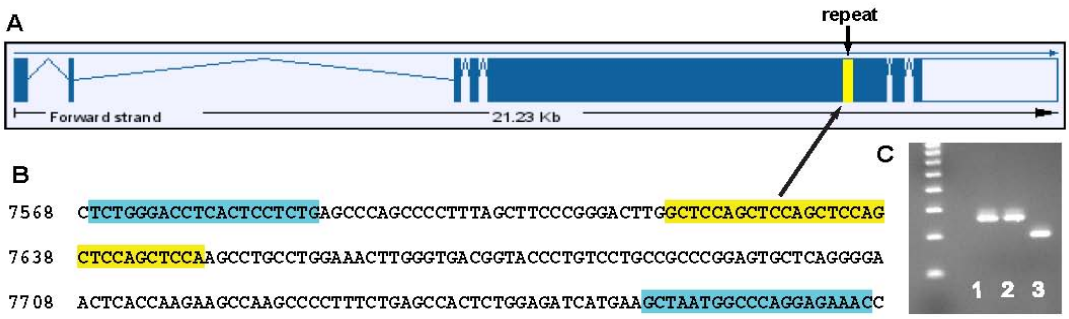

Figure 5-5. *Mtap1a* is a candidate gene for *Mdwh*.
A. Genetic structure of *Mtap1a* showing the position of a polymorphic repeat sequence (yellow bar) in the large exon 5. ***B.*** Primers (highlighted in blue) were designed to amplify the GCTCCA repeat sequence (highlighted in yellow, from C57BL/6J DNA), which encodes an alanine-proline repeat. ***C.*** Sequencing of the 268 bp PCR amplification products from CAST/Ei (lane 1) and C3H/HeJ (lane 2) showed that these strains have 15 repeats of the 6 bp sequence, whereas the 208 bp PCR product from the DW strain (lane 3) showed only 5 repeats.

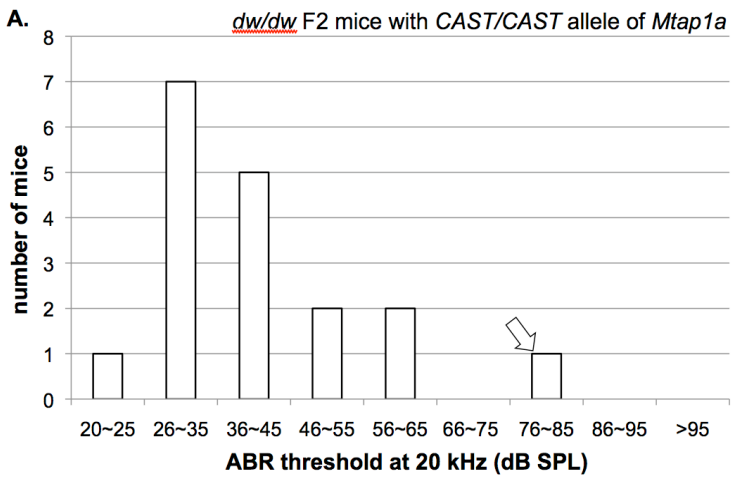
A.
dw/dw F2 mice with CAST/CAST allele of Mtap1a
number of mice
0
1
2
3
4
5
6
7
8
20~25
26~35
36~45
46~55
56~65
66~75
76~85
86~95
>95
ABR threshold at 20 kHz (dB SPL)

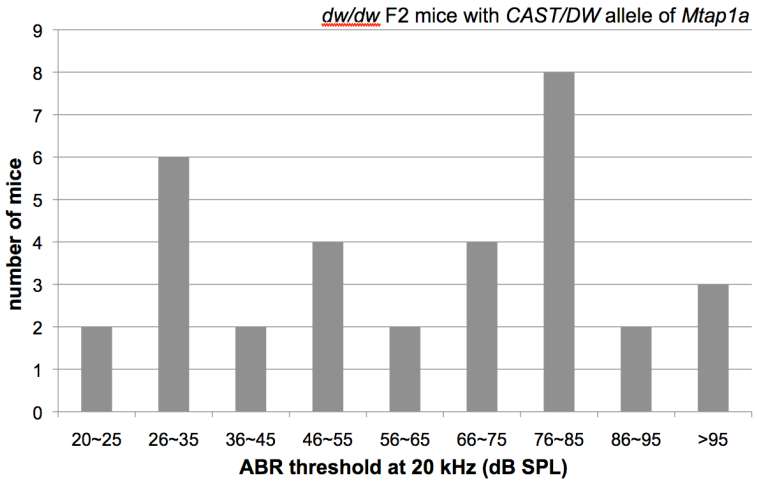
dw/dw F2 mice with CAST/DW allele of Mtap1a
number of mice
0
1
2
3
4
5
6
7
8
9
20~25
26~35
36~45
46~55
56~65
66~75
76~85
86~95
>95
ABR threshold at 20 kHz (dB SPL)

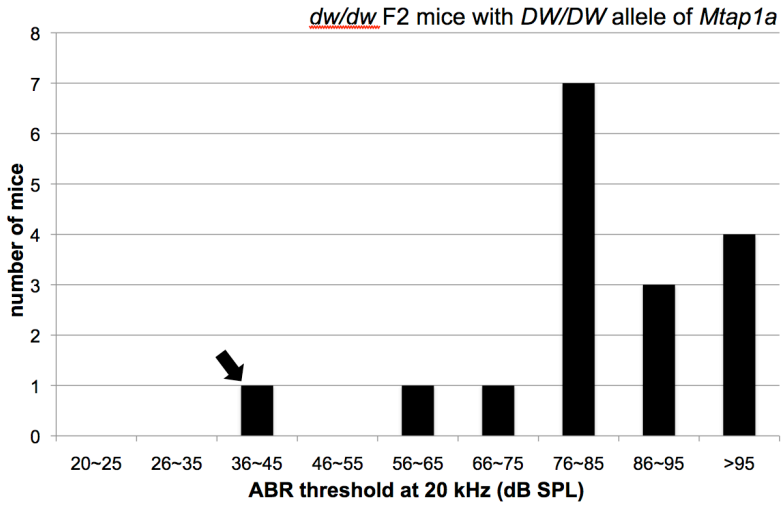
dw/dw F2 mice with DW/DW allele of Mtap1a
number of mice
0
1
2
3
4
5
6
7
8
20~25
26~35
36~45
46~55
56~65
66~75
76~85
86~95
>95
ABR threshold at 20 kHz (dB SPL)

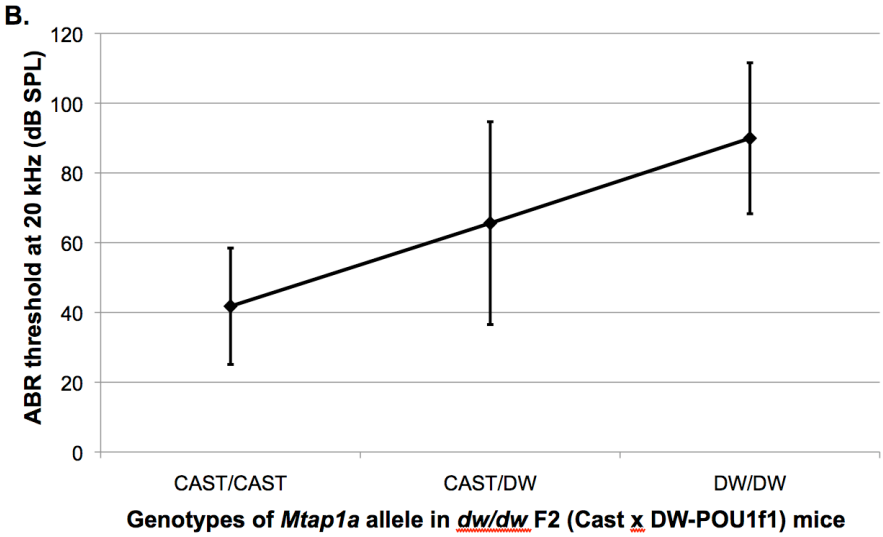

Figure 5-6. The *Mtap1a* allele correlates with, but is neither necessary nor sufficient for protection of hearing in *Pou1f1*^{dw} mice.
68 *dw/dw* F2 (DW/J-*Pou1f1*$^{dw/+}$ x CAST/EiJ) mice were tested for their hearing sensitivity and genotyped for sequence variants of GCTCCA repeats in the *Mtap1a* gene. ***A.*** Mice were grouped by their *Mtap1a* genotypes, and the number of mice with ABR thresholds in each 20 kHz interval were plotted. The open arrow indicates a mouse homozygous for CAST/EiJ *Mtap1a* alleles that exhibited a highly elevated ABR threshold. The black arrow indicates a mouse homozygous for DW/J *Mtap1a* alleles that exhibited a low threshold. ***B.*** Average ABR thresholds at 20 kHz for different *Mtap1a* genotype groups among the *dw/dw* F2 (DW/J-*Pou1f1*$^{dw/+}$ x CAST/EiJ) mice.

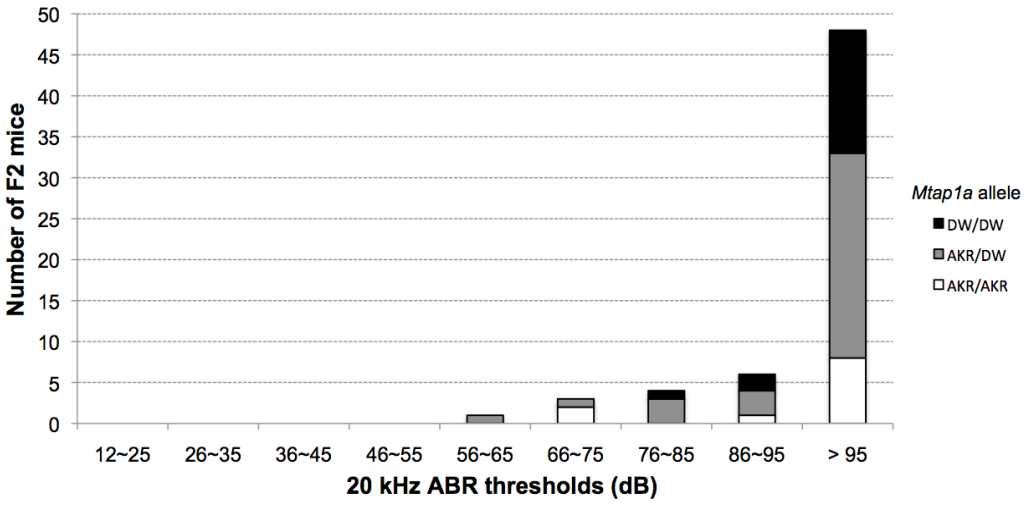

Figure 5-7. AKR genetic background is not protective against hypothyroidism for the hearing in DW/J-*Pou1f1*$^{dw/dw}$ mice.
62 *dw/dw* F2 (DW/J-*Pou1f1*$^{dw/+}$ x AKR) mice were tested for their hearing sensitivity and genotyped for sequence variants of GCTCCA repeats in the *Mtap1a* gene. None of the mice showed ABR thresholds under 35 dB SPL.

Table 5-1. The body size of dwarf intercross mice is not affected by strain background. ANOVA confirms that the similar body weights of *dw/dw* F2 mice from the (DW-*Pou1f1*^{dw} x CAST/Ei) intercross do not correspond with their highly variable ABR thresholds.

SUMMARY				ANOVA					
ABR threshold (dB SPL)	*Count*	*Average weight (gm)*	*Variance*	*Source of Variation*	*SS*	*df*	*MS*	*F*	*P-value*
15 -25	23	7.8	0.6	Between	3.20	6	0.53	0.8	0.54
30-50	27	8.0	1.0	Within	119	189	0.63		
55-60	17	7.8	0.6						
65-70	36	7.8	0.8	Total	122.2	195			
75-80	47	7.6	0.4						
85-90	35	7.7	0.6						
95-100	11	7.5	0.3						

Table 5-2. The *Mdwh* locus has a large effect on ABR thresholds of intercross mice.

Average ABR thresholds (standard deviations) of *dw/dw* F2 mice from the (DW-*Pou1f1*^{dw} x CAST/Ei) intercross are shown sorted by their *D2Mit304* (*Mdwh*) genotypes. LOD scores of linkage associations are shown for an additive inheritance model with one degree of freedom, and estimates are given for the percentage of total ABR variation that can be explained by the *Mdwh* locus. Genotype designations: DD, homozygous for DW allele; DC, heterozyous for DW and CAST alleles; CC, homozygous for CAST allele. Mice were tested at 4-8 weeks of age.

	ABR thresholds			
Genotype	click	8 kHz	16 kHz	32 kHz
DD, N=50	97.9 (8.1)	95.9 (8.2)	82.1 (12.6)	97.9 (7.5)
DC, N=96	84.8 (16.7)	81.6 (16.9)	64.3 (20.8)	87.1 (15.6)
CC, N=44	72.8 (23.7)	72.4 (21.5)	51.6 (27.1)	75.2 (22.4)
LOD score	10.1	9.5	9.9	9.0
percent variation	22	20	21	20

REFERENCES

Benjamin S, Cambray-Deakin MA, Burgoyne RD (1988) Effect of hypothyroidism on the expression of three microtubule-associated proteins (1A, 1B and 2) in developing rat cerebellum. Neuroscience 27:931-939.

Bernal J (2005) Thyroid hormones and brain development. Vitam Horm 71:95-122.

Biesiada E, Adams PM, Shanklin DR, Bloom GS, Stein SA (1996) Biology of the congenitally hypothyroid hyt/hyt mouse. Adv Neuroimmunol 6:309-346.

Brandt N, Kuhn S, Munkner S, Braig C, Winter H, Blin N, Vonthein R, Knipper M, Engel J (2007) Thyroid hormone deficiency affects postnatal spiking activity and expression of Ca2+ and K+ channels in rodent inner hair cells. J Neurosci 27:3174-3186.

Buchner DA, Trudeau M, Meisler MH (2003) SCNM1, a putative RNA splicing factor that modifies disease severity in mice. Science 301:967-969.

Cabello G, Wrutniak C (1989) Thyroid hormone and growth: relationships with growth hormone effects and regulation. Reprod Nutr Dev 29:387-402.

Camper SA, Saunders TL, Katz RW, Reeves RH (1990) The Pit-1 transcription factor gene is a candidate for the murine Snell dwarf mutation. Genomics 8:586-590.

Christ S, Biebel UW, Hoidis S, Friedrichsen S, Bauer K, Smolders JW (2004) Hearing loss in athyroid pax8 knockout mice and effects of thyroxine substitution. Audiol Neurootol 9:88-106.

Cushman LJ, Watkins-Chow DE, Brinkmeier ML, Raetzman LT, Radak AL, Lloyd RV, Camper SA (2001) Persistent Prop1 expression delays gonadotrope differentiation and enhances pituitary tumor susceptibility. Hum Mol Genet 10:1141-1153.

Darvasi A (1997) The effect of selective genotyping on QTL mapping accuracy. Mamm Genome 8:67-68.

Deol MS (1973) Congenital deafness and hypothyroidism. Lancet 2:105-106.

Dupuis J, Siegmund D (1999) Statistical methods for mapping quantitative trait loci from a dense set of markers. Genetics 151:373-386.

Eicher EM, Beamer WG (1980) New mouse dw allele: genetic location and effects on lifespan and growth hormone levels. J Hered 71:187-190.

Forrest D, Erway LC, Ng L, Altschuler R, Curran T (1996) Thyroid hormone receptor beta is essential for development of auditory function. Nat Genet 13:354-357.

Gagnon LH, Longo-Guess CM, Berryman M, Shin JB, Saylor KW, Yu H, Gillespie PG, Johnson KR (2006) The chloride intracellular channel protein CLIC5 is expressed at high levels in hair cell stereocilia and is essential for normal inner ear function. J Neurosci 26:10188-10198.

Ikeda A, Zheng QY, Zuberi AR, Johnson KR, Naggert JK, Nishina PM (2002) Microtubule-associated protein 1A is a modifier of tubby hearing (moth1). Nat Genet 30:401-405.

Johnson KR, Marden CC, Ward-Bailey P, Gagnon LH, Bronson RT, Donahue LR (2007) Congenital hypothyroidism, dwarfism, and hearing impairment caused by a missense mutation in the mouse dual oxidase 2 gene, duox2. Mol Endocrinol 21:1593-1602.

Karolyi IJ, Dootz GA, Halsey K, Beyer L, Probst FJ, Johnson KR, Parlow AF, Raphael Y, Dolan DF, Camper SA (2007) Dietary thyroid hormone replacement ameliorates hearing deficits in hypothyroid mice. Mamm Genome 18:596-608.

Lander E, Kruglyak L (1995) Genetic dissection of complex traits: guidelines for interpreting and reporting linkage results. Nat Genet 11:241-247.

Li S, Crenshaw EB, 3rd, Rawson EJ, Simmons DM, Swanson LW, Rosenfeld MG (1990) Dwarf locus mutants lacking three pituitary cell types result from mutations in the POU-domain gene pit-1. Nature 347:528-533.

Manly KF, Cudmore RH, Jr., Meer JM (2001) Map Manager QTX, cross-platform software for genetic mapping. Mamm Genome 12:930-932.

Mustapha M, Fang Q, Gong TW, Dolan DF, Raphael Y, Camper SA, Duncan RK (2009) Deafness and permanently reduced potassium channel gene expression and function in hypothyroid Pit1dw mutants. J Neurosci 29:1212-1223.

Nasonkin IO, Ward RD, Raetzman LT, Seasholtz AF, Saunders TL, Gillespie PJ, Camper SA (2004) Pituitary hypoplasia and respiratory distress syndrome in Prop1 knockout mice. Hum Mol Genet 13:2727-2735.

Ng L, Hernandez A, He W, Ren T, Srinivas M, Ma M, Galton VA, St Germain DL, Forrest D (2008) A protective role for type 3 deiodinase, a thyroid hormone-inactivating enzyme, in cochlear development and auditory function. Endocrinology.

Ng L, Goodyear RJ, Woods CA, Schneider MJ, Diamond E, Richardson GP, Kelley MW, Germain DL, Galton VA, Forrest D (2004) Hearing loss and retarded cochlear development in mice lacking type 2 iodothyronine deiodinase. Proc Natl Acad Sci U S A 101:3474-3479.

Noguchi Y, Kurima K, Makishima T, de Angelis MH, Fuchs H, Frolenkov G, Kitamura K, Griffith AJ (2006) Multiple quantitative trait loci modify cochlear hair cell degeneration in the Beethoven (Tmc1Bth) mouse model of progressive hearing loss DFNA36. Genetics 173:2111-2119.

O'Malley BW, Jr., Li D, Turner DS (1995) Hearing loss and cochlear abnormalities in the congenital hypothyroid (hyt/hyt) mouse. Hear Res 88:181-189.

Park SM, Liu G, Kubal A, Fury M, Cao L, Marx SO (2004) Direct interaction between BKCa potassium channel and microtubule-associated protein 1A. FEBS Lett 570:143-148.

Rusch A, Ng L, Goodyear R, Oliver D, Lisoukov I, Vennstrom B, Richardson G, Kelley MW, Forrest D (2001) Retardation of cochlear maturation and impaired hair cell function caused by deletion of all known thyroid hormone receptors. J Neurosci 21:9792-9800.

Ruttiger L, Sausbier M, Zimmermann U, Winter H, Braig C, Engel J, Knirsch M, Arntz C, Langer P, Hirt B, Muller M, Kopschall I, Pfister M, Munkner S,

Rohbock K, Pfaff I, Rusch A, Ruth P, Knipper M (2004) Deletion of the Ca2+-activated potassium (BK) alpha-subunit but not the BKbeta1-subunit leads to progressive hearing loss. Proc Natl Acad Sci U S A 101:12922-12927.

Sendin G, Bulankina AV, Riedel D, Moser T (2007) Maturation of ribbon synapses in hair cells is driven by thyroid hormone. J Neurosci 27:3163-3173.

Sohmer H, Freeman S (1996) The importance of thyroid hormone for auditory development in the fetus and neonate. Audiol Neurootol 1:137-147.

Sprenkle PM, McGee J, Bertoni JM, Walsh EJ (2001) Consequences of hypothyroidism on auditory system function in Tshr mutant (hyt) mice. J Assoc Res Otolaryngol 2:312-329.

Uziel A (1986) Periods of sensitivity to thyroid hormone during the development of the organ of Corti. Acta Otolaryngol Suppl 429:23-27.

Winter H, Braig C, Zimmermann U, Geisler HS, Franzer JT, Weber T, Ley M, Engel J, Knirsch M, Bauer K, Christ S, Walsh EJ, McGee J, Kopschall I, Rohbock K, Knipper M (2006) Thyroid hormone receptors TRalpha1 and TRbeta differentially regulate gene expression of Kcnq4 and prestin during final differentiation of outer hair cells. J Cell Sci 119:2975-2984.

Zheng QY, Johnson KR, Erway LC (1999) Assessment of hearing in 80 inbred strains of mice by ABR threshold analyses. Hear Res 130:94-107.

CHAPTER 6

Conclusions & Future Directions

The role of N-terminal proline-rich domain of MYO15 in the inner ear

We have generated a mouse model that recapitulates a human mutation in the proline-rich domain of MYO15 protein using knock-in technology. These knock-in mutants retain the ability to produce the MYO15 isoform that contains the motor and tail domains. They have profound deafness, but they lack circling behavior and obvious balance disorder. Subtle vestibular abnormalities were detected by vestibular evoked potentials (VsEPs) tests. Cochlear stereocilia initially appear normally elongated with whirlin localized at the tips, but the short rows of stereocilia are not maintained, implicating the role of MYO15 proline-rich region in preserving the hair bundle. Classical genetic analysis of compound heterozygous mice containing different combinations of *Myo15* mutant alleles revealed no evidence of allelic complementation for hearing or hair bundle maintenance, consistent with the functional importance of full length MYO15 isoforms containing the proline-rich domain for normal mammalian hearing. To fully uncover the roles of this proline-rich domain in the inner ear, we will focus on answering the questions posed in the following paragraphs.

What mechanisms are involved in hair bundle maintenance by the MYO15 proline-rich domain?

I will address three possible mechanisms that include roles in mechano-electrical-transduction (MET), stereocilia cohesion via tip links, and actin remodeling. These mechanisms are not mutually exclusive. It is possible that MYO15 has a role in multiple processes, each of which contribute to the hair bundle phenotype in the isoform specific knockout that we generated.

The MYO15 proline-rich domain may interact with the mechano-electrical-transduction (MET) complex in the stereocilia. We showed MYO15 isoforms containing the proline-rich domain are specifically localized at the tips of shorter rows of stereocilia. The MET channels also reside at these localizations according to the recently revised model of the MET complex (Beurg et al., 2009). Our hypothesis is that the proline-rich domain of MYO15 at the tips of short row stereocilia interacts with auxiliary elements of MET machinery to play a role in regulating the maintenance or function of ion channels. The inner hair cells of *Myo15*$^{sh2/sh2}$ mice have disrupted fast adaptation, and the transduction current is insensitive to extracellular Ca^{2+}, although the MET response has a normal amplitude and speed of activation (Stepanyan and Frolenkov, 2009). In contrast, the outer hair cells of *Myo15*$^{sh2/sh2}$ mice have normal MET and maintain a very slight staircase structure. Stepanyan and Frolenkov hypothesize that the abnormalities in *Myo15*$^{sh2/sh2}$ IHC function are attributable to the absence of the staircase pattern. If this theory were correct, then the IHC of *Myo15*$^{\Delta N/\Delta N}$ mutants

would be expected to have normal MET because the staircase is initially intact. Their preliminary results suggest this is the case. These studies, however, are limited because they have only been performed at young ages for technical reasons. It is possible that the components of the MET complex change as the mice mature. So far, the molecular composition and structure of MET channels and its anchoring at the tip of the stereocilium, however, have not been to resolved yet.

MYO15 proline-rich domain may play a role in the cohesion of stereocilia by interacting with scaffold and tip link proteins. Pulling forces applied to actin filaments are predicted to control actin polymerization (Hill and Kirschner, 1982). The tension forces on the shorter rows of stereocilia are exerted by the tip links. USH1 proteins, including Harmonin, Cadherin 23 (CDH23), Protocadherin 15 (PCDH15) and SANS, are involved in the cohesion of developing stereocilia and the maintenance of tip links. *Ush1* mouse mutants have defective elongation of the shorter rows of stereocilia, and the stereocilia regress and disappear within the fist couple of weeks after birth (Lefevre et al., 2008). This degeneration phenotype is similar to that of *Myo15*$^{\Delta N/\Delta N}$ mice, even though the ones in *Ush1* mutants are more accelerated and severe. Thus, it will be interesting to check the expression and localization of those USH1 proteins in the cochlea of *Myo15*$^{\Delta N/\Delta N}$ mice. We predict MYO15 proline-rich domain is necessary for maintaining the proper localization of USH1 proteins, either directly or indirectly through trafficking of proteins of the tip link complex or the anchoring complex, rather than affecting the expression level of USH1 proteins. This is because the

phenotype of shorter stereocilia degeneration in *Myo15*$^{\Delta N/\Delta N}$ mice is milder and starts later than *Ush1* mutants. If the degeneration of the short stereocilia in *Myo15*$^{\Delta N/\Delta N}$ mutants is caused by the breakdown of tip links, then SEM examination should detect a reduced number of tip links prior to the absorption of short stereocilia in two week old in *Myo15*$^{\Delta N/\Delta N}$ mice.

The MYO15 proline-rich domain may regulate actin dynamics in stereocilia. Proline-rich proteins are known to participate in delivering actin monomers to specific cellular locations where actin-rich membrane protrusions are formed (Holt and Koffer, 2001). The stereocilia are actin-based structures. It will be very interesting to determine whether the proline-rich domain of MYO15 is involved in regulation of actin polymerization at the plus ends of the shorter rows of stereocilia. Our hypothesis is that the degeneration of the shorter rows of stereocilia in *Myo15*$^{\Delta N/\Delta N}$ mice is due to the dysregulation of actin assembly at the tips of stereocilia. To test this idea, the actin dynamics of stereocilia will be observed in the cochlear explants from *Myo15*$^{\Delta N/\Delta N}$ mice and wild type as previously described (Schneider et al., 2002). Briefly, gene-gun system was used to transfect the cochlear explants with GFP-conjugated actin and actin filament polymerization was observed as accumulation of fluorescence signals under a confocal microscope. If the MYO15 proline-rich domain does regulate actin polymerization, the addition of actin monomers will be absent or significantly reduced at the tips of stereocilia in *Myo15*$^{\Delta N/\Delta N}$ cochlear explants. An *in vitro* actin assembly assay can test the roles of different MYO15 isoforms in actin polymerization directly. If a defect in actin dynamics or assembly is detected, the

mechanism will be explored by examining the expression of proteins that are known to interact with proline-rich domains and actin, such as profilin. Loss of MYO15 isoforms with proline-rich domain in *Myo15*$^{\Delta N/\Delta N}$ mice may affect the trafficking and localization of profilin to cause stereocilia degeneration.

Is the MYO15 proline-rich domain involved in the formation and function of synapses ?

MYO15 is associated with secretory granules in the pituitary (Lloyd et al., 2001), suggesting it may have a role in secretion or movement of secretory vesicles. MYO6 is an example of unconventional myosin present at both stereocilia and the synaptic region of cochlear hair cells. MYO6 and otoferlin interact at the IHC ribbon synapse and are involved in the recycling of synaptic vesicles (Roux et al., 2009). WHIRLIN, the only known interacting protein with MYO15, is expressed at the synaptic region of OHCs (van Wijk et al., 2006). This supports the idea that MYO15 could have a role in vesicle transport and/or neurotranmitter release at the hair cell synapses.

What proteins interact with proline-rich domain of MYO15?

To understand the biological function of MYO15 proline-rich domain, it is important to identify interacting proteins and determine how they fit into the context of known molecular networks. Yeast two hybrid is an effective way to identify novel proteins that interact. We will use three highly conserved portions of the proline-rich domain of MYO15 as bait to discover potentially interacting

proteins in a well-characterized library made from the sensory epithelia of newborn mouse cochlea. Confirmation of the bona fide interacting proteins will be performed by co-immunoprecipitation (Co-IP) tests, GST pull down assay, and co-transfection of polarized epithelia cells to validate the interaction. Alternatively, candidate proteins that are predicted to interact with the MYO15 proline-rich domain can be tested directly by Co-IP and co-localization within the transfected epithelial cells.

Does the proline-rich domain of MYO15 play a role in the vestibular function?

Unlike *sh2* or *sh2J* mice, the *Myo15*$^{\Delta N/\Delta N}$ mutants do not circle. Subtle vestibular abnormalities were detected by VsEPs tests. Linear VsEPs measures the action potential from the vestibular nerves in response to linear acceleration transients, which is strictly dependent on the saccule and utricle (also known as otolithic organ or gravity receptors) of the inner ear (Jones et al., 1999; Jones and Jones, 1999). Another routine diagnostic tool to assess otolith functions is the vestibulocollic reflex (VCR). VCR measures an animal's ability to stabilize their head at a position in space while their body is moving. VCR is used as an alternative to the vestibulo-ocular reflex (VOR), but does not require surgical preparation (Takemura and King, 2005). Abnormalities detected by VCR tests will help confirm the dysfunction of saccule and utricle in *Myo15*$^{\Delta N/\Delta N}$ mutants. Moreover, similar as VOR, VCR would reflect the function of the pathways between peripheral vestibular sensory neurons and the cervical motoneurons innervating the neck muscles (Takemura and King, 2005). Dr. Micheal King's lab

in Kresge Hearing Research Institute at the University of Michigan will do the VCR measurements on *Myo15*$^{\Delta N/\Delta N}$ mice for us.

Preliminary data show that MYO15 containing proline-rich domain isoforms are localized at the striola area within the utricle (personal communication with Dr. Jonathan Bird). The striola is an anatomically differentiated strip of the sensory epithelium within saccule and utricle. On each side of the striola, the stereocilia on vestibular hair cells are oriented 180^{o} in reverse to each other. The presence of MYO15 isoforms with proline-rich domain in the striola suggests that the proline-rich domain may be involved in establishing hair bundle polarity and orientation in the vestibular system. To test this hypothesis, measurements of the planar orientation of vestibular hair cells need to be done in our isoform specific knockout mouse as previously described (Holley et al., 2010).

Preliminary light microscopy and SEM do not reveal any differences in the stereocilia of vestibular hair cells in *Myo15*$^{\Delta N/\Delta N}$ and wild type, although more careful examination of vestibular stereocilia is necessary to draw conclusions about the effects of MYO15 proline-rich domain in the morphology of vestibular structures. These examinations include focusing on the striola to examine the position of kinocilia, measurements of stereocilia lengths, and the presence of stereocilia links. We also plan to examine the vestibular system of older mice in case there is a role for the isoforms of MYO15 with the proline rich domain in stereociliar maintenance, but with a longer time to degeneration than observed in the cochlear stereocilia.

Molecular and genetic studies of hypothyroidism-induced deafness

We showed that thyroid hormone (TH) has pleiotropic effects on cochlear development in *Pou1f1*^{dw} mutant mice. In contrast, *Prop1*^{df} mutants have very mild hearing impairment, and most of the processes that are permanently affected in *Pou1f1* mutants are normal in *Prop1* mutants. These differences in hearing are not attributable to the degree of TH deficiency, as neither mutant has detectable serum TH. Intercross experiments demonstrated that the difference is due to the protective genetic background of the stock used to carry the *Prop1*^{df} mice (DF/B) and the susceptible genetic background of the *Pou1f1*^{dw} mutants (DW/J). An intercross between F1 mice produced from a cross of DW/J-*Pou1f1*$^{dw/+}$ and wild type mice of the good hearing strain CAST/EiJ generated both hearing and deaf mutants in approximately a 1:3 ratio. A genome scan of these mutants, conducted by Dr. Ken Johnson of the Jackson Laboratory, identified a locus on chromosome 2, named modifier of dw hearing, *Mdwh*, that rescues the hearing impairment of *Pou1f1*^{dw} mutants despite persistent hypothyroidism. This chromosomal region contains a modifier of *Tubby* hearing (*Moth1*) that encodes a protective allele of the microtubule-associated protein *Mtap1a* (Ikeda et al., 2002). I present evidence that suggests *Mdwh* is not *Mtap1a*, a microtubule-associated protein that modifies the hearing of *Tubby* mice. More work is still needed, however, to make it absolutely clear that whether *Mtap1a* is not involved in the modification of hearing in hypothyroid mice.

Our future research will be focused on identifying the protective modifier gene(s) of hypothyroidism-induced deafness. Our strategies include sequencing candidate genes in the *Mdwh* critical region from the DW/J susceptible strain, generating congenic mice containing *Mdwh* locus from CAST/EiJ strain on DW/J-*Pou1f1* background, and whole genome scanning on F2 dw/dw mutants produced from an F1 intercross between 129P2/OlaHsd and DW/J-*Pou1f1* strains. I will discuss each of these experiments below.

Sequencing the candidate genes within Mdwh locus.

There are more than 1,000 genes located in the *Mdwh* locus. The way to select the most attracting genes to sequence has taken advantage of a successful microarray analysis of cochlear gene expression changes in DW-*Pou1f1*^{dw} mutants and wild types (Tzy-wen Gong, unpublished). To prepare the cochlear transcripts for the microarray, cochlear tissues were dissected from 6 wk old mutants and wild types. 4 pools of each genotype were collected. Analysis with Affy GeneChip mouse 430 version 2.0 gave 552 different probe sets with significantly altered expression between the two genotypes. 10 out of the 552 differentially expressed cochlear genes are located within *Mdwh* locus on Chromosome 2. Four genes that are known to affect hearing also map in the *Mdwh* locus. Taken together, we consider these 14 genes as the candidate genes for *Mdwh* and plan to sequence them from the *DW/J* strain.

We hypothesize that an obvious mutation such as a frame shift, splice site mutation, or stop codon in the candidate gene(s) could account for susceptibility

to the hypothyroidism-induced hearing loss on DW/J-*Pou1f1* strain. There is a precedent for this. A stop codon in sodium channel modifier 1 (SCNM1) on the genetic background of C57BL/6J strain intensifies the severity of inherited movement disease caused by mutant sodium channel gene *Scn8a* (Buchner et al., 2003). Interestingly, SCNM1 also locates in the *Mdwh* locus.

Candidate genes will be prioritized for the sequencing analysis based on knowledge of the affected process and genetic map location within the critical locus. Once a candidate gene is identified with a genetic variation that suggests it is responsible for *Mdwh*, we will check its sufficiency by introducing a transgene containing a protective allele into the genome of DW-*Pou1f1*^{dw} mutants and examine whether the hearing of DW-*Pou1f1*^{dw} mutants is rescued.

Generating congenic mice containing the Mdwh locus from Cast/EiJ strain on DW-Pou1f1 background.

To determine whether the *Mdwh* locus from the CAST/EiJ background is sufficient for protection of hearing against hypothyroidism in DW-*Pou1f1*$^{dw/dw}$ mutants, we are going to generate congenic mice by mating CAST/EiJ and DW-*Pou1f1*$^{dw/+}$ and repeatedly backcrossing the descendants with DW-*Pou1f1* (recipient strain). For each generation, genetic markers covering the whole mouse genome will be used to select the best breeders that carry the *Mdwh* locus from Cast/EiJ strain while the rest of genome comes mostly from DW-*Pou1f1* strain. Also, the possibility of hearing rescue could be checked at each generation. When congenic mice are finally generated, their hearing abilities will

be tested by ABR. If they can hear, it indicates that *Mdwh* is sufficient to protect the hearing against hypothyroidism in DW-*Pou1f1* mutants. We will further narrow down the critical region by more breeding. If the congenic mice can not hear, it suggests that genetic loci on other chromosomes are required for protection of hypothyroidism-induced deafness. which is also implied by the distribution of hearing abilities of F2 *dw/dw* mutants from crossing between 129P2/OlaHsd and DW-*Pou1f1* strains (see below).

Whole genome scanning on F2 dw/dw mutants produced from an F1 intercross between 129P2/OlaHsd and DW-Pou1f1 strains.

Our unpublished data demonstrate that the genetic background of 129P2/OlaHsd mice can rescue the hearing loss in DW-*Pou1f1*$^{dw/dw}$ mutants. The distribution of ABR thresholds among those F2 mutants is broad, in contrast to the obvious bi-modal distribution observed in the F2 mice from the CAST/EiJ and DW-*Pou1f1* F1 intercross (Fig. 6-1). This suggests that the 129P2/OlaHsd background may provide protection against hypothyroidism-induced deafness by the interaction of multiple genes. If this is true, a genome scan on F2 *dw/dw* (129P2/OlaHsd X DW- *Pou1f1*) will identify multiple loci across the genome with significant LOD scores. This result won't be too surprising since TH/THR pathway regulate a broad range of gene expressions. The significant loci other than *Mdwh* will be helpful for genotying the congenic pups if the breeding of the congenic mice described above show that Chr 2 is not enough for protection of hearing in *Pou1f1* mutants. If the congenic mice show *Mdwh* on Chr 2 is

sufficient, it suggests that the 129P2/OlaHsd background is more complex in terms of the ability to rescue the hearing loss caused by hypothyroidism.

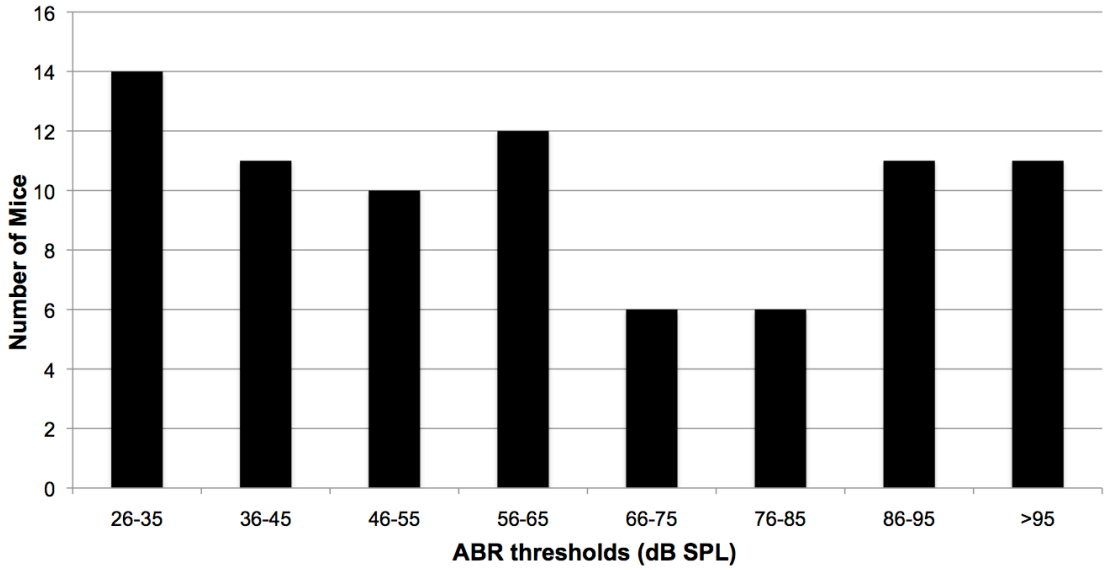

Figure 6-1. The genetic background of 129P2/OlaHsd mouse strain can rescue the hearing loss in *DW-Pou1f1*$^{dw/dw}$ mice.
A frequency distribution is shown for 77 *dw/dw* F2 mice sorted according to their 20 kHz ABR thresholds. All mice were tested at 30~60 days old.

REFERENCES

Beurg M, Fettiplace R, Nam JH, Ricci AJ (2009) Localization of inner hair cell mechanotransducer channels using high-speed calcium imaging. Nat Neurosci 12:553-558.

Buchner DA, Trudeau M, Meisler MH (2003) SCNM1, a putative RNA splicing factor that modifies disease severity in mice. Science 301:967-969.

Hill TL, Kirschner MW (1982) Subunit treadmilling of microtubules or actin in the presence of cellular barriers: possible conversion of chemical free energy into mechanical work. Proc Natl Acad Sci U S A 79:490-494.

Holley M, Rhodes C, Kneebone A, Herde MK, Fleming M, Steel KP (2010) Emx2 and early hair cell development in the mouse inner ear. Dev Biol 340:547-556.

Holt MR, Koffer A (2001) Cell motility: proline-rich proteins promote protrusions. Trends Cell Biol 11:38-46.

Ikeda A, Zheng QY, Zuberi AR, Johnson KR, Naggert JK, Nishina PM (2002) Microtubule-associated protein 1A is a modifier of tubby hearing (moth1). Nat Genet 30:401-405.

Jones SM, Erway LC, Bergstrom RA, Schimenti JC, Jones TA (1999) Vestibular responses to linear acceleration are absent in otoconia-deficient C57BL/6JEi-het mice. Hear Res 135:56-60.

Jones TA, Jones SM (1999) Short latency compound action potentials from mammalian gravity receptor organs. Hear Res 136:75-85.

Lefevre G, Michel V, Weil D, Lepelletier L, Bizard E, Wolfrum U, Hardelin JP, Petit C (2008) A core cochlear phenotype in USH1 mouse mutants implicates fibrous links of the hair bundle in its cohesion, orientation and differential growth. Development 135:1427-1437.

Lloyd RV, Vidal S, Jin L, Zhang S, Kovacs K, Horvath E, Scheithauer BW, Boger ET, Fridell RA, Friedman TB (2001) Myosin XVA expression in the pituitary and in other neuroendocrine tissues and tumors. Am J Pathol 159:1375-1382.

Roux I, Hosie S, Johnson SL, Bahloul A, Cayet N, Nouaille S, Kros CJ, Petit C, Safieddine S (2009) Myosin VI is required for the proper maturation and function of inner hair cell ribbon synapses. Hum Mol Genet 18:4615-4628.

Schneider ME, Belyantseva IA, Azevedo RB, Kachar B (2002) Rapid renewal of auditory hair bundles. Nature 418:837-838.

Stepanyan R, Frolenkov GI (2009) Fast adaptation and Ca2+ sensitivity of the mechanotransducer require myosin-XVa in inner but not outer cochlear hair cells. J Neurosci 29:4023-4034.

Takemura K, King WM (2005) Vestibulo-collic reflex (VCR) in mice. Exp Brain Res 167:103-107.

van Wijk E, van der Zwaag B, Peters T, Zimmermann U, Te Brinke H, Kersten FF, Marker T, Aller E, Hoefsloot LH, Cremers CW, Cremers FP, Wolfrum U, Knipper M, Roepman R, Kremer H (2006) The DFNB31 gene product whirlin connects to the Usher protein network in the cochlea and retina by direct association with USH2A and VLGR1. Hum Mol Genet 15:751-765.